THE UNIVERSITY OF
WAIKATO
Te Whare Wānanga o Waikato

EVIDENCE FOR A THIRD THERMAL PARAMETER OF ENZYMES

A thesis

submitted in partial fulfilment

of the requirements for the Degree

of

Doctor of Philosophy in Biological Sciences

at the

University of Waikato

by

Michelle Emma Peterson

University of Waikato

2005

Abstract

This thesis describes tests of a new hypothesis describing the effect of temperature on enzyme activity.

Traditionally, the dependence of enzyme activity on temperature has been described by a model (the 'Classical Model') consisting of two processes: the catalytic reaction defined by $\Delta G^{\ddagger}_{cat}$, and irreversible inactivation defined by $\Delta G^{\ddagger}_{inact}$.

To account for the anomalies found in the variation of enzyme activity with temperature, a new model (the 'Equilibrium Model') has been formulated to describe the effect of temperature on enzyme activity.

In addition to the processes described by $\Delta G^{\ddagger}_{cat}$ and $\Delta G^{\ddagger}_{inact}$, this model incorporates an inactive (but not denatured) form of the enzyme (E_{inact}) that is in reversible equilibrium with the active form (E_{act}). The equilibrium between E_{act} and E_{inact} is described by an equilibrium constant (K_{eq}), whose temperature dependence is characterised in terms of the enthalpy of the equilibrium, ΔH_{eq}, and a new thermal parameter, T_{eq}, which is the temperature at which the concentrations of E_{act} and E_{inact} are equal.

This research has set out to: test the 'Equilibrium Model'; investigate the molecular basis of the temperature-dependent interconversion of the active and inactive forms of the enzyme; develop methods for the reliable determination of T_{eq}, and outline the assay parameters required for accurate determination of T_{eq};

examine the biotechnological implications of T_{eq}; and finally, examine the evolutionary and ecological implications of T_{eq}

The 'Equilibrium Model' was tested by comparing 3D plots of experimental data (expressed as rate versus temperature versus time) collected for five enzymes with the 3D plots of the outputs predicted by the 'Classical' and 'Equilibrium' models. This analysis found that all five enzymes behaved as predicted by the 'Equilibrium Model', in displaying clear temperature optima at time zero, and led to the determination of plausible values for $\Delta G^{\ddagger}_{cat}$, $\Delta G^{\ddagger}_{inact}$, ΔH_{eq}, and T_{eq}.

The value of T_{eq} was affected when the enzyme-substrate interaction was altered (by the use of different substrates) but was, in general, unaffected by the addition of denaturing or stabilising agents to the assay. These results give some insight into the molecular basis of the equilibrium and, together with the fast timescale with which the E_{act}/E_{inact} equilibrium occurs, support the hypothesis that it is unlikely that E_{inact} is significantly unfolded and that the transition from E_{act} to E_{inact} involves only a local (reversible) conformational change, possibly near or at the active site; in contrast to the slower and largely irreversible (under assay conditions) global conformational changes associated with thermal denaturation.

The methodology for the determination of T_{eq} was developed and extended to allow less laborious determination of T_{eq} and to allow the determination of T_{eq} using assay systems that are less than "ideal". Minimum assay parameters were determined in terms of sampling rate and temperature range.

The potential implications of T_{eq} for enzyme evolution, protein engineering and enzyme reactor performance have been introduced and discussed.

The characterisation of three enzymes, once each from a psychrophilic, mesophilic and thermophilic source, has given some indication of the ecological and environmental implications of T_{eq}, and suggests that T_{eq} is a better indication of the source temperature of the enzyme than thermal stability and that ΔH_{eq} reflects the thermal environment from which the enzyme was sourced.

The results of this research are such that T_{eq} can now be considered a fundamental thermal parameter of enzymes and is required alongside the Arrhenius activation energy and thermal stability to completely account for the way in which enzyme activity behaves with respect to temperature.

Preface

The majority of the results presented in this thesis have been presented as papers prepared for publication. Chapter Three has been published as a Research Article in the Journal of Biological Chemistry, Chapter Four (a full length research paper) will be submitted to Biochemical Journal, Chapter Five (as part of a full length research paper) will be submitted to the Journal of Biological Chemistry and Chapter Six has been submitted as a Letter to Nature Biotechnology. These chapters are presented in the same form as that in which they were submitted to the journals, hence there are some differences in format between the chapters. There is also some minor overlap between these chapters, as each is intended to be complete in its self.

As the presentation of results in manuscript format makes up the bulk of this thesis, the numerical referencing system has been carried through out, with references collated at the end of each chapter. A complete reference list is available at the end of this thesis.

In some parts of this thesis, my own work has been placed in the context of the overall research effort. Where this has occurred, a clear distinction is made as to the extent of my contribution. It is felt that the presentation of the work in this context is necessary to enable the rationale for the conclusions to be evident.

Acknowledgements

Firstly, I thank Professor Roy Daniel for the guidance, encouragement and patience he has shown during the practical work and writing of this thesis. I am grateful to my un-official second supervisors, Professors Michael Danson and Robert Eisenthal at the University of Bath, for their hospitality during my stay in Bath and for their invaluable input throughout. Thank you also to my official second supervisor, Dr Rachel Dunn, who has not only been a suitably objective adviser but a great friend too. To the members of, and visitors to, the Thermophile Research Unit, past and present, I thank you all for making my time spent in and around TRU an entertaining and encouraging experience. A special mention goes to Charis Shepherd from the University of Auckland for providing much entertainment as she was forced to grasp the concepts of this project.

I would like to acknowledge the financial support received from the Royal Society of New Zealand, which made my visit to Michael Danson's laboratory at the University of Bath possible. A big thank you goes to the members of the "Centre for Extremophile Research" for their hospitality during my time there.

I am grateful to my wonderful friends outside of acadæmia, who had no idea what I was on about half the time but supported me 100%, and to the Peterson and Altham families for their understanding and tolerance during what could be at times, rather trying circumstances. To Tim, who has been there from the very start, I could never thank you enough for the love and support you have given me over the last six years.

Table of Contents

List of Figures

CHAPTER 3

CHAPTER 4

CHAPTER 5

CHAPTER 6

CHAPTER 7

List of Tables

Abbreviations

The abbreviations listed below follow the recommendations of the Nomenclature Committee of IUBMB and the IUPAC–IUBMB Joint Commission on Biochemical Nomenclature as far as practicable.

$[E_0]$	initial concentration of enzyme
A	the pre-exponential factor or the Arrhenius constant
APS	Adenosine 5'-phosphosulfate
ATCC	American Type Culture Collection
ATP	Adenosine triphosphate
BCV	*Bacillus caldovelox*
BPSY	*Bacillus psychrophilus*
BPSYC	*Bacillus psychrosacchrolyticus*
BSA	Bovine Serum Albumin
BSUBT	*Bacillus subtilis*
BTK	*Bacillus thuringiensis*
CTAB	Hexadecyltrimethylammonium bromide
$\Delta G^{\ddagger}$	the change in free energy for the activation
$\Delta G^{\ddagger}_{cat}$	the change in free energy of activation for the catalysed reaction
$\Delta G^{\ddagger}_{inact}$	the change in free energy of activation for thermal inactivation
ΔG_{eq}	the change in free energy for the equilibrium

$\Delta H^{\ddagger}$	the change in enthalpy for the activation
ΔH_{eq}	the change in enthalpy for the equilibrium
$\Delta S^{\ddagger}$	the change in entropy for the activation
ΔS_{eq}	the change in entropy for the equilibrium
DSMZ	Deutsche Sammlung von Mikroorganismen und Zellkulturen (German Collection of Microorganisms and Cell Cultures)
ΔU	internal energy of the products minus that of the reactants
E_a	the Arrhenius activation energy
E_{act}	active form of the enzyme
EC	Enzyme Commission Number
EDTA	ethylenediaminetetraacetic acid
E_{inact}	inactive form of the enzyme
GC-content	Guanine-cytosine content
h	Planck's constant
IPM	Isopropylmalate
IPMDH	Isopropylmalate dehydrogenase
κ	the transition co-efficient
$K^{\ddagger}$	equilibrium constant for the equilibrium between the activated complex and the un-activated molecules
k_B	the Boltzmann constant (the gas constant per molecule)
k'_b	reduced rate constant of the reverse reaction
K_c	temperature co-efficient of the equilibrium constant of a reaction in terms of concentrations

k_{cat}	the enzyme's catalytic constant
KCl	Potassium chloride
K_{eq}	equilibrium constant between active and inactive forms of enzyme
k'_f	reduced rate constant of the forward reaction
k_{inact}	thermal inactivation rate constant
K_M	Michaelis-Menten constant
k_r	rate constant of the reaction
$MgCl_2$	Magnesium chloride
$MnCl_2$	Manganese chloride
NADP(H)	nicotinamide adenine dinucleotide (phosphate)
NAD(H)	nicotinamide adenine dinucleotide
NH_4Cl	ammonium chloride
NIST	National Institute of Standards and Technology
NMR	Nuclear Magnetic Resonance
PCR	Polymerase Chain Reaction
PGK	3-phosphoglycerate kinase
pH	negative logarithm of the hydrogen ion activity
pK_a	dissociation constant
*p*NAA	*p*-nitroacetanilide
*p*NPP	*p*-nitrophenylphosphate
R	universal gas constant
SDS	sodium dodecylsulfate
T	absolute temperature
t	assay duration

$t_{½}$	half-life
T_{eq}	the temperature at which E_{act} and E_{inact} are in equilibrium
T_{opt}	the temperature optimum of an enzyme-catalysed reaction
Tris	tris (hydroxymethyl) aminomethane
UV	ultraviolet
V_{max}	maximum velocity of the enzyme
X	thermally denatured state

Chapter One

The Effect of Temperature on Enzyme Activity: A Review

Much of the information presented in section 1.4, 'Enzyme "Temperature Optima"', of this chapter has been taken directly from the paper by Daniel *et al* published in the journal, *Trends in Biochemical Sciences* (2001, volume 26, pages 223 – 225). The Models proposed in this paper are what this research project is based upon and therefore, a detailed reproduction was required here as a background to this research project.

I am indebted to Professor Robert Eisenthal at the University of Bath for an outline of the historical background to the concept of "reversible thermal enzyme inactivation" (pages 21 – 25), upon which exploration and expansion was made for the purposes of this thesis.

1.1 Introduction

It is well known that reactions in biological systems, especially those in living cells, are particularly sensitive to changes in temperature. No organism is immune to the effect of temperature, and the likelihood of exposure to extremes that may affect the integrity of cells and their components is relatively high. Organisms can tolerate only a defined range of temperatures, above and below which they are adversely affected. Life depends on a complex network of chemical reactions brought about by specific enzymes and any modification of this enzyme pattern, for example, by a change in temperature, may have significant consequences for the organism.

With very few exceptions, chemical reactions proceed at a faster velocity as the temperature is raised[1]. An increase in temperature imparts more kinetic energy to the reactant molecules resulting in more productive collisions per unit time. Enzyme catalysed reactions behave similarly. However, as the temperature is increased, the expected increase in catalytic rate resulting from increased enzyme/substrate collisions may be offset by the increasing rate of thermal denaturation of the protein and subsequent decrease in catalytic rate. The simultaneous operation of these two effects is dependent on several factors, some intrinsic to the enzyme, some due to the nature of the reaction conditions. This might suggest that the effects of temperature on enzymes are extremely complex. However, these factors can be readily analysed experimentally or eliminated by proper attention to details of technique, so that the determination of the effect of temperature on enzyme activity becomes a simple exercise and affords a useful diagnostic characteristic of an individual enzyme.

1.2 The Effect of Temperature on Catalytic Rate

The van't Hoff equation for the temperature coefficient of the equilibrium constant of a reaction, K_c, in terms of concentrations, is:

$$\frac{d\ln K_c}{dT} = \frac{\Delta U}{RT^2} \qquad \textbf{Equation 1.1}$$

where R is the universal gas constant, T is the absolute temperature and ΔU is the internal energy of the products minus that of the reactants. The Law of Mass Action[2] indicates that $K_c = k'_f/k'_b$, where k'_f and k'_b are the reduced rate constants (used where the rate equation has been expressed in concentrations relative to concentrations in a standard state) of the forward and reverse reactions, respectively.

Based on these concepts, Svante Arrhenius[3] suggested that:

$$\frac{d\ln k_r}{dT} = \frac{E_a}{RT^2} \qquad \textbf{Equation 1.2}$$

If it is assumed that E_a does not depend on temperature, Equation 1.2 gives on integration:

$$\ln k_r = -\frac{E_a}{RT} - \ln A \qquad \textbf{Equation 1.3}$$

Rearrangement of Equation 1.3 affords what is now known as the Arrhenius Equation:

$$k_r = A \cdot e^{-E_a/RT} \qquad \textbf{Equation 1.4}$$

where k_r is the rate constant of the reaction; E_a is the activation energy of the reaction; R is the universal gas constant; T is the absolute temperature and A is the pre-exponential factor or the Arrhenius constant, determined experimentally for a given reaction under given conditions.

According to Arrhenius, Equation 1.4 indicates that molecules must attain a certain critical energy E_a before they can react, and $e^{-Ea/RT}$ is the Boltzmann factor (a weighting factor determining the relative probability of a system in thermodynamic equilibrium[4]) giving the fraction of the molecules that do achieve the critical energy. This interpretation is essentially correct but considering the other shortcomings of Arrhenius Theory (empirically derived, no way of calculating E_a and A from the properties of reacting molecules, valid only if the range of temperature is not too large, assumes that the properties of the reaction medium do not change in the temperatures range examined (viscosity, diffusion of reactant species, etc.)), a more detailed theory is required to completely describe the temperature dependence of reaction rates, in terms of the physical properties of the reacting molecules.

The central point of the Theory of Absolute Reaction Rates, or Transition State Theory as it is commonly known, is that the rate of any reaction at a given temperature depends only on the concentration of an energy-rich activated complex, which is in equilibrium with the un-activated reactants[5],

$$A + B \overset{K^{\ddagger}}{\leftrightarrows} X^{\ddagger} \overset{k_r}{\rightarrow} P + Q \qquad \textbf{Equation 1.5}$$

where A and B represent the un-activated reactants, $X^{\ddagger}$ represents the activated complex, and P and Q represent the products resulting from the decomposition of $X^{\ddagger}$.

According to this theory, all activated complexes break down at a rate that can be described by:

$$k_r = \kappa \cdot \frac{k_B T}{h} \cdot K^{\ddagger} \qquad \textbf{Equation 1.6}$$

where k_r is the rate constant of the reaction, κ is the transition coefficient (which describes the probability that the breakdown of the activated complex will be in the direction of product formation rather than back to the reactants), k_B is the Boltzmann constant (the gas constant per molecule), h is Planck's constant and $K^{\ddagger}$ is the equilibrium constant for the equilibrium between the activated complex and the un-activated molecules. It must be noted that the transition coefficient κ, is often omitted on the assumption that it is equal to unity[6].

Applying the usual thermodynamic equations to this equilibrium gives:

$$\Delta G^{\ddagger} = \Delta H^{\ddagger} - T\Delta S^{\ddagger} = -RT \ln K^{\ddagger} \qquad \textbf{Equation 1.7}$$

Substituting in Equation 1.6 yields the Eyring Equation[7]:

$$k_r = \frac{k_B T}{h} \cdot e^{-\Delta G^{\ddagger}/RT} = \frac{k_B T}{h} \cdot e^{-\Delta H^{\ddagger}/RT} \cdot e^{-\Delta S^{\ddagger}/R} \qquad \textbf{Equation 1.8}$$

where $\Delta G^{\ddagger}$, $\Delta H^{\ddagger}$ and $\Delta S^{\ddagger}$ represent the change in free energy, the change in enthalpy and the change in entropy for the activation, respectively.

Assuming that $\Delta S^{\ddagger}$ does not vary with temperature (this statement may be validated by examination of an Eyring Plot, which yields $\Delta S^{\ddagger}$ as the y-intercept), the temperature coefficient of the rate constant can be derived by taking logarithms and differentiating to give:

$$\frac{d \ln k_r}{dT} = \frac{1}{T} + \frac{\Delta H^{\ddagger}}{RT^2} = \frac{\Delta H^{\ddagger} + RT}{RT^2} \qquad \textbf{Equation 1.9}$$

Comparison of the Equation 1.9 with the empirical Arrhenius Equation suggests that the energy of activation as defined by Arrhenius Theory and the change in the enthalpy of activation defined by Transition State Theory can be related as:

$$E_a = \Delta H^{\ddagger} + RT \qquad \textbf{Equation 1.10}$$

Whatever the shortcomings the Arrhenius Equation has in its description of the effect of temperature on the rate of a reaction, it does afford a very close approximation to true behaviour. Equation 1.4 predicts that a plot of the logarithm of the rate constant ($\ln k_r$) against the reciprocal of the absolute temperature (T^{-1}) should be a straight line (Figure 1.1A). The slope of the line yields E_a, which is turn can be related through Equation 1.10 to provide a fair estimation of $\Delta H^{\ddagger}$.

A more accurate estimate of $\Delta H^{\ddagger}$ can be calculated using an Eyring Plot as this does not have a temperature factor in the intercept. The slope of a plot of the logarithm of the rate constant divided by the absolute temperature ($\ln k_r/T$) against the reciprocal of the absolute temperature (T^{-1}) directly yields $\Delta H^{\ddagger}$ (see Figure 1.1B). The entropy of activation, $\Delta S^{\ddagger}$, can also be calculated from the y-axis

ordinate, therefore providing the means (via Equation 1.7) to calculate the free energy of the activation, $\Delta G^{\ddagger}$.

When the logarithm of k_r (or k_r/T in the case of an Eyring Plot) is plotted against the reciprocal of the absolute temperature (T^{-1}), a single straight line is not always obtained. In a number of cases, the graph has a discontinuity of slope and approximates to two straight lines meeting at an angle[5]. This indicates that there is a change from one value of E_a (or $\Delta H^{\ddagger}$) to another at the transition temperature. A number of explanations for such discontinuities have been suggested, such a phase change in the solvent [8,9,10], two parallel reactions with different temperature coefficients or an overall process involving two successive reactions with different temperature coefficients[11]. However, the most common cause of deviation from linearity is due to the effect of temperature on the conformation of the enzyme itself, a phenomenon that may be looked upon as simply that the enzyme exists in two (or more) forms which transform reversibly or irreversibly into one another and which differ in their catalytic activities[12].

A)

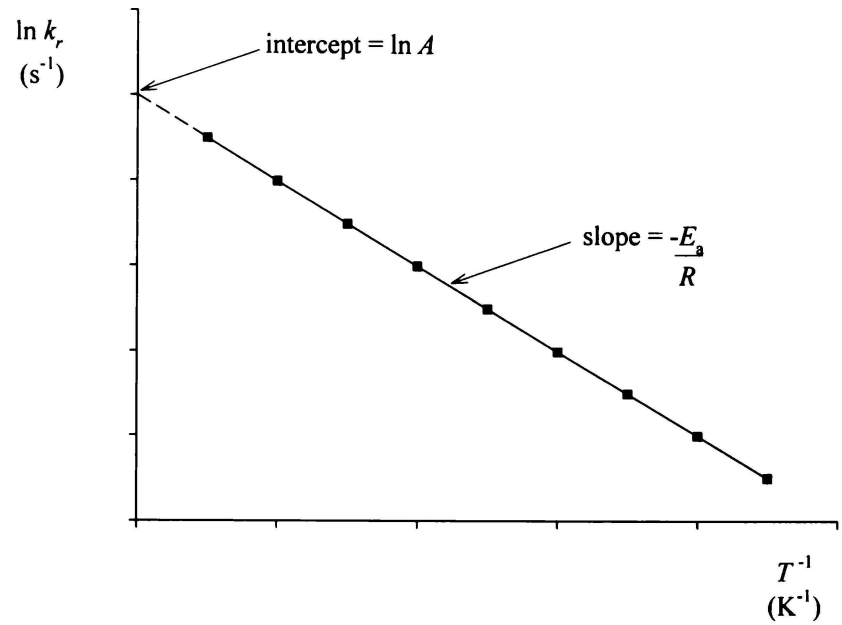

B)

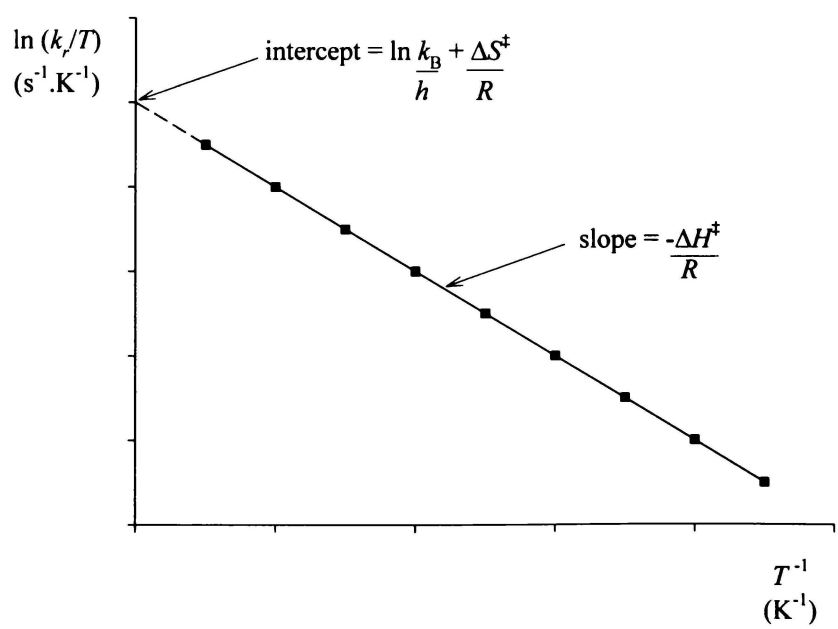

Figure 1.1 The effect of temperature on enzyme reaction velocity

Represented by **A)** an Arrhenius Plot of the natural log of the reaction rate constant (ln k_r) versus the reciprocal of the absolute temperature (T^{-1}); and **B)** an Eyring Plot of the natural log of the reaction rate constant divided by the absolute temperature (ln k_r/T) against the reciprocal of the absolute temperature (T^{-1})

1.3 The Effect of Temperature on the Conformational Integrity of an Enzyme

As the assay temperature is increased, the increase in catalytic rate is offset by the increasing rate of thermal denaturation of the protein, resulting in less functional enzyme present, and hence a decrease in observed catalytic rate. The extent of denaturation will depend on the thermal stability of the enzyme, assay temperature, assay duration, and on factors such as buffer composition and the degree of stabilisation of the enzyme by substrates, co-factors and other assay components.

In spite of the potential complications these factors may place on the mechanism of thermal denaturation, in terms of function (active cf. inactive), denaturation can be considered a two-step process. The first step is a reversible conformational change to a partially folded state. This is followed by further modifications to produce a completely and, under most assay conditions, irreversibly unfolded state. This process can be represented by:

$$N \leftrightarrows I \rightarrow D \qquad \textbf{Equation 1.11}$$

where N represents the native, catalytically active enzyme, I represents intermediate forms that are partially denatured but which rapidly interchange with the native form and D represents the denatured polypeptide, which can no longer refold but will likely then form aggregates.

Under normal conditions, the native catalytically active structure of an enzyme is only marginally stable. The conformational stability of a protein, defined as the difference in free energy between the folded and unfolded states, is the sum of a

large number of weak, non-covalent interactions (namely, hydrogen bonding, hydrophobic interactions, salt bridging and van der Waals interactions) and the destabilising forces that arise largely from conformational entropy[13].

In an "average" protein, the sum of the stabilising forces is large (approximately 1 $MJ \cdot mol^{-1}$) as is the sum of the destabilising forces, although the difference between the two is only of the order of 40 $kJ \cdot mol^{-1}$. A single weak interaction may only contribute up to 25 $kJ \cdot mol^{-1}$, therefore small changes in the number or strength of the stabilising interactions can have a major effect on the overall stability of the protein molecule[14]. An increase in temperature, for example, will instigate such changes and the protein macromolecule will begin to unfold, acquiring a less ordered conformation.

1.3.1 Reversible Thermal Inactivation

The first step in enzyme thermal denaturation is the partial unfolding of the protein molecule. As the environment of a small, single domain protein is gradually altered toward conditions that favour unfolding, the folded conformation initially changes very little, if at all[15]. There may be increases in flexibility and localised conformational alterations, but the average structure of the protein is unchanged.

If the temperature continues to increase, some of the co-operative hydrogen bonds that stabilise the helical structure will begin to break. This point in the process of enzyme thermal denaturation indicates the conversion of partially unfolded intermediate forms to a completely unfolded polypeptide, a process that occurs within a limited temperature range.

1.3.2 Irreversible Thermal Inactivation

1.3.2.1 Aggregation

The unfolding of most small proteins is reversible, and equilibrium can be attained. However, under most assay conditions, as the polypeptide completely unfolds, a number of new interactions generally occur resulting in irreversible aggregation of the protein. Water can form new hydrogen bonds with the amide nitrogen and carbonyl oxygen's of the peptide bonds. The presence of water further weakens nearby hydrogen bonds by causing an increase in the local effective dielectric constant. In addition, hydrophobic groups previously located in the interior of the protein molecule are exposed to the solvent. Such exposure is thermodynamically unfavourable, therefore the net result will be an attempt by the protein to minimise its free energy by burying as many hydrophobic groups while exposing as many polar groups as possible to the solvent. While this is analogous to what occurred when the protein folded originally, it is happening at a much higher temperature. This attempt by the protein, along with the expected decrease in the number and strength of stabilising interactions and the increase in the conformational entropy of the protein molecule as the temperature rises, dictates that the structures that form will be vastly different from the conformation of the native protein.

Upon cooling, the structures formed by the aggregated proteins may not be those of the lowest free energy but kinetic barriers prevent spontaneous refolding to the protein's native conformation. Any attempt to return to the native structure would first require that the hydrophobic interactions that caused the aggregation be broken. Directed by the energy of short-range interactions, the protein could

begin to refold, however, the exposure of such a large number of hydrophobic groups to the solvent presents a large energy barrier that makes such a refolding kinetically unlikely.

1.3.2.2 Degradation

In addition to denaturation made irreversible by the formation of aggregates, irreversible degradative processes can lead to enzyme inactivation[16, 17]. It must be noted that over the time spans considered here (minutes to hours), and at neutral pH, such degradation is only significant above 80°C[13].

In contrast to denaturation, the irreversible process of protein degradation arises from changes in covalent bonding. Deamidation of the amide side chain of asparagine and glutamine residues, succinimide formation at glutamic acid and aspartic acid residues, and oxidation of histidine, methionine, cysteine, tryptophan and tyrosine residues are the most facile and common amino acid degradations. These mechanisms of protein degradation are greatly accelerated at high temperatures, and can thus play an important role in the thermo-inactivation of enzymes[13].

1.4 Enzyme "Temperature Optima"

Thermal denaturation that then leads on to aggregation and/or protein degradative processes, and is hence irreversible, has been assumed to be solely responsible for the decrease in enzyme reaction velocity above the "temperature optimum" – the temperature at which, under a given set of conditions, maximum product is formed within a given time period. If this were the only reason for the observed loss of enzyme activity at high temperatures then, the shorter the assay duration, the higher the "temperature optimum".

As described in the preceding sections, the two established thermal parameters for the characterisation of enzymes are the Arrhenius activation energy, which describes the way enzyme reaction velocity varies with temperature, and the thermal stability of the enzyme, which is an indication of the capacity an enzyme has in maintaining its conformational integrity as temperature increases.

A graph of "enzyme activity versus temperature" is commonly presented to show the temperature optimum (T_{opt}) of an enzyme-catalysed reaction (Figure 1.2). However, as an intrinsic property of an enzyme, the temperature optimum has been regarded as a discredited concept[18, 19].

This apparent temperature optimum arises from an unknown combination of the thermal stability and the temperature coefficient of the reaction (as defined by the Arrhenius activation energy), and is dependent on assay duration – the contribution of denaturation is time dependent as well as temperature dependent, so the apparent optimum is shifted to lower temperatures for longer assays.

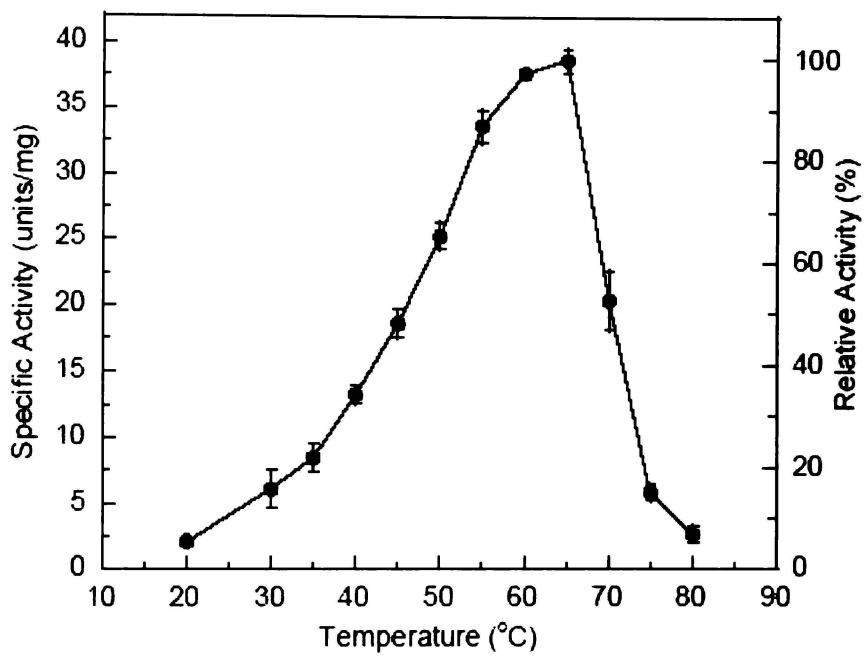

Figure 1.2 A typical graphical representation of the "temperature optimum" of an enzyme.

Reproduced from Wu *et al* (2004)[20].

In this situation, termed the 'Classical Model'[21], the variation in enzyme activity with temperature and assay duration can be described as follows:

$$V_{\max} = k_{cat} \cdot [E_0] \cdot e^{-k_{inact} \cdot t} \qquad \textbf{Equation 1.12}$$

where V_{max} = maximum velocity of the enzyme; k_{cat} = the enzyme's catalytic constant; $[E_0]$ = total concentration of enzyme; k_{inact} = thermal inactivation rate constant; t = assay duration.

The variation of the two rate constants in Equation 1.12 with temperature is given by:

$$k_{cat} = \frac{k_B T}{h} \cdot e^{-\Delta G^{\ddagger}_{cat}/RT} \qquad \textbf{Equation 1.13}$$

and

$$k_{inact} = \frac{k_B T}{h} \cdot e^{-\Delta G^{\ddagger}_{inact}/RT} \qquad \textbf{Equation 1.14}$$

where k_B = Boltzmann's constant; R = universal gas constant; T = absolute temperature; h = Planck's constant; $\Delta G^{\ddagger}_{cat}$ = Gibb's free energy of activation of the catalysed reaction; and $\Delta G^{\ddagger}_{inact}$ = Gibb's free energy of inactivation of the thermal inactivation process.

The variation in enzyme activity, in accordance with the effect of temperature and time on the rate constants k_{cat} and k_{inact}, is displayed graphically in Figure 1.3, where it can be seen that the apparent T_{opt} decreases with increasing assay duration, but at zero time (i.e. under initial rate conditions), no temperature optimum exists.

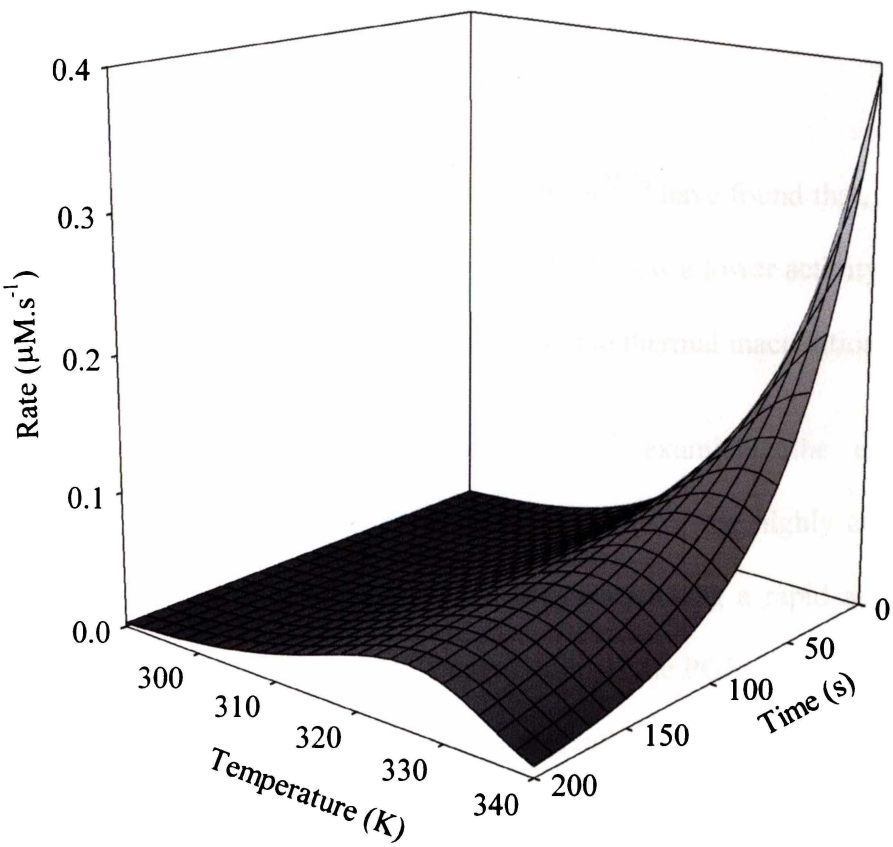

Figure 1.3 The effect of temperature on enzyme activity - the 'Classical Model'[21].

The variation of enzyme activity with temperature (290-340 K) and time during the assay (0-200 s) was simulated using Equations 1.11 – 1.13. The following parameter values were used: $\Delta G^{\ddagger}_{cat}$ = 80 kJ·mol^{-1}; $\Delta G^{\ddagger}_{inact}$ = 95 kJ·mol^{-1}; total enzyme concentration = 100 nM.

Disappointingly, this "temperature optimum" of an enzyme continues to be occasionally reported, where there is no mention of the use of initial rates nor is there any mention of assay duration in either the text or the figure captions for the determination.

A number of recent studies published on this subject[22-26] have found that, at some point in the temperature profile, the enzymes studied show a lower activity at high temperatures than can be accounted for by irreversible thermal inactivation.

The first in-depth study into this phenomenon[25] examined the effect of temperature on the kinetic parameters for three isolates of the highly conserved monomeric enzyme 3-phosphoglycerate kinase (PGK), using a rapid automated kinetics apparatus. Irreversible thermal denaturation of the PGK proteins was also investigated, in both the presence and absence of substrates. PGK was purified from the thermophilic bacterium *Thermoanaerobacter sp.* Rt8.G4 (optimum growth temperature 68°C), the mesophile *Zymomonas mobilis* (optimum growth temperature 32°C) and an unidentified soil mesophile designated *unid A* (optimum growth temperature 27°C). A comparison of the irreversible denaturation rates in the presence of substrate and the temperatures at which the PGK activities began to decline indicated that irreversible denaturation did not account for the observed reduction in activity. The rates of thermal inactivation observed indicate that irreversible denaturation would not make a significant contribution to the decrease in enzyme activity above the temperature optimum until about 66-67°C for *unid A* PGK, 73°C for *Z. mobilis* PGK and 82-83°C for *Thermoanaerobacter* PGK. (cf. temperature optima of 53°C, 63°C and 70°C, respectively). Based on these observations, the authors' postulate that another process must be occurring before

irreversible denaturation becomes the dominant detrimental influence on enzyme activity. A number of explanations for this behaviour are offered: that the overall decrease in catalytic rate may be due to the reversible temperature-mediated conversion of protein molecules to, what is likely to be, a catalytically inactive intermediate form; that the loss of activity at high temperatures relates to the hinge-bending mechanism of PGK catalysis, where as temperature increases, the conformational inter-conversions become too rapid for catalysis to occur efficiently; or, that the reduction in catalytic rate is due to localised unfolding of the protein active site. Additionally, the authors address potential failures in their experiment procedures, which may be consequent to the results observed.

In a study examining the relationship between the concepts of thermoactivity and thermostability[23], site-directed mutants of the homo-dimeric enzyme, citrate synthase, were constructed and analysed. Three sets of mutants were made: chimeric mutants where the large (inter-subunit contact) and small (catalytic) domains of *Thermoplasma acidophilum* (optimal growth temperature at 55°C) and *Pyrococcus furiosus* (optimal growth temperature at 100°C) enzymes were swapped; mutants of the *P. furiosus* citrate synthase where the inter-subunit ionic network is disrupted; and *P. furiosus* citrate synthase mutants in which the C-terminal arms that wrap around their partner subunits have been deleted. In each case, thermostability was assessed through rates of thermal inactivation, and thermoactivity via the determination of their kinetic parameters. The data for thermostability of the chimeric mutants indicated that the large domain is the main determinant of the enzyme's thermostable properties. The small, flexible, catalytic domain of the *Thermoplasma* enzyme did not confer any significant loss of thermostability when incorporated into the *Pyrococcus* enzyme, and

conversely, the small domain of the *Pyrococcus* enzyme did not increase the thermostability of the less stable *Thermoplasma* enzyme. However, a comparison of the thermal inactivation data with the dependence of catalytic activity on the temperature of the assay shows that the small domain critically influences the enzyme's catalytic properties. In the case of the wild-type *Thermoplasma* enzyme, less than 5% of the activity was lost at 85°C. However, the temperature optimum was 75°C, with the activity at 85°C being approximately 50% less than that at the optimum. Additionally, when the small catalytic domain from the *Thermoplasma* citrate synthase is combined with the *Pyrococcus* large domain, the thermostability of the whole protein is enhanced (k_{inact} = 0.017 min^{-1} at 85°C) with respect to the wild-type *Thermoplasma* enzyme (k_{inact} = 0.049 min^{-1} at 85°C), but the temperature optimum (at 75°C) remains the same. The authors postulate that this is a clear demonstration of the partial independence of thermostability and thermoactivity, which has also been reported for mesophilic and thermophilic phosphoglycerate kinases[25] (see discussion above) and for a hyperthermophilic 2-keto-3-deoxygluconate aldolase[24].

In the study by Medina *et al*[22], the effect of temperature on the initial velocity kinetics of allosteric ATP sulfurylase from *Pencillium chrysogenum* was examined. The experiments were prompted by the structural similarity between the C-terminal regulatory domain of fungal ATP sulfurylase and fungal APS kinase, a homodimer that undergoes a reversible, temperature-dependent dissociation of subunits over a narrow temperature range[27].

Initial velocity versus temperatures profiles generated were reminiscent of temperature optimum plots often observed in fixed time assays, where the

descending limb usually is the consequence of irreversible enzyme denaturation. However, in this case, the loss of activity at what is effectively "zero time" is due structural changes that result in an increase in the allosteric constant, promoting transition to the low substrate affinity/high allosteric inhibitor affinity state. Further experiments show that this loss of activity is completely reversible between 37°C and 45°C, a temperature range in which *P. chrysogenum* can survive for extended periods of time but grows poorly if at all. Additionally, it was shown that as the concentration of substrate was increased, the position of the temperature optimum was shifted to higher temperatures, consistent with previous experiments that indicate that the substrate stabilises the high substrate affinity/low allosteric inhibitor affinity state. The authors postulate that this phenomenon may play a role in cellular energy conservation at high temperatures when intracellular ATP is low and the cells have no need for sulphur amino acids.

To describe these "real" temperature optimum, the 'Equilibrium Model'[21] was formulated to account for the anomalies found in the variation of enzyme activity with temperature described in the studies discussed above.

The 'Equilibrium Model' proposes that the active form of the enzyme (E_{act}) is in equilibrium with an inactive form (E_{inact}) and it is the inactive form that undergoes irreversible thermal inactivation to the thermally denatured state (X; Equation 1.15):

$$E_{act} \leftrightarrows E_{inact} \rightarrow X \qquad \textbf{Equation 1.15}$$

In this situation, the dependence of enzyme activity on temperature has an additional component – the effect of temperature on the equilibrium position between the active and inactive forms of the enzyme (Equation 1.16):

$$V_{\max} = k_{cat} \cdot [E_{act}] \qquad \textbf{Equation 1.16}$$

where the dependence of k_{cat} on temperature remains as defined in Equation 1.12, but the concentration of active enzyme at any time point is defined by:

$$[E_{act}] = \frac{[E_0] - [X]}{1 + K_{eq}} \qquad \textbf{Equation 1.17}$$

where K_{eq} is the equilibrium constant between active and inactive forms of the enzyme (K_{eq} = [E_{inact}] / [E_{act}]), and the rate of appearance of X is given by Equation 1.16 as:

$$\frac{d[X]}{dt} = k_{inact}\{[E_0] - [E_{act}] - [X]\} \qquad \textbf{Equation 1.18}$$

The variation in K_{eq} with temperature is given by:

$$\ln K_{eq} = \frac{\Delta H_{eq}}{R}\left[\frac{1}{T_{eq}} - \frac{1}{T}\right] \qquad \textbf{Equation 1.19}$$

where ΔH_{eq} is the enthalpic change associated with the conversion of active to inactive enzyme, and T_{eq} is the temperature at which the E_{act} and E_{inact} are in equilibrium (i.e. the temperature at which $K_{eq} = 1$).

The variation of enzymic rate with temperature and time according to the 'Equilibrium Model' is shown in Figure 1.4, where it is clearly illustrated that there is an initial rate temperature optimum that is obviously independent of assay duration. Depending on the value of T_{eq} with respect to the temperatures at which significant inactivation is observed during the time course of the assay, there is a much smaller change in the apparent temperature optimum with time in the 'Equilibrium Model' than in the 'Classical Model' (Figure 1.4). Additionally, the

'Equilibrium Model' provides a "thermal buffer" that protects the enzyme from thermal inactivation, allowing enzyme activity to be maintained at a reasonably constant value with regards to time.

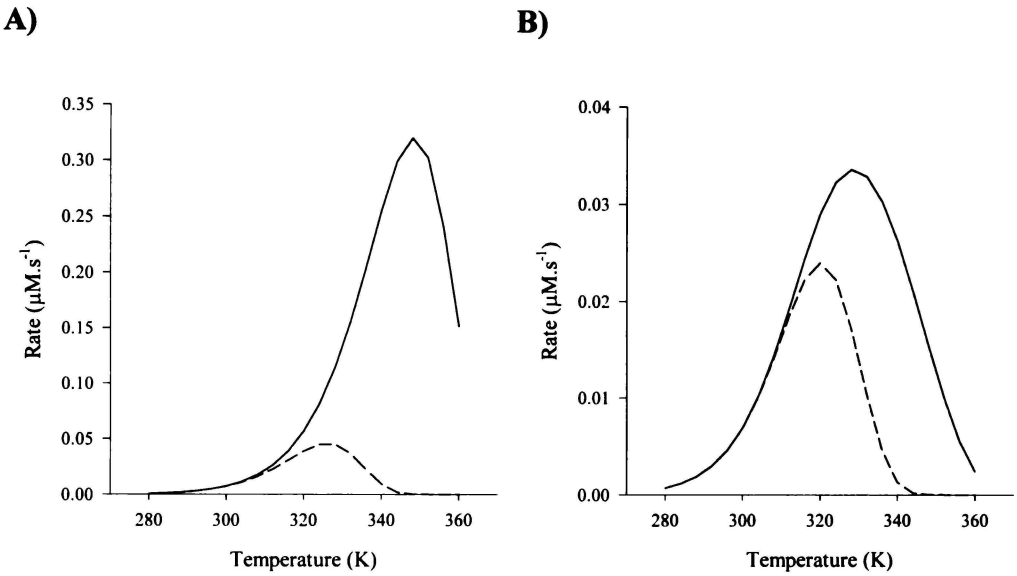

Figure 1.4 The effect of time on the position of the apparent temperature optimum and on the magnitude of enzyme activity.

According to **A**) the 'Classical Model' at an assay duration of 20 seconds (solid line) and of 200 seconds (dashed line), simulated using the following parameter values: $\Delta G^{\ddagger}_{cat}$ = 80 kJ·mol^{-1}; $\Delta G^{\ddagger}_{inact}$ = 95 kJ·mol^{-1}; total enzyme concentration = 100 nM.; and **B**) the 'Equilibrium Model' at an assay duration of 20 seconds (solid line) and of 200 seconds (dashed line), simulated using the following parameter values: $\Delta G^{\ddagger}_{cat}$ = 80 kJ·mol^{-1}; $\Delta G^{\ddagger}_{inact}$ = 95 kJ·mol^{-1}; total enzyme concentration = 100 nM; ΔH_{eq} = 100 kJ·mol^{-1}; T_{eq} = 320 K.

This zero time temperature optimum and its associated "thermal buffering" effect is seen even if the 'Equilibrium Model' is generalised to allow for the possibility

of E_{act} also undergoing thermal denaturation. If, for example, both E_{act} and E_{inact} lose activity irreversibly, each with a rate constant equal to k_{inact}, the rate-temperature-time profile looks much like that depicted in Figure 1.5. At the lower range of temperatures, the generalised Model gives somewhat lower catalytic rates, but at higher temperatures most of the enzyme is in the inactive state, and the two plots are virtually identical.

To detect a true temperature optimum, stability must be determined under the same conditions as activity (i.e. in the presence of substrates and any cofactors, and ideally at comparable protein concentrations) and, because the effects are not necessarily large, careful attention must be paid to the statistical errors of both determinations. However, it has been shown that simulated progress curves for an enzyme-catalysed reaction (concentration of product formed with time) generated by the 'Equilibrium Model' at a series of temperatures, cannot be fitted to the 'Classical Model', nor vice versa. Therefore, an experimental distinction can be made as to which of the Models any particular enzyme fits simply by collecting such progress curves at a variety of temperatures, thereby obviating the need to perform separate activity and stability measurements.

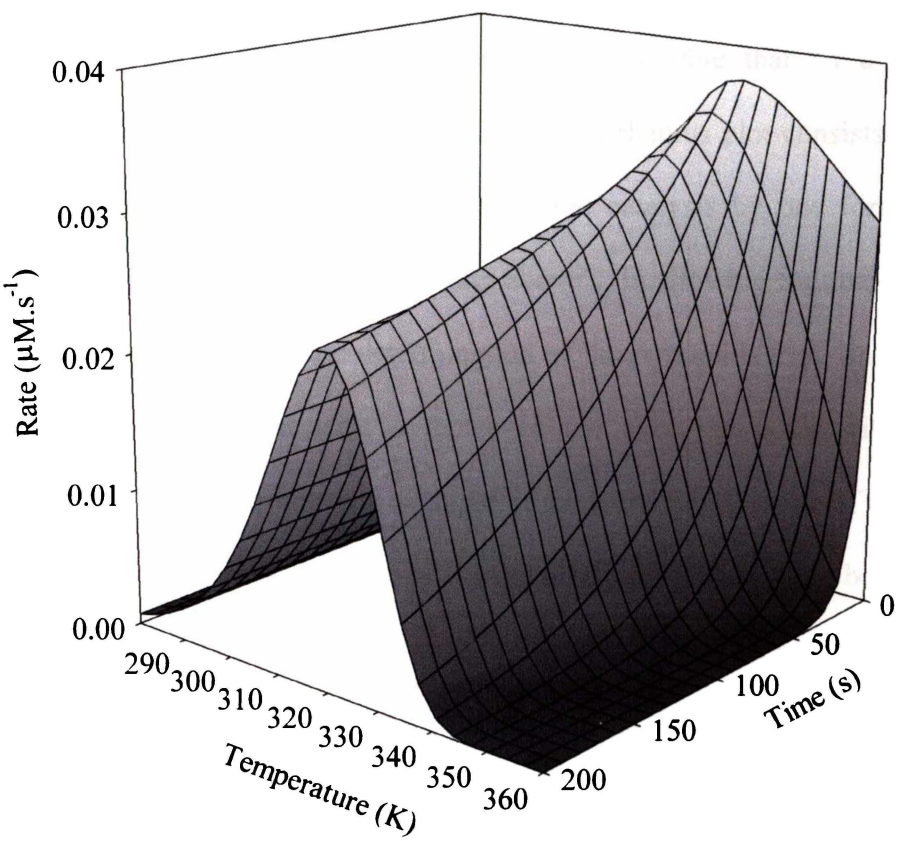

Figure 1.5 The effect of temperature on enzyme activity – the 'Equilibrium Model'[21].

The variation of enzyme activity with temperature (280-360 K) and time during the assay (0-200 s) was simulated using equations 1.14 – 1.18. The following parameter values were used: $\Delta G^{\ddagger}_{cat}$ = 80 kJ·mol^{-1}; $\Delta G^{\ddagger}_{inact}$ = 95 kJ·mol^{-1}; total enzyme concentration = 100 nM; ΔH_{eq} = 100 kJ·mol^{-1}; T_{eq} = 320 K.

Although, the Model presented above is novel (and of potentially superior technical use), the concept of reversible enzyme inactivation is not a new one.

Kistiakowsky and Lumry[12] proposed "the possibility that an enzyme may exist in two (or more) forms which transform reversibly or irreversibly into one another and which differ in their catalytic activities". They state that "if a mobile equilibrium exists between the two forms and the Arrhenius plot consists of two straight segments with a bend between them, the catalysis by one form must predominate below the bend, that by another above". In allowing for unavoidable experimental uncertainties in the determination of the Arrhenius Plot, this means that one rate must gain at least a factor of ten over the other within the temperature range of the bend. For example, if the temperature range of the bend was only over two degrees, the heat of the equilibrium reaction must be at least 200,000 calories per mole and the entropy change (if the specific activities of the two forms are comparable, so that at the temperature of the bend they are present in comparable concentrations) at least 700 entropy units.

Sizer[28] obtained parameters for the activation and thermal inactivation processes of catalase from the slopes of the (approximately) linear portions of Arrhenius Plots (logarithm of rate versus the inverse of absolute temperature). The data for these plots were obtained from initial rates, and so were effectively at zero time. Sizer was able to get reasonable parameter estimates and found that "the activation energy for the heat inactivation of catalase below 62°C is found to be 55,000 calories, and the entropy of activation is +90 calories" and "between 62-68°C the corresponding values are 255,000 and +690 calories for the energy and entropy of activation, respectively, of heat inactivation of catalase"[28]. This

observation is consistent with the proposal by Kistiakowsky and Lumry[12], and given that the data was essentially at zero time, indicates that the enzyme exists in at least two forms in equilibrium with each other. However, a model was not proposed to account for these observations.

Keith Laidler's text, "The Chemical Kinetics of Enzyme Action"[29] also addresses the problem of enzyme deactivation, and proposes several alternative mechanisms, one of which, from a paper by Wright and Schomaker[30], bears some similarity to the 'Equilibrium Model'. Wright and Schomaker studied the inactivation of diphtheria antitoxin by heat (as well as by pH and urea) and found that "the course of the reaction deviates from the typical behaviour of a first-order reaction, the specific rate of inactivation decreasing as the reaction proceeds so as to produce a strong deviation from linearity of the log activity vs. time plots". To account for this, they used the concept that a "molecule may undergo denaturation in a number of ways; that some may involve an unfolding of the antibody region, with consequent inactivation, while others may not; and that reactions of this second type can lead reversibly to a product which retains its activity but is not susceptible to the inactivation by the first type of reaction"[31].

They proposed the following model:

$$P \leftrightarrows N \rightarrow I \qquad \textbf{Equation 1.20}$$

where P is a postulated active "protected" antibody, N is the native antibody, and I is the irreversibly inactivated antibody. Using kinetic analysis, they showed that their data, which were effectively progress curves of inactivation, fitted this model. They also recognised that the model provided a reservoir of native antibody during a significant fraction of the time course. However, their model

differs from the 'Equilibrium Model' in that it assumes that the "activity" (which is based on a bioassay) is independent of temperature. Also, extrapolating from antibody to enzyme, both P and N are active, which also differs from the 'Equilibrium Model', where the equivalent forms of the protein are active enzyme (E_{act}) and an inactive (or less active) form (E_{inact}).

Sizer's analysis, as modelled by Bailey and Ollis[32] and Cornish-Bowden[33], is time-independent and only addresses the variation of the observed catalytic rate constant with temperature, total (potentially) active enzyme remaining constant. Wright and Schomaker's[31] analysis allows total active protein (in their case, antibody) to decrease with time, but assumes implicitly that the "activity" does not vary with temperature. The 'Equilibrium Model' makes neither assumption (although it does make the implicit assumption that the equilibrium between E_{act} and E_{inact} is rapid compared with the catalytic reaction and the thermal denaturation). The 'Equilibrium Model' therefore differs qualitatively from both although the underlying theory remains the same.

It has been suggested[34] that the mechanism on which the 'Equilibrium Model' is based (Equation 1.14) is not an entirely new concept and is the same as the autolysis model of Henley and Sadana[35] and that Ahern and Klibanov[16] have applied this mechanism to the thermal denaturation of lysozyme.

Henley and Sadana's autolysis model[35] is based on the observation that some proteolytic enzymes will hydrolyse inactivated enzymes of their own type. This is more likely to occur when some of the enzyme is denatured, thus losing the resistance to autolysis inherent in the native form. Kawamura *et al*[36] have proposed a model based on the existence of a single active form; thus activity is

simply given by [E]/ $[E]_0$. Their proposed mechanism consists of two reactions. The first reaction, and the only one evident at low protease concentrations, is a monomolecular series deactivation:

$$E_a \overset{K}{\leftrightarrows} E_i \overset{k_1}{\rightarrow} E' \qquad \textbf{Equation 1.21}$$

where $K = [E_i/E_a]$, k_1 is the denaturation constant, E_a and E_i are the active and inactive forms, and E′ is the denatured form (random coil).

However, at higher enzyme concentrations, a second reaction becomes more evident due to the higher order of the first step. It is assumed that the reversibly inactivated form is the one that is acted upon by the protease:

$$E_a + E_i \overset{K_m}{\leftrightarrows} E_aE_i \overset{k_2}{\rightarrow} E_a + P \qquad \textbf{Equation 1.22}$$

where $K_m = [E_a]\cdot[E_i]/[E_aE_i]$, k_2 is the digestion constant and P represents the decomposed products.

While the deactivation mechanism evident at low protease concentration shows similarities to that proposed by the 'Equilibrium Model', the mechanism applied by the 'Equilibrium Model' differs as it retains its validity across the range of enzyme concentrations. Additionally, the assumption that the reversibly inactivated form of the enzyme is the one that is acted upon by the protease is probably incorrect, given that, while it is well known that denatured proteins are particularly susceptible to proteolysis[37], increased temperature will also increase the susceptibility of a protein to proteolytic attack in its undenatured, active state[38].

In the study by Ahern and Klibanov[16], the focus was on the pathways and mechanisms of irreversible thermo-inactivation (covalent processes) rather than reversible temperature-induced conformational transitions and they did not propose a model to account for their observations.

In the article by Patnaik[34], the author states that the 'Equilibrium Model' "too has some drawbacks" in that "at short assay times, there are two peaks on the rate-temperature-time surface", illustrated in the paper by re-orienting the 'Equilibrium Model' figure, to show the back of the plot (Figure 1.5). He states, "while there is a peak at the transition temperatures, the surface twists eccentrically beyond this temperature" and that "this twist generates additional local maxima for short assay times ($t < 50s$)." Examination of this plot in this orientation shows what could be mistaken for "two peaks", but at any given assay duration only one maximum exists. It must be emphasised that the shift in the position of the peak with increasing assay duration is due to the contribution of thermal inactivation and that the point of the original paper was to illustrate the presence of a temperature optima at *zero time*, where no thermal inactivation can have taken place.

The author suggests, "this problem disappears on increasing the order of the irreversible step from one to two, suggesting that a second-order equilibrium model may be appropriate for some thermal inactivations". The basis for the proposal of the second-order model is that "a rapid assay, which is desirable, may have to span a wider range of temperature so as to strike the global maximum in a multi-peak domain. A slow assay avoids this problem but carries greater risk of denaturation". One of the main features of the 'Equilibrium Model' is the presence of a "zero time" temperature optimum that is independent of assay

duration. Therefore, it does not matter how "rapid" the assay is, as long as initial rates are determined. Additionally, temperature optima determinations, however they are performed, generally span a wide temperature range. These two points invalidate Patnaik's criticism of the 'Equilibrium Model'.

The comment that "the presence of two optima is itself an unusual feature and raises doubts about the validity of the mass action kinetics inherent in the 'Equilibrium Model' has resulted in a misguided attempt to propose a model that gives only one temperature optimum, irrespective of the length of the assay[34].

It must be noted, that Patnaik's version of the 'Equilibrium Model' 1st-order equation is erroneous (attempts to simulate the equation proposed were unsuccessful). Additionally, the author managed to reproduce graphs for the 'Classical' and 'Equilibrium Model' from the original paper[21] that were mistakenly altered in proof by the publisher and thus published incorrectly (for which an amendment was published in a subsequent issue[39]) indicating that both his analysis and attempted rebuttal of the 'Equilibrium Model' are flawed.

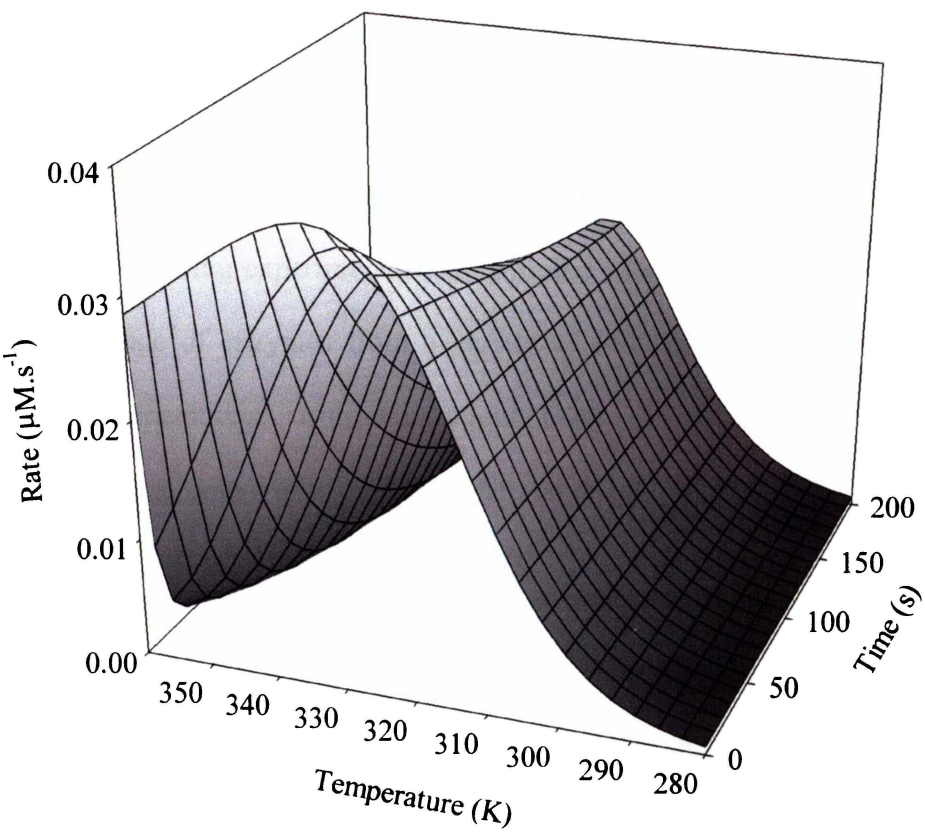

Figure 1.6 The re-oriented 'Equilibrium Model' figure

This figure is oriented as per Patnaik's paper[34], but simulated correctly as per the paper by Daniel *et al*[21].

1.5 Thesis Objectives

Daniel *et al*[21] have proposed the concept of real temperature optima for enzymes, and the means to distinguish this phenomenon from cases of apparent optima in which protein instability is a major factor in the temperature-dependence of enzyme activity.

This project has the following objectives to fulfil:

a) determine the validity of the concept of true temperature optima by comparing experimental data with the Models. The aim is to assay a range of enzymes from a variety of sources for activity at different temperatures, using continuous assays to allow the simultaneous measurement of activity and thermal stability in the same cuvette.

b) describe completely the data collection and analysis process for determining T_{eq}, and extend the data collection and analysis process to a range of enzymes and assay systems. The collection of experimental data has the potential to be complicated by a number of factors coincident with increasing the temperature of an enzyme assay.

c) investigate the molecular basis of the temperature-dependent interconversion of the active and inactive forms of the enzyme. It is likely that the equilibrium mechanism involves local rather than global conformational changes.

d) examine the biotechnological implications of T_{eq}. If real temperature optima exist, there is the additional consideration for the enzyme

engineer; for example, engineering an enzyme to operate at high temperatures might no longer be merely a question of creating a more stable variant: thermoactivity will need to be considered in addition to thermostability.

e) examine the evolutionary and ecological implications of T_{eq}. There is no evidence connecting the Arrhenius activation energy of an enzyme to its thermal environment, and we predict that T_{eq} will be a better expression of the effect of environmental temperature on the evolution of the enzyme than thermal stability.

1.6 References

1. Chang, R (1994) In *Chemistry*, 5th Edition, McGraw-Hill, Inc., New York.

2. Guldberg, C. M. & Waage, P. (1879) Über die chemische Affinität. *Journal für praktische Chemie*, **127**, 69 – 114.

3. Arrhenius, S. (1889) On the Reaction Velocity of the Inversion of Cane Sugar by Acids. *Zeitschrift für physikalische Chemie*, **4**, 226ff.

4. Kittel, C. & Kroemer, H. (1980) In *Thermal Physics*, 2nd Edition, Freeman & Co, New York.

5. Dixon, M. & Webb, E.C. (1979) In *Enzymes*, 3rd Edition (assisted by Thorne, C.J.R. & Tipton, K.F.), p 170, Longman Group Ltd, London.

6. Garcia-Viloca, M., Gao, J., Karplus, M. & Truhlar, D.G. (2004) How Enzymes Work: Analysis by Modern Rate Theory and Computer Simulations. *Science*, **303**, 186 – 195.

7. Eyring, H. (1935) The activated complex in chemical reactions. *Journal of Chemical Physics*, **3**,107 – 115.

8. Sizer, I.W. (1943) Effects of temperature on enzyme kinetics. *Advances in Enzymology*, **3**, 35 – 62.

9. Ladbrooke, B.D. & Chapman, D. (1969) Thermal analysis of lipids, proteins and biological membranes. A review and summary of some recent studies. *Chemistry and Physical Lipids*, **3**, 304 – 356.

10. Raison, J.K. (1973) Temperature-induced phase changes in membrane lipids and their influence on metabolic regulation. *Symposia of the Society for Experimental Biology*, **27**, 485 – 512.

11. Stearn, A.E. (1949) Kinetics of biological reactions with special references to enzymatic processes. *Advances in Enzymology*, **9**, 25 – 74.

12. Kistiakowsky, G.B. & Lumry, R. (1949) Anomalous Temperature Effects in the Hydrolysis of Urea by Urease. *Journal of the American Chemical Society*, **71**, 2006 – 2013.

13. Daniel, R.M. Dines, M. & Petach, H.H. (1996) The denaturation and degradation of stable enzymes at high temperatures. *Biochemical Journal*, **317**, 1 – 11.

14. Matthews, B.W. (1993) Structural and genetic analysis of protein stability. *Annual Review of Biochemistry*, **62**, 139 – 160.

15. Creighton, T.E. (1993) In *Proteins*, 2nd Edition, W.H. Freeman & Co, New York.

16. Ahern, T.J. & Klibanov, A.M. (1985) The mechanisms of irreversible enzyme inactivation at 100°C. *Science*, **228**, 1280 – 1283.

17. Zale, S.E. & Klibanov, A.M. (1986) Mechanisms of irreversible thermoinactivation of enzymes. *Biochemistry*, **25**, 5432 – 5444.

18. Cornish-Bowden, A. (1995) In *Fundamentals of Enzyme Kinetics*, pp 193 – 197, Portland Press Ltd, London, UK.

19. Daniel, R.M. & Danson, M.J. (2001) Assaying activity and assessing thermostability of hyperthermophilic enzymes. *Methods in Enzymology*, **334**, 283 – 293.

20. Wu, J., Patel, M.A., Sundaram, A.K. & Woodard, R.W. (2004) Functional and biochemical characterization of a recombinant Arabidopsis thaliana 3-deoxy-D-manno-octulosonic 8-phosphate synthase. *Biochemical Journal*, **381**,185 – 193.

21. Daniel, R.M., Danson, M.J. & Eisenthal, R. (2001) The temperature optima of enzymes: a new perspective on an old phenomenon. *Trends in Biochemical Sciences*, **26**(4), 223 – 225.

22. Medina, D.C., Hanna, E., MacRae, I.J., Fisher, A.J., & Segel, I.H. (2001) Temperature Effects on the Allosteric Transition of ATP Sulfurylase from *Penicillium chrysogenum*. *Archives of Biochemistry and Biophysics,* **393**(1), 51 – 60.

23. Arnott, M.A., Michael, R.A., Thompson, C.R., Hough, D.W. & Danson, M.J. (2000) Thermostability and Thermoactivity of Citrate Synthases from the Thermophilic and Hyperthermophilic Archaea. *Thermoplasma acidophilum* and *Pyrococcus furiosus, Journal of Molecular Biology*, **304**, 657 – 668.

24. Buchanan, C.L, Connaris, H., Danson, M.J., Reeve, C.D., & Hough, D.W. (1999) An extremely thermostable aldolase from *Sulfolobus solfataricus* with specificity for non-phosphorylated substrates. *Biochemical Journal*, **343**, 563 – 570.

25. Thomas, T.M. & Scopes, R.K. (1998) The effects of temperature on the kinetics and stability of mesophilic and thermophilic 3-phosphogylcerate kinases. *Biochemical Journal*, **330**, 1087 – 1095.

26. Gerike, U., Danson, M.J., Russell, N.J & Hough, D.W. (1997) Sequencing and expression of the gene encoding a cold-active citrate synthase from an Antarctic bacterium, strain DS2-3R. *European Journal of Biochemistry*, **248**, 49 – 57.

27. Renosto, F., Seubert, P.A., Knudson, P. & Segel, I.H. (1985) Adenosine 5'-phosphosulfate kinase from Penicillium chrysogenum. Determining ligand dissociation constants of binary and ternary complexes from the kinetics of enzyme inactivation. *Journal of Biological Chemistry*, **260**, 11903 – 11913.

28. Sizer, I.W. (1944) Temperature activation and inactivation of the crystalline catalase-hydrogen peroxide system. *Journal of Biological Chemistry*, **154**, 461 – 473.

29. Laidler, K.J. & Bunting, P.S. (1973) In *The Chemical Kinetics of Enzyme Action*, 2nd Ed., pp426, Clarendon Press, Oxford, UK.

30. Wright, G.G. & Schomaker, V. (1948) Studies on the Denaturation of Antibody III. Kinetic Aspects of the Inactivation of Diphtheria Antitoxin by Urea. *Journal of the American Chemical Society*, **70**, 356 – 364.

31. Wright, G. G. & Pauling, L. (1944) A note on the Serological Activity of Denatured Antibodies. *Science* **99**, 198 – 199.

32. Bailey, J.E. & Ollis, D.F. (1977) In *Biochemical Engineering Fundamentals*, pp132 – 134, McGraw-Hill, New York.

33. Cornish-Bowden, A. (1976) In *Principles of Enzyme Kinetics*, Butterworth's, London, UK.

34. Patnaik, P.R. (2002) Temperature optima of enzymes: sifting fact from fiction. *Enzyme and Microbial Technology*, **31**, 198 – 200.

35. Henley, J.P. & Sadana, A. (1986) Deactivation Theory. *Biotechnology and Bioengineering*, **28**, 1277 – 1285.

36. Kawamura, Y., Nakanishi, K., Matsuno, R. & Kamikubo, T. (1981) Stability of immobilized α-chymotrypsin. *Biotechnology and Bioengineering*, **23**, 1219 – 1236.

37. Anson, M.L. (1938) The Estimation of Pepsin, Trypsin, Papain and Cathepsin with Hemoglobin. *Journal of General Physiology*, **22**, 79.

38. Daniel, R.M., Cowan, D.A., Morgan, H.W. & Curran, M.P. (1982) A correlation between protein thermostability and resistance to proteolysis. *Biochemical Journal*, **207**, 641 – 644.

39. Erratum. *Trends in Biochemical Sciences*, Volume 26, Issue 6, 1 June 2001, Page 401.

Chapter Two

The Effect of Temperature on Enzyme Activity: Practical Considerations, Data Collection and Analysis

---

2.1 Introduction

The detection of reversible enzyme inactivation, which forms the basis for the theory of true temperature optima[1], is not entirely straightforward due to the number of conflicting influences that arise when increasing the temperature of an enzyme assay.

During the course of this project, it was established that there are a number of practical considerations that might easily be overlooked. This observation deemed it necessary to make a number of choices that ensured that the enzyme activity was readily measured and guaranteed that any decrease in activity observed is due solely to thermal inactivation and not some other process.

Therefore, this chapter seeks to:

a) emphasise "good assay practice" and to alert readers to possible pitfalls when measuring the temperature dependence of enzyme activity, and

b) clearly demonstrate exactly what and how data were collected and subsequently manipulated, with examples to illustrate.

2.2 Enzyme Selection

In attempting to select a range of enzymes from different sources (mammalian, bacterial etc), of different localisation (intracellular versus extracellular) and of varying subunits/molecular weight for testing the theory, there was a trend toward sampling oxidoreductases (EC 1.x.x.x) and hydrolases (EC 3.x.x.x).

Enzymes from these two groups generally have simple spectrophotometric assays that also fit the original criteria that were put in place, so that the detection of reversible enzyme inactivation of enzymes, and therefore the calculation of T_{eq}, was simplified.

The criteria were:

- *An enzyme reaction that can be continuously assayed*

  Following the reaction continuously produces progress curves (product produced versus time plots as related to absorbance decrease or increase) which provide an abundance of valuable information[2].

  Using continuous assays allows the measurement of activity versus time and of thermal inactivation all in the same cuvette, and therefore under identical conditions. It has been pointed out that difficulties in the past arise partly because thermostability and thermoactivity have been carried out in separate experiments, often under different conditions[1].

- *An enzyme that shows no product or substrate inhibition*

  If an enzyme experiences product inhibition, the observed decrease in activity due to denaturation will be simultaneously affected by the increase in product

concentration, resulting in an over-estimation of the extent of denaturation. In the case of substrate inhibition, a "lag-phase" will be observed, obscuring the true initial rate of the reaction.

- *A reaction that is essentially irreversible*

  The approach to reaction equilibrium is a common factor in the decrease of enzyme reaction velocity with time. As the reaction proceeds the contribution of the back reaction to the overall rate increases. To minimise this, the enzyme assay must be able to be run under conditions that shift the equilibrium of the reaction in the direction that favours product formation.

- *Operation at V_{max}*

  Operation at V_{max} ensures that the decrease in enzyme reaction velocity will be due to thermal inactivation and not substrate depletion. This is vital as the theoretical models hypothesised[1] assume that the enzyme remains saturated with substrate throughout the assay.

Initially, there were the additional criteria that the enzymes selected needed to be monomeric (avoiding complications due to subunit dissociation) and intracellular (avoiding the presence of oxidisable disulfide bonds; the chemical environment inside a typical cell is reducing[3, 4]). However, it appears that the models can be extended to cover cases of oligomeric enzymes where dissociation into monomers (reversible or otherwise) may be part of the thermal inactivation process/es (Danson, M.J. & Eisenthal, R. *pers. comm.*).

Because of these "rules", the other classes of enzymes (transferases, lyases, isomerases, and ligases) have been sampled less frequently when testing the 'Equilibrium Model', mainly due to factors such as a lack of a continuous spectrophotometric assay method, and substrate instability or substrate insolubility. There are, however, examples in the literature where a reversible thermal inactivation, independent of denaturation, has been observed for some representatives of these enzyme classes (Table 2.1).

Table 2.1 – Enzymes exhibiting reversible enzyme inactivation.

The list below details the enzymes examined by our laboratories and others (indicated by a reference) that have been shown to exhibit reversible enzyme inactivation. * indicates enzymes that show this phenomenon but that have not been fitted to the 'Equilibrium Model'.

E.C. Nº	Enzyme Name	Source
1.1.1.37	Malate dehydrogenase	*Bacillus cereus* ATCC 14579
		Escherichia coli (unknown strain)
		Bos taurus
		Thermus thermophilus ATCC 33923.
1.1.1.67	Mannitol dehydrogenase	*Pseudomonas fluorescens*
1.1.1.85	Isopropylmalate dehydrogenase	*Bacillus psychrophilus*
		Bacillus psychrosacchrolyticus
		Bacillus subtilis
		Bacillus thuringiensis

Table 2.1 continued – Enzymes exhibiting reversible enzyme inactivation

E.C. Nº	Enzyme	Source
1.1.1.85	Isopropylmalate dehydrogenase	*Bacillus caldovelox*
		LUB12 (inferred "ancestral gene" product)
		LUB18 (inferred "ancestral gene" product)
		LUB20 (inferred "ancestral gene" product)
1.4.1.3/4	Glutamate dehydrogenase	*Bos taurus*
		Candida utilis
		Thermococcus zilligii ATCC 700529
1.5.1.3	Dihydrofolate reductase	*Moritella profunda*
		Bacillus cereus ATCC 14579
		Escherichia coli ATCC 700928
		Geobacillus stearothermophilus DSM 13240
1.11.1.10	Chloroperoxidase*	*Caldariomyces fumago*
2.7.2.3	3-phosphoglycerate kinase*[5]	*Thermoanaerobacter sp.* Rt8 G4
		Zymomonas mobilus
		unid A (unidentified soil mesophile)
2.7.7.4	ATP sulfurylase*[6]	*Penicillium chrysogenum*
3.1.3.1	Alkaline phosphatase	Calf Intestinal muscosa
		Antarctic sea bacterium HK47
		Escherichia coli (unknown strain)
3.1.3.2	Acid phosphatase	Wheat germ
3.2.1.1	α-amylase	Porcine pancreas
3.5.1.13	Aryl acylamidase	*Pseudomonas fluorescens* ATCC 70095
3.5.2.6	β-lactamase	*Bacillus cereus*
3.5.4.4	Adenosine deaminase	Bovine spleen
4.1.2.20	KDG aldolase*[7]	*Sulfolobus solfataricus*
4.1.3.7	Citrate synthase*[8]	*Thermoplasma acidophilum*
		Pyrococcus furiosus

2.3 The Importance of "Good Assay Practice"

A succinct discussion on assaying activity and assessing thermostability of hyperthermophilic enzymes has been published[9], from which much of the material presented below has been adapted to suit the purpose of describing possible pitfalls encountered when determining T_{eq}.

2.3.1 Temperature Control

Equilibration of a cuvette in a spectrophotometer at 37°C is a relatively quick procedure, although a plastic cuvette may still require over 5 minutes[10]. At higher temperatures not only is the slower temperature equilibration a more serious drawback, but the cuvettes may distort.

Above 60°C not only is equilibration of any cuvette slow but also for liquid-jacketed cuvette holders, heat losses during circulation may be significant. This will necessitate a significant offset between the (higher) water-bath temperature circulating the liquid and the temperature required in the water-jacketed cuvette holder. For the most reliable results, the water-bath will need to be controlled by a temperature sensor actually inside the cuvette. Above 80°C, the temperature offset between the water-bath and the cuvette becomes so significant that this method is rendered impractical, and electrically heated cuvette holders must be used for accurate temperature control. In all cases, the only reliable estimate of the temperature of the cuvette contents is a direct measurement.

Temperature gradients within cuvettes can be significant at high temperatures despite lowered viscosity, and often necessitates the use of a stirred cuvette.

However, if this is not a feasible approach, temperature measurements at both the top and bottom of the cuvette need to be performed under experimental conditions.

2.3.2 Evaporation and Condensation

Evaporation of cuvette contents is an aspect that is often overlooked when assaying at high temperature. Vaporisation of aqueous and volatile assay components (such as buffers and organic phases) may lead to an increase in the concentration or even the precipitation of solubilised assay components. This problem can be remedied by using sealed capillaries when determining the stability of an enzyme. When directly assaying for activity at high temperature, cuvettes fitted with plastic lids can be used. Additionally, shorter assays should be used to minimise the extent of condensation on the walls of the cuvette.

When assaying at low temperatures (<10°C), condensation of water vapour on the walls of the cuvette can be prevented by blowing a continuous stream of a dry inert gas (e.g. nitrogen) across the face of the cuvette.

2.3.3 Assay Component Stability

If the substrate(s) or cofactor(s) are significantly heat-labile during the assay period, the results will obviously be affected. The same applies to the product if product measurement is being used to follow the progress of the assay. This is especially important in the case of NAD(P), where its oxidation/reduction is very widely used to follow enzyme reaction progress, but which is quite unstable at high temperatures and where the pH of the assay solution is less then neutral[11]. An additional complication is the possibility that the product of substrate thermal

degradation may be inhibitory. Little work has been carried out with regard to this possibility, and for many cases where enzyme reaction components are known to degrade at high temperature, the products of this degradation are unknown or are poorly characterised. Overall, not enough is known of reactant temperature stability, and if a reactant is known to occur *in vivo* in, say a hyperthermophile, this does not necessarily mean it will be stable in an *in vitro* enzyme assay, considering that the organism may overcome reactant instability by a variety of means.

There are few satisfactory solutions to reactant instability. In some cases, it may be possible to modify reaction conditions (pH, metal concentrations) to enhance stability; however, this is likely to mean that the enzyme is assayed under sub-optimal conditions.

An additional complication is that many metabolites and cofactors have temperature-dependent extinction coefficients[12]. It has been pointed out that the effect of temperature on the absorbance and λ_{max} of *p*-nitrophenol can lead to substantial errors in k_{cat} values measured by the continuous release of *p*-nitrophenol, if the calibration curve is not determined at the same temperature as the assay[13].

2.3.4 Buffer Choice

Of particular importance when attempting to determine T_{eq} is the maintenance of the pH so that it remains constant throughout the course of the assay. Many enzymes are particularly sensitive to changes in pH, especially when this effect is combined with an increase in temperature. Additionally, the frequent use of

continuous assays based on the release of *p*-nitrophenol or *p*-nitroaniline necessitates strict maintenance of pH as the extinction coefficient changes dramatically with very little change in pH. Care must be taken with such assays to ensure that the value used as extinction coefficient takes the pH of the assay into account. In the case of *p*-nitrophenol, the extinction coefficient that should be applied at different pH values takes the pK of the ionisation into account (Equation 2.1)[10].

$$\varepsilon_{pH} = 18000 \times [10^{(pH - 7.15)} / (10^{(pH-7.15)} + 1)] \qquad \textbf{Equation 2.1}$$

According to Equation 2.1, for a pH change of 0.5 from say, 8.0 to 8.5, the extinction coefficient changes by approximately 10%.

Buffers should be chosen on the basis that:

a) the buffer has a low or has no temperature coefficient,

b) the buffer is stable with regards to temperature and time,

c) the buffer does not react with the enzyme or the reaction components, and,

d) the buffer does not inhibit the enzyme reaction in any way, either by precipitating ions essential for catalytic activity or by supplying inhibiting metabolites.

Often it is not possible to use buffers that have a low temperature coefficient as they react with or inhibit the enzyme under investigation, or have pK_as outside the buffering range required. Therefore, the use of buffers with a large temperature coefficient requires that the solutions be adjusted to the required pH at the correct temperature with a pH meter standardised at the temperature required.

Alternatively, using published $d\text{pK}_a/d\text{T}$ values[14], the pH of the buffer solution can be adjusted at room temperature so that it gives the correct pH at the required assay temperature. This method is quicker but is potentially less accurate.

2.3.5 Variation of K_M with Temperature

A number of enzymes are known to have different K_M values at different temperatures (Table 2.2). Given that the 'Equilibrium Model' assumes that the enzyme remains saturated with substrate throughout the assay, these findings emphasise the need to carry out a K_M determination at either end of the temperature range likely to be used in the determination of T_{eq}.

2.3.6 Preparation of Substrate and Enzyme Solutions

Substrate and enzyme solutions should be dissolved or diluted in buffer and the pH checked, and if necessary, adjusted. This step is essential for *p*-nitrophenol/*p*-nitroaniline substrates where the leaving group is sometimes pH-labile.

For those solutions containing organic solvents, the volumes added to the reaction system must be minimised, so that the solvent is diluted sufficiently so that it has little or no effect on the enzyme or reaction.

2.3.7 Maintenance of Protein Concentration

The 'Equilibrium Model' assumes that the concentration of protein in the system is constant throughout the determination. Addition of non-ionic detergents[15], salts or another protein[16] to assay solutions to prevent loss of protein to the walls of the cuvette may be necessary where the enzyme concentration is very low.

Table 2.2 Examples of K_M variation with Temperature

Enzyme	Substrate	K_M (mM)	Temperature (°C)
3-phosphoglycerate kinase[5]	3-phosphoglycerate	0.8	40
		1.1	65
		1.9	76
	ATP	0.7	40
		0.7	65
		1.5	77
Glutamate dehydrogenase[17]	2-oxoglutarate	0.2	14
		0.52	60
		1.7	80
	NH_4Cl	2.0	14
		5.7	60
		15.5	80
	Glutamate	1.4	40
		1.9	60
		9.1	80
Alkaline phosphatase[18]	*p*-nitrophenyl phosphate	0.5	30
		1.0	70
Aryl acylamidase[18]	*p*-nitroacetanilide	0.015	20
		0.15	50

2.4 Data Collection

2.4.1 Management of Assay Temperature

The temperature of each assay was recorded using a Cole-Parmer Digi-Sense® thermocouple thermometer accurate to ± 0.1% of the reading and calibrated using a Cole-Parmer NIST-traceable high-resolution glass thermometer. The temperature probe was placed inside the cuvette adjacent to the light path during temperature equilibration prior to the initiation of the reaction and again immediately after completion of each enzyme reaction. Measurements of temperature were also taken at the top and bottom of the cuvette to check for temperature gradients. Where the temperature measured before and after the reaction differed by more than 0.1°C, the reaction was repeated.

2.4.2 Determination of Protein Concentration

Determinations of protein concentration were performed for each enzyme to check the protein concentrations stated by the manufacturers. The far UV method of Scopes[19] was used in each case as this method is non-destructive and it is much less affected by the protein amino acid composition[20, 21]. This method makes use of the approximate relationship between a protein at a concentration of 1 $mg \cdot mL^{-1}$ and its corresponding extinction coefficient and gives sufficiently accurate results provided that the absorbance is kept below 0.5.

Final protein concentrations were determined by taking the mean value of protein concentrations calculated from absorption readings made at five UV wavelengths (Table 2.3).

The extinction coefficient values vary from protein to protein because aromatic and some other residues contribute to the absorbance in this range, and the secondary structure has some influence on the shape and exact position of the peptide absorption peak. By analysing at all five wavelengths, interferences can be easily identified and anomalies discarded whilst leaving enough absorption readings to give an accurate estimation of the protein concentration.

Table 2.3 Wavelengths for protein determination and their corresponding extinction coefficient for a 1 mg·mL^{-1} solution of protein[19].

Wavelength (nm)	extinction coefficient ($M^{-1} \cdot cm^{-1}$)
220	~ 11
215	~ 15
210	~ 20
205	~ 31
200	~45

2.4.3 Instrumentation

All enzymic activities were measured using a Thermospectronic™ Helios γ-spectrophotometer equipped with a Thermospectronic™ single cell peltier-effect cuvette holder. This system was networked to a computer installed with Vision32™ (Version 1.25, Unicam Ltd) software including the Vision Enhanced Rate Programme capable of recording absorbance changes over time intervals of down to 0.125 seconds.

2.4.4 Assays

Substrate concentrations were maintained at ~10 times K_M to minimise the effects of any possible increases in K_M with temperature and to ensure that the enzyme remains saturated with substrate for the entire assay duration. Where these concentrations could not be maintained (e.g. because of substrate solubility), tests were conducted to confirm that there was no decrease in rate over the assay period because of substrate depletion.

For each enzyme, progress curves (absorbance versus time) were collected at a variety of temperatures; the time interval set so that an absorbance reading was collected every second, this value being a trade off between collecting a sufficient number of data points and unnecessary introduction of error due to instrument noise.

Assays reactions were initiated by the addition of microlitre amounts of enzyme (less than 2% of the total assay volume) that had no significant effect on the temperature of the solution inside the cuvette.

Three progress curves were collected at each temperature (see Figure 2.1) - where the slope for these triplicates deviated by more than 10%, the reactions were repeated.

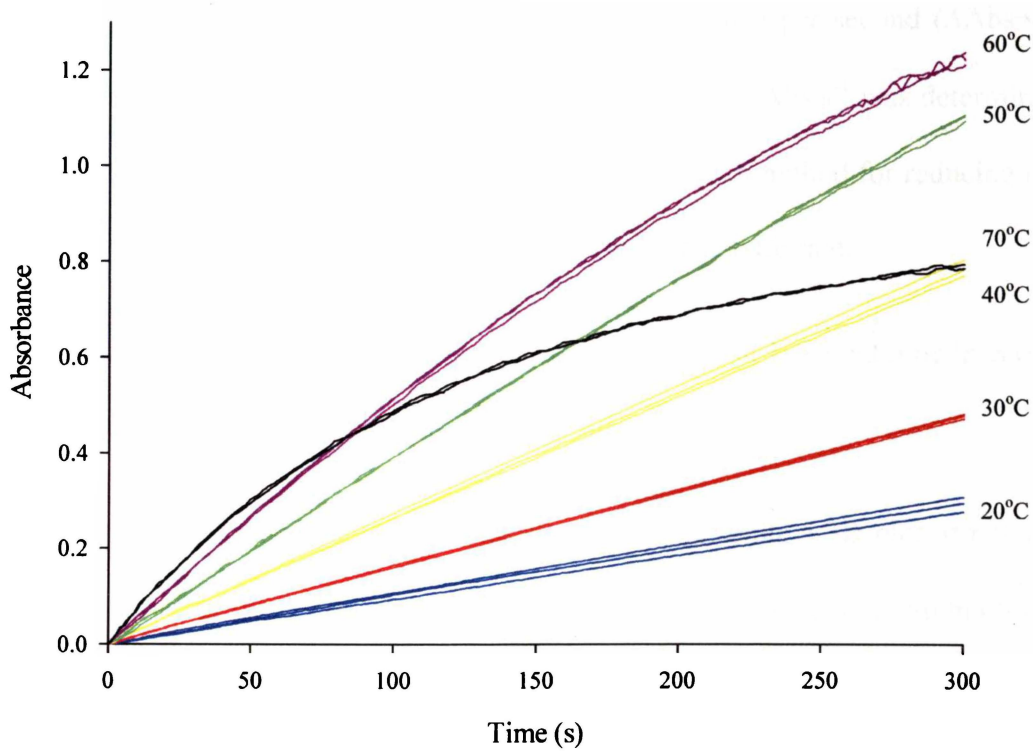

Figure 2.1 **A typical set of progress curves, shown in triplicate, generated by the Vision Rate Enhanced Program for a continuous assay.**

2.5 Data Analysis

2.5.1 Generation of 3-D Plots from Experimental Data

For each enzyme, each progress curve was exported from the Vision Rate Enhanced Program to Microsoft Excel, in the form of "data points of rates" as absolute absorbance versus time.

Using the spreadsheet function, the change in absorbance per second ($\Delta Abs \cdot s^{-1}$) was determined for each of the triplicates. The average $\Delta Abs \cdot s^{-1}$ was determined for the triplicates, averaging being the statistically correct method for reducing the contribution of random error in the determination of catalytic rate.

The catalytic rates (expressed as $M \cdot s^{-1}$) were calculated at 1 second time intervals along the averaged progress curve at each temperature.

Each time-point value for catalytic rate was used to generate a 3D plot of rate (in $\mu M \cdot s^{-1}$) versus temperature (in Kelvin) versus time (in seconds) [SigmaPlot® 2001 for Windows™, Version 7.101, SPSS Inc.]. Data were smoothed using a Loess algorithm; a curve-fitting technique based on local regression that applies a tricube weight function to elicit trends from noisy data[22] (Figure 2.2). A discussion on the use of this smoothing technique can be found in Appendix B. The first data point was obtained at approximately 2 seconds, owing to the delay between the addition of enzyme to the reaction mixture and the start of data collection. The data for zero time were obtained during the smoothing process, which extrapolates back to zero using the trend elicited from the data.

A) **B)**

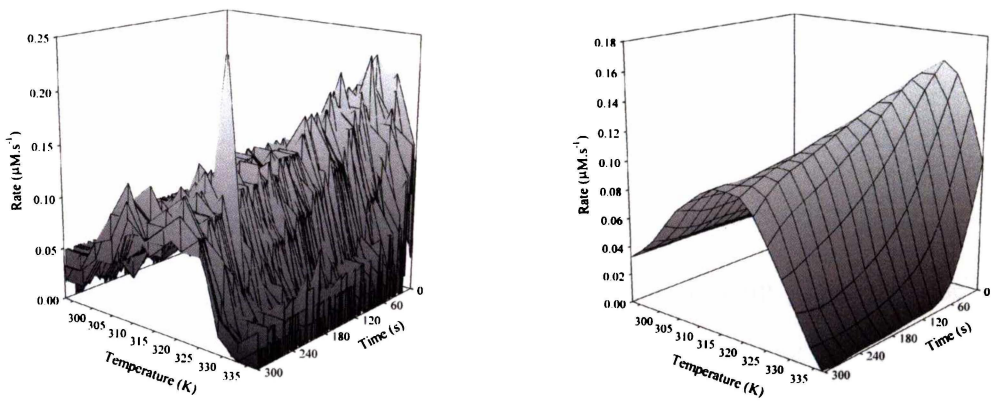

Figure 2.2 **The effect of smoothing raw data using the Loess algorithm.**

A) raw data; **B)** smoothed data

2.5.2 Estimation of Thermodynamic Parameters by 2D Analysis

The values for rate, temperature and time determined by the smoothing process for each enzyme were analysed to provide initial estimates of $\Delta G^{\ddagger}_{cat}$ (the activation energy of the catalytic reaction), $\Delta G^{\ddagger}_{inact}$ (the activation energy of the thermal inactivation process), ΔH_{eq} (the enthalpy change for the transition between active and inactive forms of the enzyme) and T_{eq} (the temperature for the mid-point of this transition) by 2D analyses.

2.5.2.1 Estimation of $\Delta G^{\ddagger}_{cat}$

For the data at zero time (where there is no thermal inactivation), the linear portion of an Eyring plot of $\ln(v/T)$ versus $1/T$ gives values of $\Delta H^{\ddagger}_{cat}$ and $\Delta S^{\ddagger}_{cat}$ (from the gradient and intercept, respectively), from which $\Delta G^{\ddagger}_{cat}$ can thus be calculated at any temperature of assay, via the relationship $\Delta G = \Delta H - T\Delta S$. The

mean of $\Delta G^{\ddagger}_{cat}$ calculated for each temperature was taken to give the final estimate.

2.5.2.2 Estimation of $\Delta G^{\ddagger}_{inact}$

At each assay temperature, plots of ln(v) versus time were used to calculate rate constants (k_{inact}) for the thermal inactivation process; Eyring plots of these data [ln(k_{inact}/T) versus $1/T$] similarly give values of $\Delta H^{\ddagger}_{inact}$ and $\Delta S^{\ddagger}_{inact}$, and hence of $\Delta G^{\ddagger}_{inact}$.

2.5.2.3 Calculation of ΔH_{eq} and T_{eq}

Values of K_{eq} were calculated from an Eyring plot [ln(v/T) versus $1/T$] for the data at zero time. According to the 'Equilibrium Model', in the absence of any thermal inactivation, the deviation from linearity in the Arrhenius plot is attributed to a shifting of the equilibrium from active to inactive forms, therefore a comparison of the observed values with those from the extrapolated linear portion can thus be used to calculate the value of K_{eq} at any temperature (Figure 2.3).

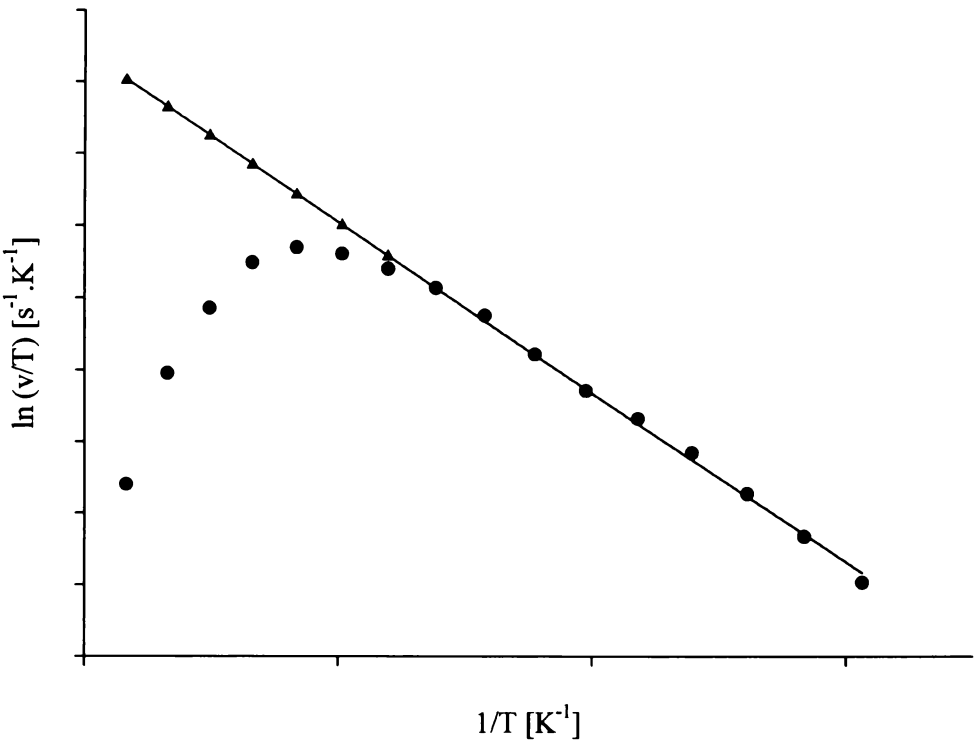

Figure 2.3 An Eyring plot illustrating the deviation from linearity attributed to a shifting of the equilibrium from active to inactive forms.

(●) experimentally determined data points. (▲) theoretical data points illustrating what the activity might have been in the absence of reversible thermal inactivation.

As rate is directly proportional to enzyme concentration, the difference in the measured velocity with respect to the velocity determined from the extrapolations is a measure of ratio between the concentration of active enzyme and the concentration of inactive enzyme.

Using the equation,

$$\ln K_{eq} = \frac{\Delta H_{eq}}{R}\left[\frac{1}{T_{eq}} - \frac{1}{T}\right] \qquad \textbf{Equation 2.2}$$

values of ΔH_{eq} and T_{eq} can be subsequently determined from a plot of $\ln(K_{eq})$ versus $1/T$ (from the gradient and x-axis intercept, respectively).

2.6 Fitting of the Data to the 'Equilibrium Model'

It must be noted here that a numerically integrated rate equation (see Appendix C.1) was used in the simulation and fitting of early experimental data to the 'Equilibrium Model'.

An analytic solution for the rate equation (the derivation of which can be found in Appendix C.2) has now been derived, providing a more accurate and robust method for simulating and fitting the data.

Using the estimates of the thermodynamic parameters, the complete, averaged data set for each enzyme (rate versus time versus temperature) was then fitted to the 'Equilibrium Model'. The fits were performed using the program, MicroMath® Scientist® for Windows™ (Version 2.01, MicroMath Scientific Software Inc.) to derive final values for the parameters of $\Delta G^{\ddagger}_{cat}$, $\Delta G^{\ddagger}_{cat}$, ΔH_{eq} and T_{eq}.

The parameters from the 2D estimation were first "improved" by Simplex searching[23, 24]. The parameters derived from the Simplex search were then fitted alongside the "raw" data, employing a re-iterative, non-linear minimisation of the least squares function of the analytical rate equation. This minimisation utilises Powell's algorithm[25], to find a local minimum, possibly a global minimum, of the sum of squared deviations between the experimental data and the model calculations.

In each case, the fitting routine was set to take minimum and maximum iterative step-sizes of 1 $x10^{-12}$ and 1, respectively. The sum of squares goal – the termination criterion for the fitting routine – was set to 1 x 10^{-12}.

The "fit" of the raw data to the 'Equilibrium Model' was then verified by visual means, by comparing the 3D plot of the smoothed raw data with the 3D plot generated by the 'Equilibrium Model' (Figure 2.4).

A) **B)**

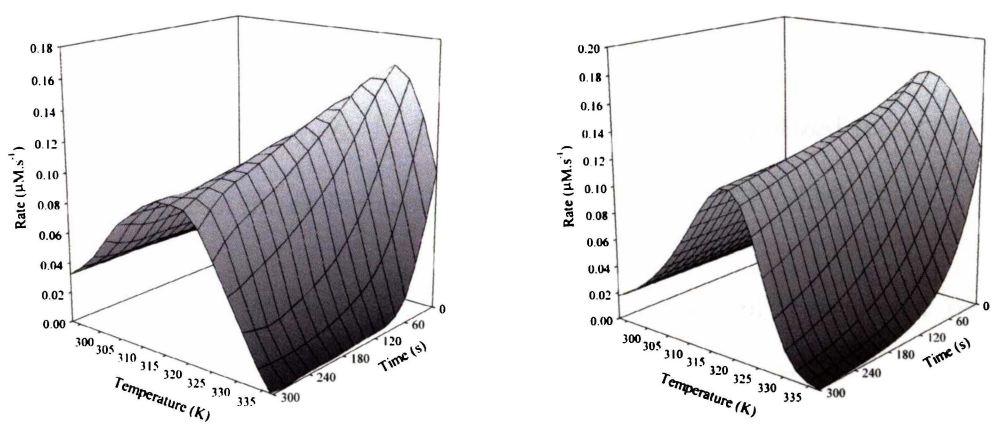

Figure 2.4 Comparison of 3D plots of experimental data smoothed using the Loess algorithm (A) with that generated by fitting the raw data to the 'Equilibrium Model' (B).

2.7 References

1. Daniel, R.M., Danson, M.J. & Eisenthal, R. (2001) The temperature optima of enzymes: a new perspective on an old phenomenon. *Trends in Biochemical Sciences*, **26**(4), 223 – 225.

2. Cornish-Bowden, A. J. (1972) Analysis of progress curves in enzyme kinetics. *Biochemical Journal*, **130,** 637 – 639.

3. Gilbert, H. F. (1990) Molecular and cellular aspects of thiol-disulfide exchange. *Advances in enzymology & related areas of molecular biology,* **63**, 69 – 172.

4. Hwang, C., Sinskey, A. J., & Lodish, H. F. (1992) Oxidized redox state of glutathione in the endoplasmic reticulum. *Science* **257**, 1496 – 1502.

5. Thomas, T.M. & Scopes, R.K (1998) The effects of temperature on the kinetics and stability of mesophilic and thermophilic 3-phosphoglycerate kinases. *Biochemical Journal*, **330**, 1087 – 1095.

6. Medina, D.C., Hanna, E., MacRae, I.J., Fisher, A.J., & Segel, I.H. (2001) Temperature Effects on the Allosteric Transition of ATP Sulfurylase from *Penicillium chrysogenum*. *Archives of Biochemistry and Biophysics,* **393**(1), 51 – 60.

7. Buchanan, C.L, Connaris, H., Danson, M.J., Reeve, C.D., & Hough, D.W. (1999) An extremely thermostable aldolase from *Sulfolobus solfataricus* with specificity for non-phosphorylated substrates. *Biochemical Journal*, **343**, 563 – 570.

8. Arnott, M.A., Michael, R.A., Thompson, C.R., Hough, D.W. & Danson, M.J. (2000) Thermostability and Thermoactivity of Citrate Synthases from the Thermophilic and Hyperthermophilic Archaea, *Thermoplasma acidophilum* and *Pyrococcus furiosus*. *Journal of Molecular Biology*, **304**, 657 – 668..

9. Daniel, R.M. & Danson, M.J. (2001) Assaying Activity and Assessing Thermostability of Hyperthermophilic Enzymes. *Methods in Enzymology*, **334**, 283 – 293..

10. John, R.A. (1992) in *Enzyme Assays, a Practical Approach* (ed. Eisenthal, R. & Danson, M.J.) p70. Oxford University Press, Oxford, UK.

11. Daniel, R.M. & Cowan, D.A. (2000) Biomolecular stability and life at high temperatures. *Cellular and Molecular Life Sciences*, **57**, 250 – 264.

12. Walsh, K.A.J., Daniel, R.M. & Morgan, H.W. (1983) A soluble NADH dehydrogenase (NADH: ferricyanide oxidoreductase) from *Thermus aquaticus* strain T351. *Biochemical Journal*, **209**, 427 – 433.

13. Fourage, L., Helbert, M., Nicholet, P. & Colas, B. (1999) Temperature Dependence of the Ultraviolet–Visible Spectra of Ionized and Un-ionized Forms of Nitrophenol: Consequence for the Determination of Enzymatic Activities Using Nitrophenyl Derivatives – A Warning. *Analytical Biochemistry*, **270**, 184 – 185.

14. Stevens, L. (1992) in *Enzyme Assays, a Practical Approach* (ed. Eisenthal, R. & Danson, M.J.) p320. Oxford University Press, Oxford, UK.

15. Millipore Corporation, Improving Protein and RNA Recovery with Microcon™ microconcentrators. *Fax Solutions Document 301*, Millipore Corporation, Bedford, Massachusetts, USA.

16. Allison, R.D.(1996) Kinetic Assay Methods, in *Current Protocols in Protein Science*, (eds. Coligan, J.E., Dunn, B.M., Ploegh, H.L., Speicher, D.W. & Wingfield, P.T.), pp 3.5.4, John Wiley & Sons Inc., New York, New York, USA.

17. Hudson, R.C., Ruttersmith, L.D. & Daniel, R.M. (1993) Glutamate dehydrogenase from the extremely thermophilic archaebacterial isolate AN1. *Biochimica et Biophysica Acta*, **1202**, 244 – 250.

18. Peterson, M.E. (2002) The Effect of Temperature on Enzyme Activity. MSc thesis, University of Waikato.

19. Scopes, R. K. (1994) in *Protein Purification: Principles and Practice,* 3rd Edition, (ed. Cantor, C. R.), pp44-50, Springer Verlag: San Diego, California, USA.

20. Goldfarb, A.R., Saidel, L.J., Mosovich, E. (1951) The ultraviolet absorption spectra of proteins. *Journal of Biological Chemistry*, **193**, 397 – 404.

21. Goldfarb, A.R. & Saidel, L.J. (1951) Ultraviolet absorption spectra of proteins. *Science*, **114**,156 – 157.

22. Cleveland, W. S. (1993) *Visualizing Data.* Hobart Press, New Jersey, USA.

23. Deming, S.N. & Morgan, S.L. (1973) Simplex Optimization of Variables in Analytical Chemistry. *Analytical Chemistry*, **45**, 278A – 283A.

24. Caceci, M.S. & Cacheris, W.P. (1984) Fitting Curves to Data. *Byte*, **May**, 340 – 362.

25. Powell, M.J.D. (1970) In *Numerical Methods for Nonlinear Algebraic Equations*, (ed. Robinowitz, P.) Chapter 7, Gordon & Breach Science Publishers, New York, New York, USA.

Chapter Three

The Effect of Temperature on Enzyme Activity - Testing the Theory

---

This chapter deals with the collection and analysis of experimental data that essentially proves the theory presented in the paper, "The temperature optima of enzymes: a new perspective on an old phenomenon" (see Appendix A). This work was published as a Research Article in the Journal of Biological Chemistry.

My contribution to this work included all of the experimental work, preparation of early drafts of the paper and submission of the final manuscript to the Journal. The version included here is the final manuscript submitted and subsequently published, and is the result of considerable input from all four authors.

A new, intrinsic, thermal parameter for enzymes reveals true temperature optima

Michelle E. Peterson*, Robert Eisenthal[†], Michael J. Danson[††], Alastair Spence[†††] and Roy M. Daniel*

The Journal of Biological Chemistry (2004) Vol. 279, No. 20, pp. 20717-20722

* Department of Biological Sciences, University of Waikato, Private Bag 3105, Hamilton, New Zealand.

[†] Department of Biology and Biochemistry, University of Bath, Bath, BA2 7AY, UK.

[††] Centre for Extremophile Research, Department of Biology and Biochemistry, University of Bath, Bath, BA2 7AY, UK.

[†††] Department of Mathematical Sciences, University of Bath, Bath, BA2 7AY, UK.

Corresponding Author:

Professor Roy Daniel,

Department of Biological Sciences, University of Waikato, Private Bag 3105, Hamilton, New Zealand

Tel: +64-7-8384213

Fax: +64-7-8384324

Email: r.daniel@waikato.ac.nz

Running Title: A new thermal parameter for enzymes

Summary

Two established thermal properties of enzymes are the Arrhenius activation energy and thermal stability. Arising from anomalies found in the variation of enzyme activity with temperature, a comparison has been made of experimental data for the activity and stability properties of 5 different enzymes with theoretical models. The results provide evidence for a new and fundamental third thermal parameter of enzymes, T_{eq}, arising from a sub-second timescale, reversible, temperature-dependent equilibrium between the active enzyme and an inactive (or less active) form. Thus, at temperatures above its optimum, the decrease in enzyme activity arising from the temperature-dependent shift in this equilibrium is up to two orders of magnitude greater than occurs through thermal denaturation. This parameter has important implications for our understanding of the connection between catalytic activity and thermostability, and of the effect of temperature on enzyme reactions within the cell. Unlike the Arrhenius activation energy, which is unaffected by the source ("evolved") temperature of the enzyme, and enzyme stability, which is not necessarily related to activity, T_{eq} is central to the physiological adaptation of an enzyme to its environmental temperature and links the molecular, physiological, and environmental aspects of the adaptation of life to temperature in a way that has not been previously described. We may therefore expect the effect of evolution on T_{eq} with respect to enzyme temperature/activity effects to be more important than on thermal stability. T_{eq} is also an important parameter to consider when engineering enzymes to modify their thermal properties by both rational design and by directed enzyme evolution.

Introduction

A graph of rate of product generation against temperature is sometimes presented to show the "temperature optimum" (T_{opt}) of an enzyme; however, it is a misconception that this optimum is an intrinsic enzyme property. The descending limb of this plot arises mostly from the denaturation of the enzyme and, since denaturation is both time and temperature dependent, shorter assays give a higher T_{opt}. In this classical description, the variation in enzyme activity with temperature can be described as follows:

$$V_{max} = k_{cat} . [E_0] . e^{-k_{inact} . t} \qquad \textbf{Equation (1)}$$

where V_{max} = maximum velocity of the enzyme; k_{cat} = the enzyme's catalytic constant; $[E_0]$ = total concentration of enzyme; k_{inact} = thermal inactivation rate constant; t = assay duration. Both rate constants, k_{cat} and k_{inact}, are dependent on temperature. This gives rise to temperature-activity graphs as shown in Figure 1A, where it can be seen that the apparent T_{opt} decreases with increasing time during the assay, but at zero time (i.e., under initial rate conditions), no temperature optimum exists (1). In this Classical Model, the temperature–dependent behaviour of the enzyme arises from the activation energy of the reaction and the thermal stability of the enzyme.

Arising from anomalies found in the variation of enzyme activity with temperature (2-6), a proposal (1) has been made for a third temperature-dependent property of enzymes, involving the reversible equilibrium between active and inactive forms of an enzyme, and implying a "true" temperature optimum. In this model (The Equilibrium Model), the active form of the enzyme (E_{act}) is in

reversible equilibrium with an inactive form (E_{inact}) and it is the inactive form that undergoes irreversible thermal inactivation to the thermally denatured state (X):

$$E_{act} \leftrightarrows E_{inact} \rightarrow X$$

In this situation, the concentration of active enzyme at any time point is defined by:

$$[E_{act}] = \frac{[E_o] - [X]}{1 + K_{eq}} \qquad \textbf{Equation (2)}$$

where K_{eq} is the equilibrium constant between active and inactive forms of the enzyme (K_{eq} = [E_{inact}] / [E_{act}]). Thus, K_{eq} becomes a new temperature-dependent property of an enzyme, in addition to k_{cat} and k_{inact}, and its variation with temperature is given by:

$$\ln (K_{eq}) = \frac{\Delta H_{eq}}{R} \left[\frac{1}{T_{eq}} - \frac{1}{T} \right] \qquad \textbf{Equation (3)}$$

where ΔH_{eq} is the enthalpic change associated with the conversion of active to inactive enzyme, and T_{eq} is the temperature at the mid-point of transition between the two forms. That is, T_{eq} is the temperature at which K_{eq} = 1 and ΔG_{eq} = 0; therefore $T_{eq} = \Delta H_{eq}/\Delta S_{eq}$. [We previously (1) used the term T_m to designate this temperature, but now prefer the term T_{eq}, as it is the temperature at which the concentrations of E_{inact} and E_{act} are at equilibrium]. In this Equilibrium Model, the temperature-dependent behaviour of an enzyme can be explained only by the inclusion of an additional intrinsic thermal parameter, T_{eq}.

The effect of incorporating the parameters K_{eq} and T_{eq} into simulated progress curves (Figure 1B) yields major differences from the Classical Model shown in Figure 1A, showing an initial rate temperature optimum that is obviously independent of assay duration and enabling an experimental distinction between the two models.

To compare the experimental data with the models, five enzymes from a variety of sources were assayed for activity at different temperatures, using continuous assays to allow the simultaneous measurement of activity and thermal stability in the same cuvette, and therefore under identical conditions. These measurements allow the generation of a unique temperature profile for each enzyme. Most of this work has been carried out on monomeric enzymes to avoid the potentially complicating effects of subunit dissociation.

The data presented support the Equilibrium Model hypothesis, involving K_{eq} as an intrinsic, temperature-dependent property of enzymes. The consequence is that, in such cases, T_{eq} must now be considered as a new thermal parameter that is a characteristic of any particular enzyme and which gives rise to a true temperature optimum.

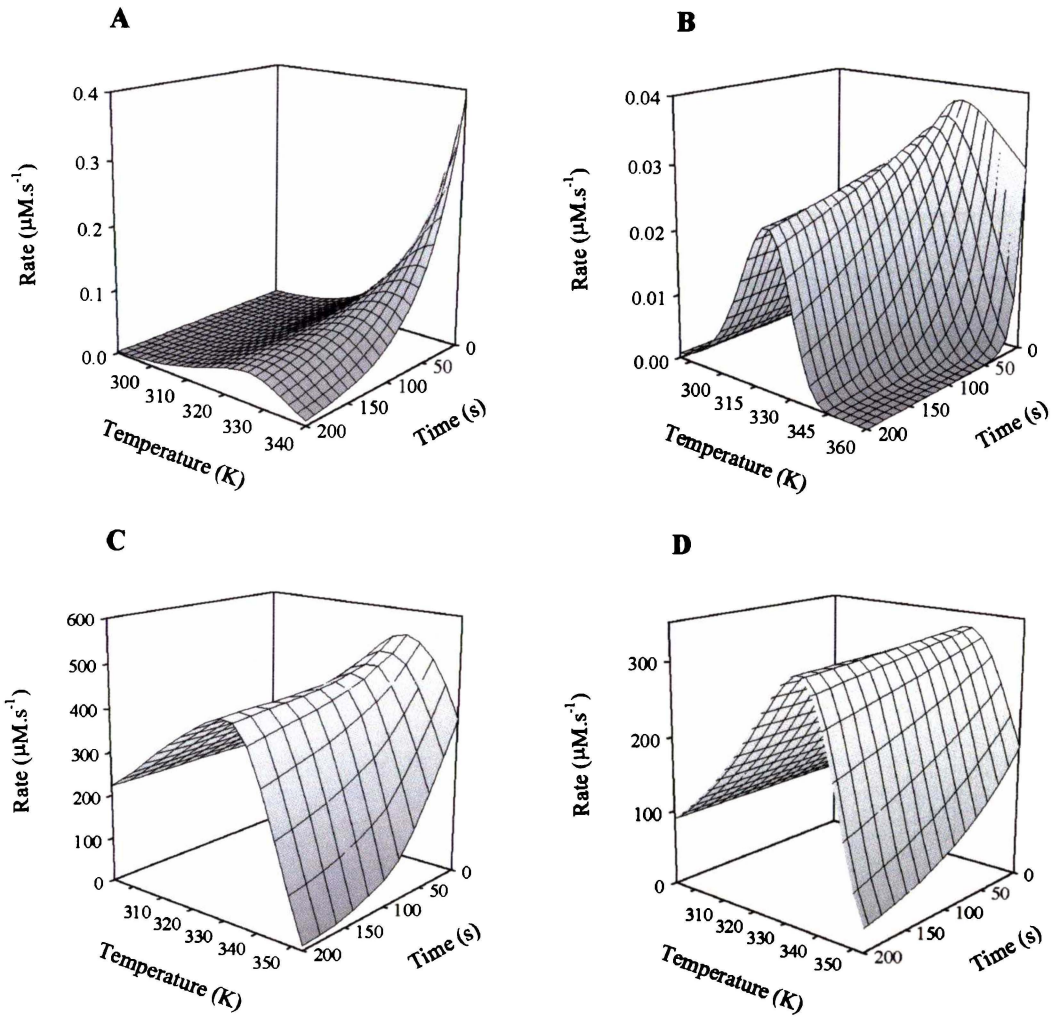

Figure 3.1 **The temperature dependence of enzyme activity**

(**A**) Simulated plot for the Classical Model (1). The variation of enzyme activity with temperature (290-340 K) and time during the assay (0-200 s) was simulated using Equation (1). The variation of the two rate constants in Equation (1) with temperature is given by $k_{cat} = (k_B T/h)\, e^{-(\Delta G^{\ddagger}_{cat}/RT)}$ and $k_{inact} = (k_B T/h)\, e^{-(\Delta G^{\ddagger}_{inact}/RT)}$ where k_B = Boltzmann's constant; R = Gas constant; T = absolute temperature; h = Planck's constant; $\Delta G^{\ddagger}_{cat}$ = activation energy of the catalysed reaction; $\Delta G^{\ddagger}_{inact}$ = activation energy of the thermal inactivation process. The following parameter values were used: $\Delta G^{\ddagger}_{cat}$ = 80 kJ·mol^{-1}; $\Delta G^{\ddagger}_{inact}$ = 95 kJ·mol^{-1}; total enzyme concentration = 100 nM. (**B**) Simulated plot for the Equilibrium Model (1). The variation of enzyme activity with temperature (280-360 K) and time during the assay (0-200 s) was simulated using the equation $V_{max} = k_{cat}[E_{act}]$, where the concentration of E_{act} at any time point is defined by Equation (2) and the variation of K_{eq} with

temperature is given by Equation (3). The rate of formation of X is given by $d[X]/dt = k_{inact}\{[E_0] - [E_{act}] - [X]\}$. The following parameter values were used: $\Delta G^{\ddagger}_{cat}$ = 80 kJ·mol^{-1}; $\Delta G^{\ddagger}_{inact}$ = 95 kJ·mol^{-1}; total enzyme concentration = 100 nM; ΔH_{eq} = 100 kJ·mol^{-1}; T_{eq} = 320 K. (**C**) Experimental data for adenosine deaminase. The enzyme was assayed spectrophotometrically at 265nm as described in Materials and Methods; the data are plotted as rate (μM.s^{-1}) versus temperature (K) versus time during assay (s). (**D**) Simulated data for adenosine deaminase. The experimental data from (C) were analysed as described in Materials and Methods to give estimated values of $\Delta G^{\ddagger}_{cat}$, $\Delta G^{\ddagger}_{inact}$, ΔH_{eq}, and T_{eq}. Using these values, the complete data set was fitted to the Equilibrium Model to give final values, which were then used to simulate the plot of rate (μM.s^{-1}) versus temperature (K) versus time during assay (s).

Experimental Procedures

Enzymes and reagents

Alkaline phosphatase from calf intestinal mucosa was purchased from Roche Applied Science, Basel, Switzerland. Adenosine deaminase from bovine spleen, aryl acylamidase from *Pseudomonas fluorescens* and β-lactamase from *Bacillus cereus* were purchased from Sigma-Aldrich Inc. (St. Louis, MO., USA). Acid phosphatase from wheat germ was purchased from Serva Electrophoresis GmbH (Heidelberg, Germany). Reagents for the analysis of the activity of these enzymes were purchased from Sigma-Aldrich, Merck KGaA (Darmstadt, Germany) and Oxoid Ltd (Basingstoke, UK). All other chemicals used were of analytical grade. Buffers were adjusted to the appropriate pH value at the assay temperature, using a combination electrode calibrated at this temperature.

Enzyme Assays

All enzymic activities were measured using continuous assays on a Thermospectronic™ Helios γ-spectrophotometer equipped with a Thermospectronic™ single cell peltier-effect cuvette holder. This system was networked to a computer installed with Vision32™ (Version 1.25, Unicam Ltd) software including the Vision Enhanced Rate Programme capable of recording absorbance changes over time intervals of down to 0.125 seconds. Substrate concentrations were maintained at approximately 10 times K_M to minimise the effects of any possible increases in K_M with temperature. Where these concentrations could not be maintained (e.g. due to substrate solubility), tests were conducted to confirm that there was no decrease in rate over the assay period

due to substrate depletion. No evidence was found for either substrate or product inhibition under the experimental conditions described.

Adenosine deaminase [E.C. 3.5.4.4, adenosine aminohydrolyase] activity was measured by following the decrease in absorbance at 265nm ($\Delta\varepsilon_{265}$ = 8.1 $mM^{-1}\cdot cm^{-1}$) resulting from the deamination of adenosine to inosine (7). Reaction mixtures (1 mL) contained 0.1 M sodium phosphate pH 7.4, 0.12 mM adenosine and 0.003 units of enzyme. One unit is defined as the amount of enzyme that hydrolyses one μmole of adenosine to inosine per minute at 30°C.

Acid phosphatase [E.C. 3.1.3.2, orthophosphoric-monoester phosphohydrolase (acid optimum)] activity was measured using *p*-nitrophenylphosphate (*p*NPP) as substrate (8). Reaction mixtures (1 mL) contained 0.1 M sodium acetate pH 5.0, 10 mM *p*NPP and 0.024 units of enzyme. The release of *p*-nitrophenol was monitored at 410 nm ($\Delta\varepsilon_{410}$ = 3.4 $mM^{-1}\cdot cm^{-1}$). One unit is defined as the amount of enzyme that hydrolyses one μmole of *p*NPP to *p*-nitrophenol per minute at 37°C.

Alkaline phosphatase [E.C. 3.1.3.1, orthophosphoric-monoester phosphohydrolase (alkaline optimum)] activity was measured using *p*NPP as substrate (9). Reaction mixtures (1 mL) contained 0.1 M diethanolamine/HCl pH 8.5, 0.5 mM $MgCl_2$, 10 mM *p*NPP and 0.02 units of enzyme. The release of *p*-nitrophenol was monitored at 405 nm ($\Delta\varepsilon_{405}$ = 18.3 $mM^{-1}\cdot cm^{-1}$). One unit is defined as the amount of enzyme that hydrolyses one μmole of *p*NPP to *p*-nitrophenol per minute at 37°C.

Aryl acylamidase [E.C. 3.5.1.13, aryl-acylamide amidohydrolyase] activity was measured by following the increase in absorbance at 382nm ($\Delta\varepsilon_{382}$ = 18.4 mM^{-1}

$^{1}\cdot cm^{-1}$) corresponding to the release of *p*-nitroaniline from the *p*-nitroacetanilide (*p*NAA) substrate (10). Reaction mixtures contained 0.1 M Tris/HCl pH 8.6, 0.75 mM *p*NAA and 0.018 units of enzyme. One unit is defined as the amount of enzyme required to catalyse the hydrolysis of one μmole of *p*NAA per minute at 37°C.

β-lactamase [E.C. 3.5.2.6, β-lactamhydrolase] activity was measured by following the increase in absorbance at 485nm ($\Delta\varepsilon_{485}$ = 20.5 $mM^{-1}\cdot cm^{-1}$) associated with the hydrolysis of the β-lactam ring of nitrocefin (11). Reaction mixtures contained 0.05 M sodium phosphate pH 7.0, 0.1 mM nitrocefin and 0.003 U of enzyme. One unit is defined as that which will hydrolyse the β-lactam ring of one μmole of cephalosporin per minute at 25°C.

Data collection

For each enzyme, progress curves (absorbance versus time) at a variety of temperatures were collected; the time interval was set so that an absorbance reading was collected every second. Assay reactions were initiated by the addition of microlitre amounts of enzyme that had no significant effect on the temperature. Three progress curves were collected at each temperature, each for a five-minute period. Where the slope for these triplicates deviated by more than 10%, the reactions were repeated. Temperature was recorded using a Cole-Palmer Digi-Sense® thermocouple thermometer accurate to ± 0.1°C of the reading and calibrated using a Cole-Parmer NIST-traceable high-resolution glass thermometer. The temperature probe was placed inside the cuvette adjacent to the light path during temperature equilibration prior to the initiation of the reaction and again

immediately after completion of each enzyme reaction. Measurements of temperature were also taken at the top and bottom of the cuvette to check for temperature gradients. Where the temperature measured before and after the reaction differed by more than 0.1°C, the reaction was repeated.

Data analysis

For each enzyme, the catalytic rates (expressed as $\mu M.s^{-1}$) were calculated at 1s time intervals along the three progress curves at each temperature. The averages of each time-point value were used to generate 3D plots of rate (v) versus temperature (T in Kelvin) versus time (t in seconds) [SigmaPlot® 2001 for Windows, Version 7.101, SPSS Inc.]. Data were smoothed using a Loess transformation, a curve-fitting technique based on local regression that applies a tricube weight function to elicit trends from noisy data (12). The first data point was obtained at approximately 2 seconds, owing to the lag between the addition of enzyme to the reaction mixture and the start of data collection. The data for zero time were obtained during the smoothing process, which extrapolates back to zero using the trend elicited from the data.

The data for each enzyme were analysed to provide values of $\Delta G^{\ddagger}_{cat}$ (the activation energy of the catalytic reaction), $\Delta G^{\ddagger}_{inact}$ (the activation energy of the thermal inactivation process), ΔH_{eq} (the enthalpy change for the transition between active and inactive forms of the enzyme) and T_{eq} (the temperature for the mid-point of this transition). Initial estimates of these parameters were calculated from 2D analyses. Firstly, for the data at $t = 0$ (where there is no thermal inactivation), Eyring plots of $\ln(v/T)$ versus $1/T$ give values of $\Delta H^{\ddagger}_{cat}$ and $\Delta S^{\ddagger}_{cat}$

(from the slope and intercept, respectively), from which $\Delta G^{\ddagger}_{cat}$ can thus be calculated at any temperature of assay. Secondly, at each assay temperature, plots of ln(v) versus time were used to calculate rate constants (k_{inact}) for the thermal inactivation process; Eyring plots of these data [ln(k_{inact}/T) versus $1/T$] similarly give values of $\Delta H^{\ddagger}_{inact}$ and $\Delta S^{\ddagger}_{inact}$, and hence of $\Delta G^{\ddagger}_{inact}$. Values of K_{eq} were calculated from an Arrhenius plot [ln(v) versus $1/T$] for the data at $t = 0$. That is, according to the Equilibrium Model (1), in the absence of any thermal inactivation, the deviation from linearity in the Arrhenius plot is attributed to a shifting of the equilibrium from active to inactive forms; a comparison of the observed values with those from the extrapolated linear portion can thus be used to calculate the value of K_{eq} at any temperature. Using equation (3), values of ΔH_{eq} and T_{eq} were subsequently determined from a plot of ln(K_{eq}) versus $1/T$.

Using these estimates of the thermodynamic parameters, the complete data set for each enzyme (rate versus time versus temperature) was fitted to the Equilibrium Model equations to derive the values given in Table 1. The fits were performed using Scientist (MicroMath) software, employing a non-linear least squares minimisation of the numerically integrated rate equations utilising Powell's algorithm.

Protein determination

Protein concentrations were determined from A_{280} measurements or by the colorimetric methods of Bradford and Biuret (13).

Results

The overall dependence of velocity on temperature with time can be described in our model by the relationship:

$$V_{\max} = \frac{\dfrac{k_B T}{h} . e^{\left(-\frac{\Delta G^{\ddagger}_{cat}}{RT}\right)} . E_0 . e^{\left(-\frac{\frac{k_B T}{h} . e^{\left(-\frac{\Delta G^{\ddagger}_{inact}}{RT}\right)} . e^{\left(\frac{\Delta H_{eq}\left(\frac{1}{Teq}-\frac{1}{T}\right)}{R}\right)}}{1+e^{\left(\frac{\Delta H_{eq}\left(\frac{1}{Teq}-\frac{1}{T}\right)}{R}\right)}} . t \right)}}{1+e^{\left(\frac{\Delta H_{eq}\left(\frac{1}{Teq}-\frac{1}{T}\right)}{R}\right)}}$$

Equation (4)

where k_B is Boltzmann's constant and h is Planck's constant. A comparison of the simulated plots for the Classical and Equilibrium models (Fig.1A & 1B) with the experimentally-determined 3D plots of rate versus time versus temperature (Fig. 1C and 2A-D) shows that all the enzymes studied conform to the Equilibrium Model; that is, they display clear temperature optima at time = 0 when there can be no loss of activity due to thermal inactivation. Analysis of the data gives values for $\Delta G^{\ddagger}_{cat}$, $\Delta G^{\ddagger}_{inact}$, ΔH_{eq} and T_{eq} for each enzyme (Table 1), assuming that the data can be described by the Equilibrium Model. Taking adenosine deaminase

as the example, these parameters were used to simulate the 3D plot (Fig. 1D), and a comparison with the plot of the experimental data (Fig. 1C) shows excellent agreement. Similarly good agreement has been obtained with the 4 other enzymes (data not shown).

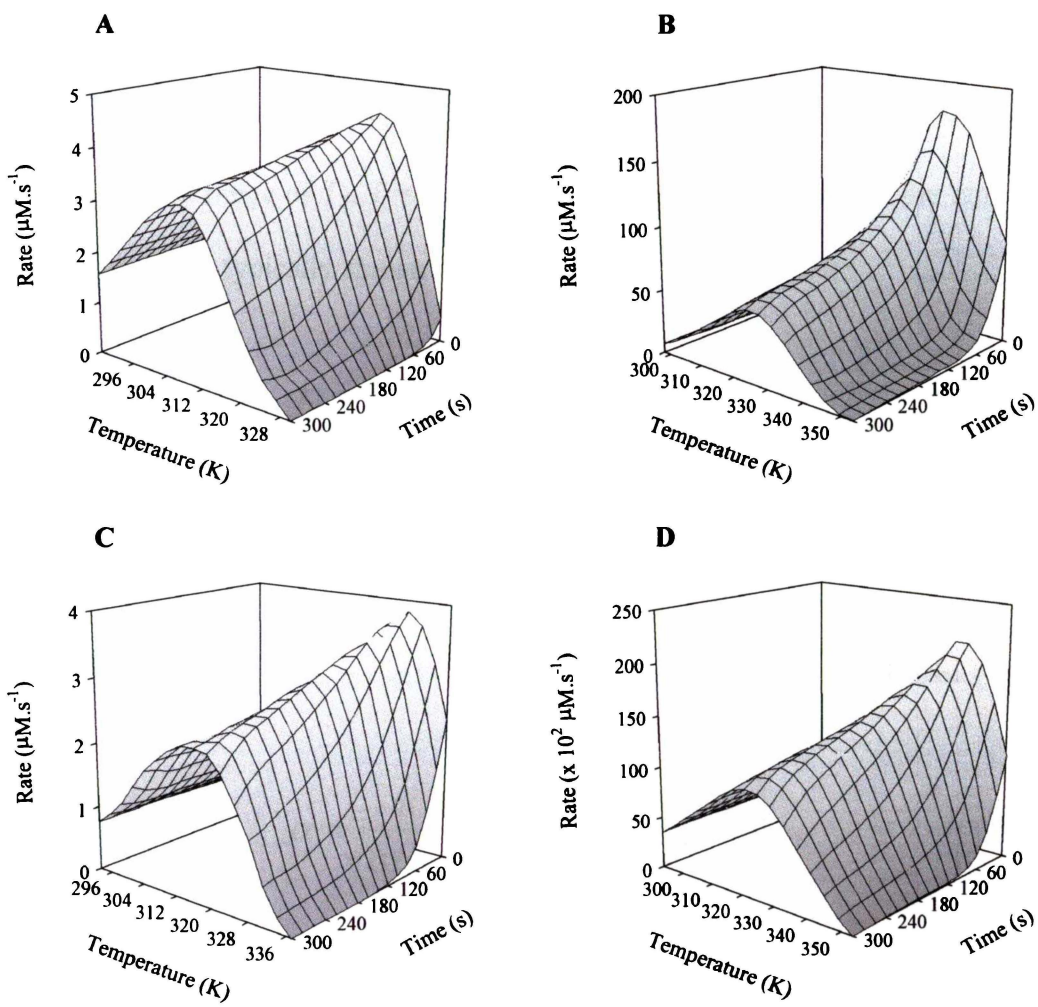

Figure 3.2 Experimentally-determined temperature dependence of enzymic activity.

Enzymes were assayed spectrophotometrically as described in Materials and Methods, and the data plotted as rate ($\mu M.s^{-1}$) versus temperature (K) versus time during assay (s).

(**A**) aryl acylamidase; (**B**) acid phosphatase; (**C**) β-lactamase; (**D**) alkaline phosphatase.

Setting $t = 0$ in equation (4) and differentiating with respect to T gives

$$\frac{dV_{\max}}{dT} = \frac{T + \dfrac{\Delta G^{\ddagger}_{cat}}{R}}{\dfrac{\Delta H_{eq}}{R} - \dfrac{\Delta G^{\ddagger}_{cat}}{R} - T} - e^{\left(\frac{\Delta H_{eq}\left(\frac{1}{T_{eq}} - \frac{1}{T}\right)}{R}\right)} \qquad \textbf{Equation (5)}$$

When $dV_{\max}/dT$ is set to zero (i.e. at the maximum of the rate/temperature profile in the observed range of T), $T = T_{opt}$. It can be demonstrated that for the range of parameter values typically shown for enzymes:

$$\frac{1}{T_{eq}} - \frac{1}{T_{opt}} \approx -\frac{R}{\Delta H_{eq}} \ln\left(\frac{\Delta H_{eq} - \Delta G^{\ddagger}_{cat}}{\Delta G^{\ddagger}_{cat}}\right) \qquad \textbf{Equation (6)}$$

Further manipulation provides the relationship:

$$T_{\text{opt}} \approx T_{\text{eq}}(1 - \alpha T_{\text{eq}}) \qquad \textbf{Equation (7)}$$

where $$\alpha \approx \frac{R}{\Delta H_{eq}} \ln\left(\frac{\Delta H_{eq} - \Delta G^{\ddagger}_{cat}}{\Delta G^{\ddagger}_{cat}}\right)$$

and α is small (such that $\alpha T_{\text{eq}} << 1$). Thus in general, for enzymes whose thermal activity dependence follows the Equilibrium Model, T_{opt} will be close in value to T_{eq} and always smaller (by the term αT_{eq}^2). Over the range of values of $\Delta G^{\ddagger}_{\text{cat}}$ and ΔH_{eq} encountered in this study, T_{opt} and T_{eq} follow an essentially linear relationship.

A plot of relative activity at zero time versus temperature (Fig. 3) illustrates that all five enzymes display true temperature optima of catalytic activity as defined by the Equilibrium Model, and that the values of T_{opt} are essentially in accordance with the determined values of T_{eq} (Table 1). For β-lactamase and adenosine deaminase, the difference between T_{opt} and T_{eq} is greater than for the other enzymes; both enzymes have relatively low ΔH_{eq} values, which will have a major influence on this difference (Equation 7). It should be stressed that $\Delta G^{\ddagger}_{inact}$ is not a factor in the position of the peaks illustrated in Figure 3 as the curves are determined at "time zero" where there is no thermal inactivation process. As also noted by Thomas and Scopes (2), in all cases reported here the T_{opt} is approximately 20-40°C above the optimum growth temperature/body temperature of the source organisms.

Although the application of the Equilibrium Model has the potential to be complicated by temperature-induced subunit dissociation in the case of oligomeric enzymes, we find no evidence to suggest that this treatment is restricted to monomeric enzymes; the data for the dimeric alkaline phosphatase adhere equally well to the Equilibrium Model as do the other, monomeric, enzymes investigated here.

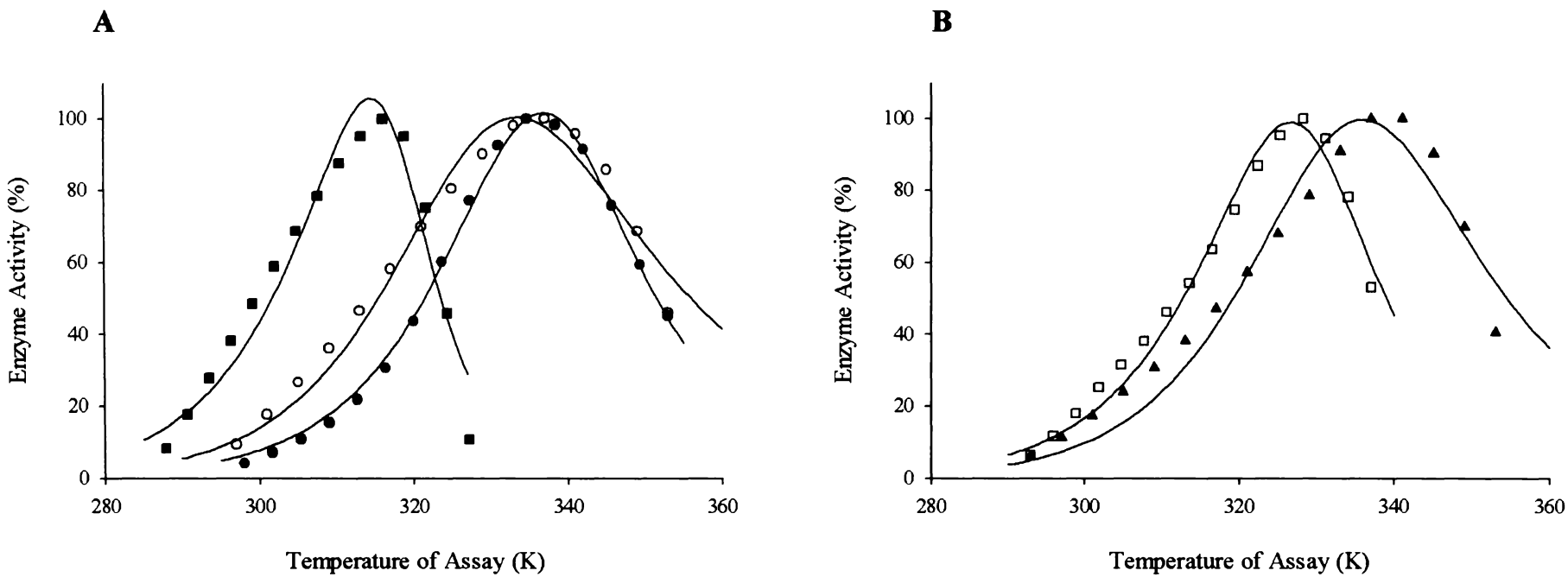

Figure 3 **Temperature dependence of enzymic activity at time zero**

From the experimental data in Figure 1C and Figure 2A-D, the enzymic activities at time zero were plotted against temperature to demonstrate the dependence of enzymic activity on temperature in the absence of thermal inactivation. For clarity, the data have been divided into two graphs. The activity data for each enzyme are scaled from 5-100% relative to the maximum activity for that enzyme. (A): (●) acid phosphatase; (○) adenosine deaminase; (■) aryl acylamidase. (B): (□) β-lactamase; (▲) alkaline phosphatase. The solid curves through the points are fits to the data using equation (4) with time (t) set to zero.

Table I **Summary of experimentally-determined thermodynamic parameters**

T_{opt} values were determined from the data in Figure 3 using the peaks of the fitted curves. Values of T_{eq}, $\Delta G^{\ddagger}_{cat}$, $\Delta G^{\ddagger}_{inact}$, and ΔH_{eq} were determined as described in the Materials and Methods.

Enzyme	*Origin*	Growth Temp. °C	T_{opt} °C	T_{eq} °C	$\Delta G^{\ddagger}_{cat}$ (kJ·mol^{-1})	$\Delta G^{\ddagger}_{inact}$ (kJ·mol^{-1})	ΔH_{eq} (kJ·mol^{-1})
Aryl acylamidase	*P. fluorescens*	25	41	44	37	93	165
β-lactamase	*Bacillus cereus*	30	53	75	38	91	103
Acid phosphatase	Wheat germ	15-25*	64	65	31	138	183
Adenosine deaminase	Bovine spleen	39	59	73	26	100	146
Alkaline phosphatase	Bovine intestine	39	63	70	18	108	220

* Spring germination temperatures

Discussion

The results and their analysis indicate that the experimental velocity data as a function of temperature can be described by the Equilibrium Model, suggesting K_{eq} as an intrinsic, temperature-dependent property of enzymes, and supporting the hypothesis that these enzymes possess a third thermal parameter (T_{eq}), alongside the Arrhenius activation energy and the activation energy for thermal stability.

Currently, we have no evidence bearing on the molecular basis of the equilibrium between E_{act} and E_{inact}, although it is clearly a fast process relative to thermal denaturation. All the variation of activity with temperature at zero time [Figures 2 and 3] occurs as a result of changes in the E_{act}/E_{inact} equilibrium, and is thus attained over timescales shorter than the mixing process, say less than 1 second, whereas the measured rate of irreversible thermal inactivation (conversion from E_{inact} to denatured state) is at least two orders of magnitude slower over the same temperature range. For example, in the case of aryl acylamidase [Fig 2A], at 51°C the activity at time zero is approximately 40% lower than at the "optimum" temperature [46°C], whereas the activity/time line at this temperature shows that it takes approximately 60 seconds for 40% denaturation to occur.

Since the Native/Denatured transition is generally a two-state process for single-domain proteins (14), E_{inact} is unlikely to be significantly unfolded. A reversible conformational change is most likely, and we speculate that the differing effects of temperature on the various weak interactions stabilising protein structure offer an opportunity for a shift of structure with changing temperature, leading to a change in activity. The existence of conformational sub-states in equilibrium over

sub-second timescales is widely accepted (15, 16), and it has recently been suggested that adaptation to thermal stability may involve a change in the scale of fluctuations about the average state (17).

T_{eq} is important in describing the effect of temperature on enzymes, and in particular on the role of temperature as a selection pressure on enzyme structure and function. There is no evidence connecting the Arrhenius activation energy of an enzyme to its thermal environment, and although there is a strong correlation between thermal stability and the environmental temperature of the source organism, it is known that enzyme thermal stability also reflects resistance to other cellular conditions such as the action of proteases (18). T_{eq} is central to the physiological adaptation of an enzyme to its environmental temperature and links the molecular, physiological, and environmental aspects of the adaptation of life to temperature in a way that has not been previously possible. We predict that T_{eq} will be a better expression of the effect of environmental temperature on the evolution of the enzyme than thermal stability; and thus we might expect differences in the overall shapes of the curves such as those shown in Figure 2 to describe the fit of an enzyme to its thermal environment, especially at the high temperature part of the graph, since the shape of the low temperature part of the graph will be determined largely by the Arrhenius activation energy. T_{eq} thus provides an important new parameter for matching an enzyme's properties to its cellular and environmental function.

In terms of protein engineering, T_{eq} provides an additional parameter that determines the *thermoactivity* of an enzyme and so must be considered when designing enzymes for particular functions. Much enzyme engineering is directed

at stabilising enzymes against denaturation. The results here suggest that engineering to manipulate the E_{act}/E_{inact} equilibrium [i.e., T_{eq}] may be equally productive, and that T_{eq} must also be shifted to higher temperatures to obtain the expected catalytic benefits of enhanced enzyme thermostability. It will be important to distinguish between mutations that affect stability from those that affect T_{eq}.

Acknowledgements

We thank C. Collet for some of the preliminary work on β-lactamase, and C. Cary and C. Monk for assistance in collecting some of the data presented in this paper. The work was partially supported by the National Science Foundation (Biocomplexity 0120648) and by the Biotechnological and Biological Sciences Research Council, U.K.

References

1. Daniel, R. M., Danson, M. J. & Eisenthal, R. (2001) *Trends Biochem. Sci.* **26**, 223 – 225.

2. Thomas, T. M. & Scopes, R. K. (1998) *Biochem. J.* **330**, 1087 – 1095.

3. Gerike, U., Russell, N. J., Danson, M. J. & Hough, D. W. (1997) *Eur. J. Biochem.* **248**, 49 – 57.

4. Buchanan, C. L., Connaris, H., Hough, D. W., Reeve, C. D. & Danson, M. J. (1999) *Biochem. J.* **343**, 563 – 570.

5. Arnott, M. A., Michael, R. A., Thompson, C. R., Hough, D. W. & Danson, M. J. (2000) *J. Mol. Biol.* **304**, 655 – 666.

6. Medina, D. C., Hanna, E., MacRae, I. J., Fisher, A. J. & Segel, I. H. (2001) *Arch. Biochem. Biophys.* **393**, 51 – 60.

7. Pfrogner, N. (1967) *Arch. Biochem. Biophys.* **119**, 141 – 146.

8. Hollander, V. P. (1971) in *The Enzymes*, Vol. 4 (ed. Boyer, P. D.) 449 – 498 (Academic Press, New York).

9. Fernley, H. N. (1971) in *The Enzymes*, Vol. 4 (ed. Boyer, P. D.) 417 – 447 (Academic Press, New York).

10. Hammond, P. M., Price, C. P. & Scawen, M. D. (1983) *Eur. J. Biochem.* **132**, 651 – 655.

11. O'Callaghan, C. H., Morris, A., Kirby, S. M. & Shingler, A. H. (1972) *Antimicrob. Agents Chemother.* **1**, 283 – 288.

12. Cleveland, W. S. (1993) *Visualizing Data*, Hobart Press, New Jersey.

13. Scopes, R. K. (1994) in *Protein Purification: Principles and Practice*, 3rd Edition, (ed. Cantor, C. R.) 44 – 50 (Springer Verlag: San Diego).

14. Creighton, T. E. (1993) *Proteins*, 2nd Ed., W H Freeman, New York.

15. Brooks, C. L., Karplus, M. & Pettitt, B. M. (1988) *Proteins*, John Wiley, New York.

16. Svensson, A-K. E., O'Neill, J. C. & Matthews, C. R. (2003) *J. Mol. Biol.* **326**, 569 – 583.

17. Wintrode, P. L., Zhang, D., Vaidehi, N., Arnold, F. H. and Goddard III, W. A. (2003) *J. Mol. Biol.* **327**, 745 – 757.

18. Daniel, R. M., Dines, M. & Petach, H. H. (1996) *Biochem. J.* **317**, 1 – 11.

Additions and Corrections

Vol. 279 (2004) 20717-20722

A new, intrinsic, thermal parameter for enzymes reveals true temperature optima.

Michelle E. Peterson, Robert Eisenthal, Michael J. Danson, Alastair Spence and Roy M. Daniel

Page 20720, Table I: It has become apparent to us that incorrect units were used for the fitting of experimental data to the 'Equilibrium Model', and that the values for $\Delta G^{\ddagger}_{cat}$, $\Delta G^{\ddagger}_{inact}$, ΔH_{eq} and T_{eq} published in this paper are therefore incorrect; a corrected table is below. The main conclusion of the paper is unaffected, namely that:

> "*The results and their analysis indicate that the experimental velocity data as a function of temperature can be described by the Equilibrium Model, suggesting K_{eq} as an intrinsic, temperature-dependent property of enzymes, and supporting the hypothesis that these enzymes possess a third thermal parameter (T_{eq}), alongside the Arrhenius activation energy and the activation energy for thermal stability.*".

However, based on the original table we stated:

> "*For β-lactamase and adenosine deaminase, the difference between T_{opt} and T_{eq} is greater than for the other enzymes;*"

This statement no longer applies.

In addition, as a result of the corrected values, the statement that

> *"T_{opt} will be close in value to T_{eq} and always smaller"*

should read

> *"T_{opt} will almost always be close in value to T_{eq} but depending on the relative values of $\Delta G^{\ddagger}_{cat}$ and ΔH_{eq}, may be smaller or larger than T_{eq}.*

Table I **Summary of experimentally-determined thermodynamic parameters**

T_{opt} values were determined from the data in Figure 3 using the peaks of the fitted curves. Values of T_{eq}, $\Delta G^{\ddagger}_{cat}$, $\Delta G^{\ddagger}_{inact}$, and ΔH_{eq} were determined as described in the Materials and Methods.

Enzyme	*Origin*	Growth Temp. °C	T_{opt} °C	T_{eq} °C	$\Delta G^{\ddagger}_{cat}$ (kJ·mol^{-1})	$\Delta G^{\ddagger}_{inact}$ (kJ·mol^{-1})	ΔH_{eq} (kJ·mol^{-1})
Aryl acylamidase	*P. fluorescens*	25	38	36	74	92	133
β-lactamase	*Bacillus cereus*	30	53	53	69	94	146
Acid phosphatase	Wheat germ	15-25*	66	63	79	95	133
Adenosine deaminase	Bovine spleen	39	62	56	65	99	101
Alkaline phosphatase	Bovine intestine	39	68	60	57	97	86

* Spring germination temperatures

Chapter Four

Data Collection & Analysis – Improvements to the Method and Extension to Other Enzyme and Assay Systems

---

This chapter consists of the draft manuscript of a paper ready to be submitted to Biochemical Journal, describing how to determine T_{eq} and its associated thermodynamic constants for any enzyme.

My contribution to this work involved all of the experimental work, data analysis and the majority of the preparation, and submission, of the manuscript.

The determination of T_{eq}, the new and fundamental third thermal parameter of enzymes

Michelle E. Peterson*, Robert Eisenthal†, Michael J. Danson††, and Roy M. Daniel*

* Department of Biological Sciences, University of Waikato, Private Bag 3105, Hamilton, New Zealand.

† Department of Biology and Biochemistry, University of Bath, Bath, BA2 7AY, UK.

†† Centre for Extremophile Research, Department of Biology and Biochemistry, University of Bath, Bath, BA2 7AY, UK.

Key words: enzyme, method, activity, stability, T_{eq}, Equilibrium Model, temperature

Corresponding Author: Professor Roy Daniel, Department of Biological Sciences, University of Waikato, Private Bag 3105, Hamilton, New Zealand

Tel: +64-7-8384213

Fax: +64-7-8384324

Email: r.daniel@waikato.ac.nz

Running Title: Determination of T_{eq}

Synopsis

Traditionally, the dependence of enzyme activity on temperature has been described by a model consisting of two processes: the catalytic reaction defined by k_{cat}, and irreversible inactivation defined by k_{inact}. To account for observed anomalies in the temperature-dependent behaviour of enzymes, a new model for the temperature dependence of enzyme behaviour has been developed and validated. This model (the 'Equilibrium Model') includes an inactive form of the enzyme (E_{inact}) that is in reversible equilibrium with the active form (E_{act}); it is the inactive form that undergoes irreversible thermal inactivation to the thermally denatured state.

The equilibrium is described by an equilibrium constant (K_{eq}), whose temperature dependence is characterised in terms of the enthalpy of the equilibrium, ΔH_{eq}, and a new thermal parameter, T_{eq}, which is the temperature at which the concentrations of E_{act} and E_{inact} are equal: T_{eq} may therefore be regarded as the thermal equivalent of K_M. The Equilibrium Model has major implications for enzymology, biotechnology, and evolution of enzymes.

This paper determines the minimum assay parameters needed for the accurate determination of T_{eq} and it's associated parameters, and describes simpler methods for their determination than have been previously available, including those required for the application of the Equilibrium model to enzyme reactions catalysed under non-ideal conditions. Additionally, it presents more accurate methods based on fitting progress curves directly to the Equilibrium Model.

Introduction

The effect of temperature on enzyme activity has been described by two well established thermal parameters: the Arrhenius activation energy, which describes the effect of temperature on the catalytic rate constant; and thermal stability, which describes the effect of temperature on the thermal inactivation rate constant. Anomalies arising from this description have been resolved by the development [1] and validation [2] of a new model for the effect of temperature on enzyme activity, the "Equilibrium Model", incorporating an additional thermal parameter, T_{eq}. In this Model, the active form of the enzyme (E_{act}) is in reversible equilibrium with an inactive form (E_{inact}), and it is the inactive form that undergoes irreversible thermal inactivation to the thermally denatured state (X):

$$E_{act} \leftrightarrows E_{inact} \rightarrow X$$

The effect of the third parameter, T_{eq}, is most evident from a plot of enzyme activity versus temperature versus time, which shows a temperature optimum at zero time (Figure 1A). In contrast, the 'Classical Model', which assumes a simple two-state equilibrium between an active and a thermally-denatured state ($E_{act} \leftrightarrows$ X), and can be described in terms of only two parameters (Arrhenius activation energy and thermal stability) shows, when graphed in three dimensions, the absence of a temperature optimum at zero time (Figure 1B).

In addition to the obvious differences in the graphs representing each Model, it has been observed experimentally that at any temperature above the maximum of enzyme activity, the loss of activity attributed to the shift in the E_{inact}/ E_{act}

equilibrium is fast (<1s) relative to the loss of activity due to thermal denaturation [2].

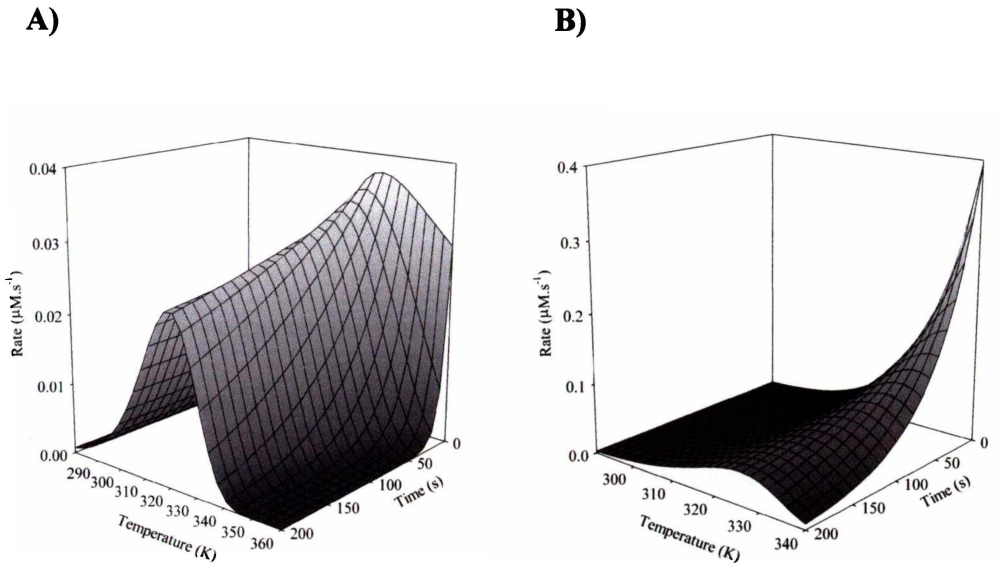

Figure 1 The temperature dependence of enzyme activity [1]

A comparison of plots of rate ($\mu M \cdot s^{-1}$) versus temperature (K) versus time (s) as described by **A)** The Equilibrium model, and **B)** The Classical Model. The data were simulated using parameter values: **A)** $\Delta G^{\ddagger}_{cat}$ = 80 kJ $\cdot mol^{-1}$, $\Delta G^{\ddagger}_{inact}$ = 95 kJ $\cdot mol^{-1}$, ΔH_{eq} = 100 kJ $\cdot mol^{-1}$, T_{eq} = 320 K; **B)** $\Delta G^{\ddagger}_{cat}$ = 80 kJ $\cdot mol^{-1}$, $\Delta G^{\ddagger}_{inact}$ = 95 kJ $\cdot mol^{-1}$.

T_{eq} has both fundamental and technological significance. T_{eq} has important implications for our understanding of the effect of temperature on enzyme reactions within the cell and of enzyme evolution in response to temperature. T_{eq} will possibly be a better expression of the effect of environmental temperature on the evolution of the enzyme than thermal stability; T_{eq} thus provides an important new parameter for matching an enzyme's properties to its cellular and environmental function.

T_{eq} must also be considered in engineering enzymes for biotechnological applications at high temperatures. In general, enzyme engineering is directed at stabilising enzymes against denaturation; however, enhanced thermal stability does not guarantee thermoactivity. It is possible that engineering to manipulate the E_{act}/E_{inact} equilibrium [i.e., T_{eq}] may be equally productive, and that T_{eq} must also be shifted to higher temperatures to obtain the expected catalytic benefits of enhanced enzyme thermostability [3].

The detection of the reversible enzyme inactivation, which forms the basis of the 'Equilibrium Model', is not entirely straightforward due to the number of conflicting influences that arise when increasing the temperature of an enzyme assay. Determination of T_{eq} to date has used continuous assays, because this method produces progress curves directly and obviates the need to perform separate activity and stability experiments, and has utilised enzymes whose reactions are essentially irreversible (far from reaction equilibrium), do not show any substrate or product inhibition and remain saturated with substrate for the duration of the assay. However, there are a large number of enzymes that do not fit these criteria, narrowing the potential utility of determining T_{eq}.

This paper describes simple methods for the reliable determination of T_{eq} using either continuous or discontinuous assays, and outlines the assay parameters required for accurate determination of T_{eq} and the associated thermodynamic constants ($\Delta G^{\ddagger}_{cat}$, $\Delta G^{\ddagger}_{inact}$ and ΔH_{eq}) associated with the 'Equilibrium Model'. It also introduces a more detailed alternative method of fitting progress curves directly to the Model.

Materials

Enzymes and Reagents

Aryl acylamidase from *Pseudomonas fluorescens* was purchased from Sigma-Aldrich Inc. (St. Louis, MO., USA). The substrate, *p*-nitroacetanilide, for this enzyme was purchased from Merck KGaA (Darmstadt, Germany). Acid phosphatase from wheat germ was purchased from Serva Electrophoresis GmbH (Heidelberg, Germany). β-lactamase from *Bacillus cereus* was purchased from Sigma-Aldrich Inc and its substrate, nitrocefin, was purchased from Oxoid. Malate dehydrogenase from *Escherichia coli* was purchased from Megazyme International Ireland Ltd (Bray, County Wicklow, Ireland). *p*-nitrophenylphosphate, malic acid, semicarbazide and NAD^+ were purchased from Sigma-Aldrich. All other chemicals used were of analytical grade.

Instrumentation

All enzymic activities were measured using a Thermospectronic™ Helios γ-spectrophotometer equipped with a Thermospectronic™ single cell peltier-effect cuvette holder. This system was networked to a computer installed with Vision32™ (Version 1.25, Unicam Ltd) software including the Vision Enhanced Rate Programme capable of recording absorbance changes over time intervals down to 0.125 seconds.

Temperature Control

The temperature of each assay was recorded directly, using a Cole-Parmer Digi-Sense® thermocouple thermometer accurate to ± 0.1°C of the reading and

calibrated using a Cole-Parmer NIST-traceable high-resolution glass thermometer. The temperature probe was placed inside the cuvette adjacent to the light path during temperature equilibration prior to the initiation of the reaction and again immediately after completion of each enzyme reaction. Measurements of temperature were also taken at the top and bottom of the cuvette to check for temperature gradients. Where the temperature measured before and after the reaction differed by more than 0.1°C, the reaction was repeated [2].

Assay conditions

Assays at high temperature (or over any wide temperature range) can sometimes pose special problems and may need additional care [4, 5, 6]. Quartz cuvettes were used in all experiments, for their relatively quick temperature equilibration and heat-retaining capacity. Where required, a plastic cap was fitted to the cuvette to prevent loss of solvent due to evaporation (at higher temperatures), or a constant stream of a dry, inert gas (e.g. nitrogen) was blown across the cuvette to prevent condensation (at temperatures below ambient).

Buffers were adjusted to the appropriate pH value at the assay temperature, using a combination electrode calibrated at this temperature.

Where very low concentrations of enzyme were used, salts or low concentrations of non-ionic detergents were added to prevent loss of protein to the walls of the cuvette.

Substrate concentrations were maintained at ~10 times K_M to minimise the effects of any increases in K_M with temperature and to ensure that the enzyme remains saturated with substrate for the entire assay duration. Where these concentrations

could not be maintained (e.g. because of substrate solubility), tests were conducted to confirm that there was no decrease in rate over the assay period arising from to substrate depletion.

Assays reactions were initiated by the addition of microlitre amounts of enzyme that had no significant effect on the temperature of the solution inside the cuvette.

Methods

Enzyme Assays

Aryl acylamidase [E.C. 3.5.1.13, aryl-acylamide amidohydrolyase] activity was measured by following the increase in absorbance at 382 nm ($\Delta\varepsilon_{382}$ = 18.4 $mM^{-1} \cdot cm^{-1}$) corresponding to the release of *p*-nitroaniline from the *p*-nitroacetanilide (*p*NAA) substrate [7]. Reaction mixtures contained 0.1 M Tris/HCl pH 8.6, 0.75 mM *p*NAA and 0.003 units of enzyme. One unit is defined as the amount of enzyme required to catalyse the hydrolysis of one μmole of *p*NAA per minute at 37°C.

Acid phosphatase [E.C. 3.1.3.2, orthophosphoric-monoester phosphohydrolase (acid optimum)] activity was measured using *p*-nitrophenylphosphate (*p*NPP) as substrate [8]. Reaction mixtures (1 mL) contained 0.1 M sodium acetate pH 5.0, 10 mM *p*NPP and 8 x 10^{-6} units of enzyme. The assay was stopped using 0.5 mL of 1 M sodium hydroxide. The amount of *p*-nitrophenol released was measured at 410 nm ($\Delta\varepsilon_{410}$ = 18.4 $mM^{-1} \cdot cm^{-1}$). One unit is defined as the amount of enzyme that hydrolyses one μmole of *p*NPP to *p*-nitrophenol per minute at 37°C.

β-lactamase [E.C. 3.5.2.6, β-lactamhydrolase] activity was measured by following the increase in absorbance at 485nm ($\Delta\varepsilon_{485}$ = 20.5 $mM^{-1}\cdot cm^{-1}$) associated with the hydrolysis of the β-lactam ring of nitrocefin [9]. Reaction mixtures contained 0.05 M sodium phosphate pH 7.0, 1 mM EDTA, 0.1 mM nitrocefin and 0.003 U of enzyme. One unit is defined as that which will hydrolyse the β-lactam ring of one μmole of cephalosporin per minute at 25°C.

Malate dehydrogenase [E.C. 1.1.1.37, (S)-malate:NAD+ oxidoreductase] activity was measured in the direction of oxaloacetate formation using malate as substrate [10]. Reaction mixtures (1 mL) contained 100 mM sodium pyrophosphate pH 8.0, 20 mM malate, 20 mM NAD^+, 10mM semicarbazide and 0.25 units of enzyme. The reaction was monitored at 340nm ($\Delta\varepsilon_{340}$ = 6.23 $mM^{-1}\cdot cm^{-1}$), which corresponds to the formation of NADH. One unit is defined as the amount of enzyme that hydrolyses one μmole of oxaloacetate to malate per minute at 25°C.

Protein determination

Protein concentrations claimed by the manufacturers (determined by Biuret) were checked using the far UV method of Scopes [11].

Data analysis

Although earlier determinations of $\Delta G^{\ddagger}_{cat}$, $\Delta G^{\ddagger}_{inact}$, ΔH_{eq} and T_{eq} used initial parameter estimates derived from "2-D" analysis (described in [2]), more recent analysis of results indicates that the method described below is simpler and equally accurate.

Using the values for $\Delta G^{\ddagger}_{cat}$, $\Delta G^{\ddagger}_{inact}$, ΔH_{eq} and T_{eq} described in the original paper [1] as initial parameter estimates (deemed to be "typical" or "plausible" values for each of the parameters, see Table 1) and the concentration of protein in each assay (expressed in M), the experimental data (expressed as rates, in $M \cdot s^{-1}$) was fitted to the 'Equilibrium Model' using MicroMath® Scientist® for Windows™ (Version 2.01, MicroMath Scientific Software, Inc.) software.

Table 1 **"Typical" or "plausible" values for $\Delta G^{\ddagger}_{cat}$, $\Delta G^{\ddagger}_{inact}$, ΔH_{eq} and T_{eq}**

Parameter	*Value*
$\Delta G^{\ddagger}_{cat}$ ($kJ \cdot mol^{-1}$)	80
$\Delta G^{\ddagger}_{inact}$ ($kJ \cdot mol^{-1}$)	95
ΔH_{eq} ($kJ \cdot mol^{-1}$)	100
T_{eq} (K)	320

As described in [1].

The values for each parameter were first "improved" by Simplex searching [12, 13]. The experimental data was then fitted to the 'Equilibrium Model' using the parameters derived from the Simplex search, employing a re-iterative, non-linear minimisation of the least squares function of the analytical rate equation. This minimisation utilises Powell's algorithm [14], to find a local minimum, possibly a global minimum, of the sum of squared deviations between the experimental data and the model calculations.

In each case, the fitting routine was set to take minimum and maximum iterative step-sizes of 1 $x10^{-12}$ and 1, respectively. The sum of squares goal – the termination criterion for the fitting routine – was set to 1 x 10^{-12}.

The "fit" of the raw data to the 'Equilibrium Model' was then verified by visual means, by comparing the 3D plot of rate (in $\mu M \cdot s^{-1}$) versus temperature (in Kelvin) versus time (in seconds) of the smoothed raw data (generated by SigmaPlot® 2001 for Windows (Version 7.101, SPSS Inc.) applying a Loess algorithm [15] (a curve-fitting technique based on local regression that applies a tricube weight function to elicit trends from noisy data) to the 3D plot generated in Scientist® by the 'Equilibrium Model'.

Results

Robustness of the fitted constants

When fitting experimental data to a model, the results of the fitting can only be as good as the data provided to the Model. The 'Equilibrium Model' has two inputs – enzyme concentration and rate of reaction.

Unless the enzyme preparation used in the determination of T_{eq} is pure, then over-estimation of the enzyme concentration is likely. Additionally, few methods of determining the concentration of protein in a sample give answers that are unequivocally correct; apart from each method having its limitations, in terms of sensitivity and interferences, most are based on a comparison with a standard of uncertain equivalence to the enzyme under investigation. Therefore, the determination of protein concentration yields, at best, only a fairly good estimate of the enzyme concentration.

Likewise, considering unavoidable sources of error (limits of detectability, instrument noise, instrument response delays), the rate of reaction measured can only be a fair estimation of the true rate of reaction. This effect is magnified when measuring rates over short time scales and over small changes in absolute absorbance.

To determine how dependent the fitted constants are on the accuracy of the protein concentration and enzyme reaction rate, the data for β-lactamase was fitted against the experimentally determined rates with the enzyme concentration reduced five-fold. The data was then refitted with the correct enzyme concentration but with the experimentally determined rates reduced by 15%.

Table 2 illustrates the effect of input data accuracy on the final parameter values returned by fitting data to the 'Equilibrium Model'.

In changing the enzyme concentration five-fold, there is very little difference in parameter values for $\Delta G^{\ddagger}_{inact}$, ΔH_{eq} and T_{eq} (all differences are with errors) in comparison to the parameters derived using the correct enzyme rate. Unsurprisingly, the value of $\Delta G^{\ddagger}_{cat}$ is reduced as the model attempts to relate the reduced enzyme concentration to the observed rates of reaction. However, in reducing the enzyme rates fitted to the Model by 15%, the values for $\Delta G^{\ddagger}_{cat}$ and $\Delta G^{\ddagger}_{inact}$ remain unchanged (within errors) but the values for ΔH_{eq} and T_{eq} fall well outside the error range.

One of the criteria for collecting rate data for fitting to the 'Equilibrium Model' is that "three progress curves are collected at each temperature - where the slope for these triplicates deviates by more than 10%, the reactions are repeated". The data shown here support this criterion, where it is seen that it is not until there is a 15% reduction in reaction rates that the parameter values start to deviate. This suggests that rates of reaction could be underestimated by up to 15% across the temperature range yet still yield a good estimation of the true parameter values. Beyond a 15% reduction, fitting the data to the 'Equilibrium Model' becomes more difficult and results in greater deviation of the parameter values (data not shown).

Table 2 **The effect of input data accuracy on parameter values**

Parameter values are quoted ± 1 standard deviation

	Correct [E_0] *Correct rate*	*[E_0] reduced five-fold* *Correct rate*	*Correct [E_0]* *Rate reduced 15%*
$\Delta G^{\ddagger}_{cat}$ ($kJ \cdot mol^{-1}$)	68.9±0.1	64.8±0.1	69.0±0.1
$\Delta G^{\ddagger}_{inact}$ ($kJ \cdot mol^{-1}$)	93.7±0.1	93.5±0.1	94.0±0.1
ΔH_{eq} ($kJ \cdot mol^{-1}$)	146±2	144±2	120±2
T_{eq} (K)	326±1	327±1	324±1
$[E_0]$ (M)	5.5×10^{-9}	1.1×10^{-9}	5.5×10^{-9}

Data Sampling Requirements - Sampling Rate

To determine the sampling requirement for discontinuous assays, progress curves for the reaction catalysed by aryl acylamidase were collected over a 30 minute period at a variety of temperatures. Three progress curves were collected at each temperature - where the slope for these triplicates deviated by more than 10%, the reactions were repeated. Data was collected every second. Progress curves were then manipulated by the removal of data points to determine the effect of sampling rate on the fitting of the data to the 'Equilibrium Model' and on the resulting parameters

Each manipulated data set was then fitted to the 'Equilibrium Model' and the corresponding parameters derived. Table 3 shows the parameters from each fit for the different sampling rates.

The results indicate that across the range of sampling rates, although the standard error increases, the values for each parameter are relatively constant, except in the case of ΔH_{eq} where the value begins to drift upwards as the sampling interval is increased. If it is assumed that the 1-second sampling interval represents the "correct" value for each parameter, then all sampling intervals give values which are within the limits of the standard deviation.

Using the 1-second sampling interval as a reference, the differences on the absolute values of $\Delta G^{\ddagger}_{cat}$, $\Delta G^{\ddagger}_{inact}$ and T_{eq} at all sampling rates (up to 120 seconds) are less than 1% despite the increase in the standard deviation as the sampling interval increases.

The differences in the absolute values of ΔH_{eq} up to and including a sampling interval of 60-seconds are less than 8%. Beyond the 60-second sampling interval (at 120-seconds), the difference in the estimate of ΔH_{eq} is large.

The results indicate that discontinuous enzyme assays can be used for the accurate determination of T_{eq}; stopping the reaction at, say, 60 second intervals will potentially give quite adequate results, except possibly for ΔH_{eq}. It also indicates that accuracy is not dominated by a requirement for "early" data, taken very soon after zero time. The data also suggests that the value of ΔH_{eq} is much more sensitive to experimental error than the other parameters; this is not surprising since ΔH_{eq} arises in the 'Equilibrium Model' from an exponential function raised to an exponential function.

Table 3 **Data sampling requirements – sampling rate**

Final parameter values for fitting data at various sampling rates to the 'Equilibrium Model'. Parameter values are quoted ± 1 standard deviation.

Sampling rate	*1s*	*5s*	*10s*	*20s*	*60s*	*120s*
Assay duration	*1800s*	*1800s*	*1800s*	*1800s*	*1800s*	*1800s*
Nº. of points	*1800 points*	*360 points*	*180 points*	*90 points*	*30 points*	*15 points*
$\Delta G^{\ddagger}_{cat}$ ($kJ \cdot mol^{-1}$)	74.3±0.2	74.1±0.2	74.4±0.3	74.4±0.4	74.4±0.6	74.5±0.7
$\Delta G^{\ddagger}_{inact}$ ($kJ \cdot mol^{-1}$)	94.1±0.4	94.1±0.7	93.4 ± 1.0	93.1±1.4	93.4±2.3	94.0±4.0
ΔH_{eq} ($kJ \cdot mol^{-1}$)	134±12	136±20	141±29	149±43	138±69	188±129
T_{eq} (K)	310±1	309±1	311±2	311±2	310±4	311±5
T_{opt} (K)	312	311.5	312	312	311.5	311.5

Data Sampling Requirements - Temperature Range

In previous determinations of T_{eq} and associated thermodynamic parameters [2], enzymes have been assayed at 12-15 temperatures, at 3-5°C intervals depending on the temperature range of the enzyme (usually estimated by examining previous characterisation studies of the target enzyme).

Progress curves at twelve temperatures were collected for the enzyme, β-lactamase. Analysis of the initial rate of reaction (and therefore, at zero time) shows two points above the temperature at which maximum product is formed (Figure 2).

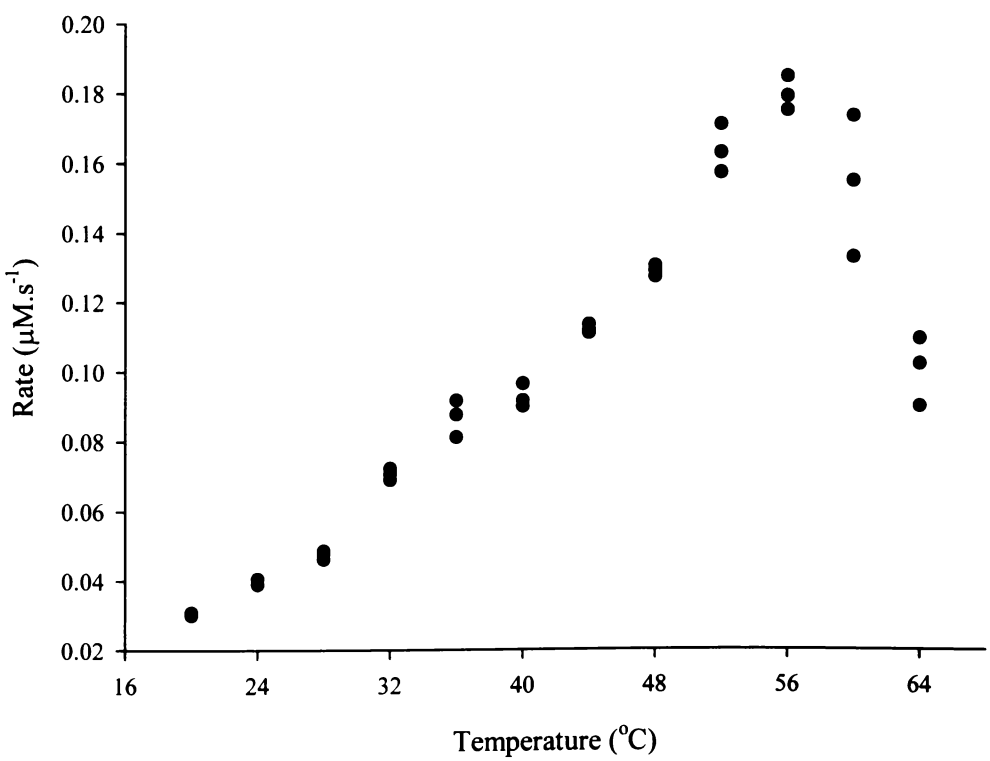

Figure 2 **The effect of temperature on the initial rate of reaction - β-lactamase**

For each assay triplicate, the initial rate of reaction was determined using the linear search function in the program, Vision32™.

By re-fitting the data, firstly excluding the last data point and then fitting again excluding the last two data points, we gain some insight into the dependence of the fitting routine and accurate estimation of the parameters on the data points above the "temperature optimum". Table 4 illustrates the differences in the final parameter estimates for the three fitting procedures.

As expected, the values of $\Delta G^{\ddagger}_{cat}$, as with the previously examined data sets, do not vary wildly with the various data treatments. Using the values for the full data set as a reference, the difference is less than 1%. For the data set excluding the last data point, the values $\Delta G^{\ddagger}_{inact}$, and T_{eq} are also in good agreement, but for the fit excluding the last two data points, there are substantial differences as well as increases in the standard deviation.

Table 4 The effect of data points "over the top" on the final parameter estimates for data fitted to the Equilibrium Model.

Parameter values are quoted ± 1 standard deviation

	Full data set	*Minus last point*	*Minus last 2 points*
$\Delta G^{\ddagger}_{cat}$ ($kJ \cdot mol^{-1}$)	68.9±0.1	68.8±0.1	69.8±2.0
$\Delta G^{\ddagger}_{inact}$ ($kJ \cdot mol^{-1}$)	93.7±0.1	93.7 ±0.1	80.3±17
ΔH_{eq} ($kJ \cdot mol^{-1}$)	146±2	122±2	84±16
T_{eq} (K)	326±1	325±1	392±84

Again, the results suggest that determining ΔH_{eq} with accuracy is more difficult than for the other parameters. The results show a ~10% difference in ΔH_{eq} for the fit excluding the last data point and a ~33% difference in ΔH_{eq} for the fit excluding the last two data points. Figure 3 illustrates the differences in each fitting of the truncated data sets to the 'Equilibrium Model' presented as a 3D plot of rate (in $\mu M \cdot s^{-1}$) versus temperature (in Kelvin) versus time (in seconds).

The plots indicate that, although when only one data point is removed there is very little difference in the shape of the plot when the data are simulated in three dimensions, without a data point above the T_{opt}, the equilibrium model effectively relapses towards the 'Classical Model' (Figure 1B), with a sharp decline in ΔH_{eq} and a sharp increase in T_{eq}. However, the results suggest that it is possible to obtain reasonable estimates of the parameters (except ΔH_{eq}) with only one temperature point above the "temperature optimum". This result has been confirmed by treating data for other enzymes in a similar manner (data not shown).

To determine how many points in total, above and below the temperature optimum, are required for the accurate determination of T_{eq} and the other thermodynamic parameters, temperature points were sequentially truncated lowest temperature point to highest from the data set for β-lactamase. Each data set included both points above the temperature at which maximum product was formed. Each truncated data set was then fitted to the 'Equilibrium Model'.

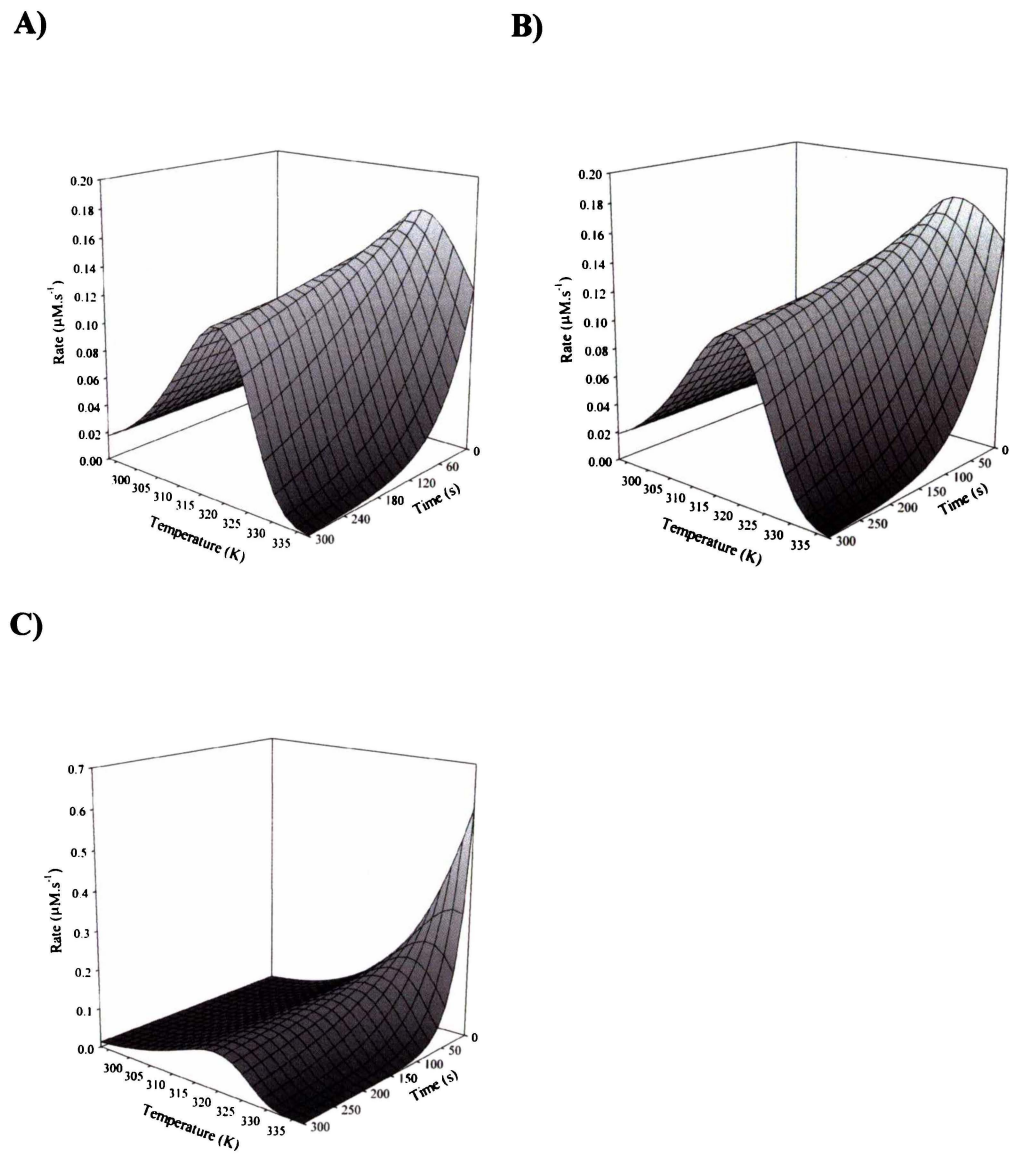

Figure 3 The effect of the number of data points "over the top" on the fit of the experimental data to the 'Equilibrium Model'

Results for the fit of β-lactamase data to the 'Equilibrium Model' using **A**), the full data set; **B**), the data set minus the last data point; and **C**), the data set minus the last two data points.

A trend in the parameter values was seen with each deletion of a temperature point (Table 5). $\Delta G^{\ddagger}_{cat}$ was fairly well conserved with each deletion; using the complete data set (twelve temperature points) as a reference, values were within errors up to and including the fit with eight temperature points. The value of $\Delta G^{\ddagger}_{inact}$ was successively reduced with each deletion; there was only a 2% difference in $\Delta G^{\ddagger}_{inact}$ between fitting all twelve of the temperature points and fitting only five temperature points, however, this difference is equivalent to a 3-fold change in k_{inact} (the inactivation rate constant) at 320 K. In this case, the values of $\Delta G^{\ddagger}_{inact}$ were within errors up to and including the fit with ten temperature points.

Again, the results suggest that determining ΔH_{eq} with accuracy is more difficult than for the other parameters, the trend being that ΔH_{eq} and T_{eq} drift upwards. A large difference in ΔH_{eq} is seen between fitting all twelve of the temperature points and fitting only five temperature points, and although the values of T_{eq} are within four degrees, the values are outside the error limits.

It is obvious that if a reduced number of data points fitted to the Model, then the accuracy of the final parameter values will suffer, as shown by the observed increase in the standard deviation on each parameter value.

The results of this data manipulation suggest that progress curves at no less than nine temperature points should be collected for accurate determination of $\Delta G^{\ddagger}_{cat}$, $\Delta G^{\ddagger}_{inact}$, ΔH_{eq} and T_{eq} including at least one temperature point beyond the "temperature optimum".

Table 5 **The effect of truncating temperature data points from the β-lactamase data set**

Temperature points were sequentially truncated, from lowest temperature point to highest, from the complete data set for β-lactamase. All values are quoted ± one standard deviation.

	5 points	*6 points*	*7 points*	*8 points*	*9 points*	*10 points*	*11 points*	*12 points*
ΔG_{cat}	70.3±0.1	70.0±0.1	69.7±0.1	69.3±0.1	69.1±0.1	69.0±0.1	69.0±0.1	68.9±0.1
ΔG_{inact}	91.6±0.2	92.0±0.2	92.7±0.2	93.3±0.1	93.6±0.1	93.6±0.1	93.7±0.1	93.7±0.1
ΔH_{eq}	233±5	213±4	195±3	165±3	159±3	152±3	146±2	146±2
T_{eq}	332±1	332±1	330±1	328±1	327±1	327±1	326±1	326±1

Discontinuous Assays

The results presented above imply that adequate data can be obtained from an assay that is sampled at time intervals up to and including 60 seconds before the error on the determination of the parameters by fitting the data to the 'Equilibrium Model' becomes prohibitive. Thus, data collected using discontinuous assays can be fitted to the 'Equilibrium Model' and the parameters derived with good accuracy.

It must be emphasised that the use of discontinuous assays over a significant period of time requires, as for continuous assays, that the reaction be "ideal"; that is, the reaction must be essentially irreversible (far from equilibrium), the enzyme must not be inhibited by substrate or product and must remain saturated with substrate throughout the assay.

Although we would expect the "data sampling" to be a satisfactory proxy for a discontinuous assay, this has been confirmed using a discontinuous assay to determine T_{eq}. Acid phosphatase was incubated with the substrate, *p*-nitrophenylphosphate for total assay duration of 30 minutes. The reaction was sampled in triplicate every 60 seconds, stopped with sodium hydroxide, and the absorbance read at 410nm. Three progress curves (absorbance versus time) at each temperature were generated from the triplicate absorbance values obtained when the reaction was stopped (Figure 4).

The catalytic rates (expressed as $M.s^{-1}$) were then calculated for each absorbance reading, and the data set fitted to the 'Equilibrium Model' as previously described. The parameter values generated from fitting this data can be found in Table 6.

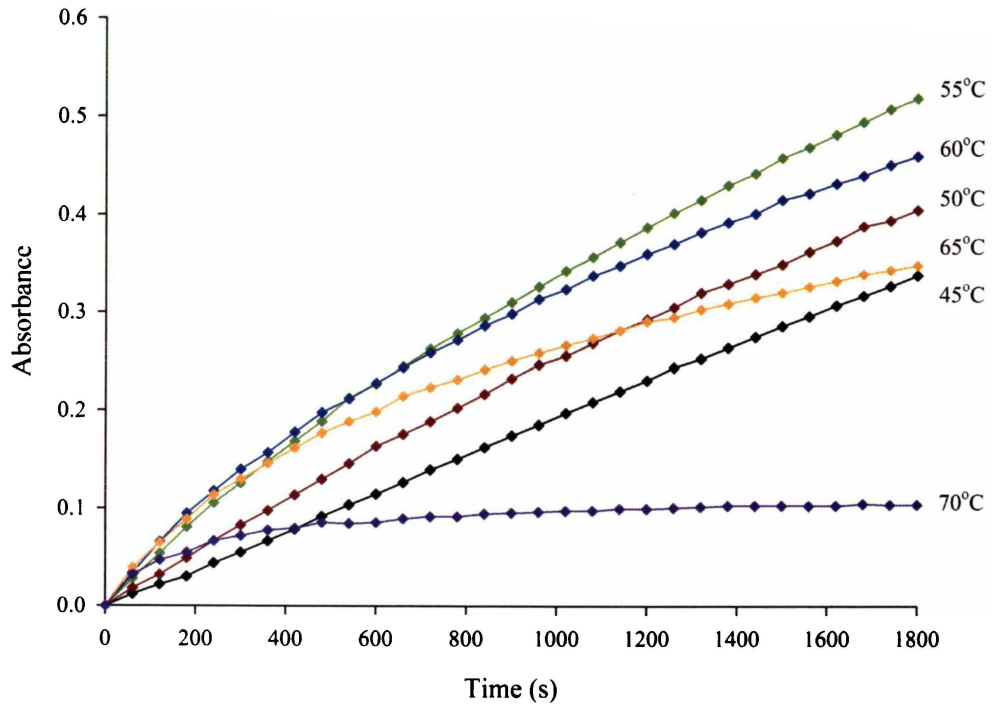

Figure 4 **Progress curves generated for acid phosphatase employing a discontinuous assay**

The values of $\Delta G^{\ddagger}_{inact}$, ΔH_{eq} and T_{eq} determined for acid phosphatase using a discontinuous assay agree with those determined for the same enzyme using a continuous assay (Table 6) within the errors calculated on each parameter determination. This is not the case for $\Delta G^{\ddagger}_{cat}$, however, the values are only just outside the error range and simulating these parameters produces graphs of rate (in $\mu M \cdot s^{-1}$) versus temperature (in Kelvin) versus time (in seconds) that are virtually indistinguishable (Figure 5).

The increased value of the errors on each parameter determined using the discontinuous data is consistent with previous results that show an increase in error as the sampling interval is increased.

Table 6 **Final parameter values for an enzyme employing a discontinuous assay**

The results of fitting data collected using a continuous assay for the same enzyme have been included for comparison. Parameter values are quoted ± 1 standard deviation.

Parameter	*Discontinuous assay*	*Continuous assay*
ΔG_{cat}	78.3 ± 0.1	79.0 ± 0.1
ΔG_{inact}	95.2 ± 0.4	94.8 ± 0.1
ΔH_{eq}	126 ± 6	133 ± 2
T_{eq}	339 ± 2	336 ± 1

A) **B)**

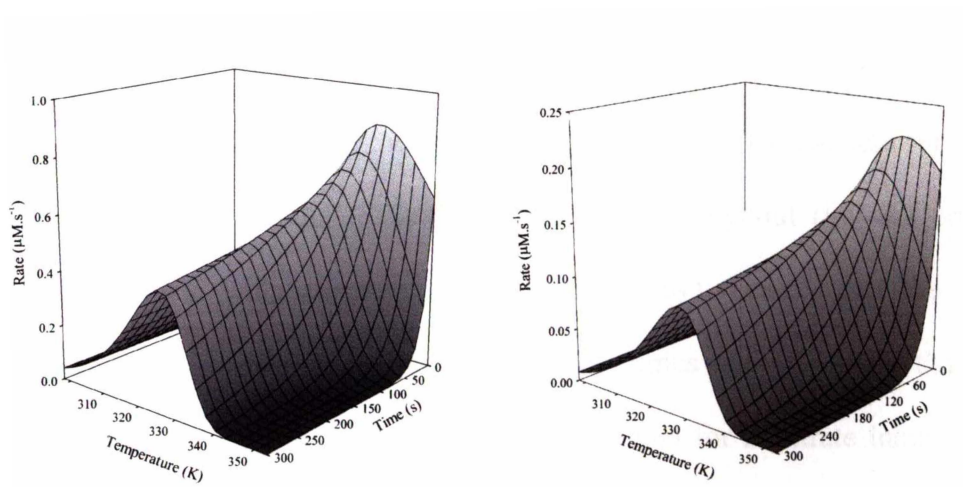

Figure 5 **Simulation of parameters determined for acid phosphatase, using A) continuous assays; and B) discontinuous assays.**

Enzymes operating under "non-ideal" conditions: the use of initial rates

Both inhibition of enzyme activity by either substrate or product and the position of the reaction equilibrium play an important role in the regulation of many biological systems. It is not uncommon for enzymes to be inhibited by high concentrations of one or more of their substrates, and the products of enzyme-catalysed reactions are frequently reversible inhibitors of the reaction. Nor is it uncommon that an enzyme strongly favours the forward direction over the reverse direction.

Up until now, all the enzymes fitted to the 'Equilibrium Model' have been "ideal"; that is the enzyme is neither product nor substrate inhibited, the reaction is essentially irreversible (far from equilibrium) and the enzyme operates at V_{max}. This allows the collection of progress curves from which a wealth of information can be derived.

However, not all enzymes are "ideal" when it comes to collecting data for fitting to the 'Equilibrium Model'. To operate at V_{max} throughout (i.e. the enzyme remains saturated with substrate for the entire assay) requires that the initial concentration of substrate be more than 10 times K_M. Given that this concentration may be non-physiological, the potential for substrate inhibition of the reaction is great. Additionally, there are a number of substrates that are unable to be dissolved at concentrations above K_M, and therefore saturating substrate concentrations can not be attained.

To collect progress curves over an extended period of time for fitting to the 'Equilibrium Model' requires that any decrease in activity observed is due solely to thermal inactivation and not some other process. Product inhibition or achievement of equilibrium prohibits this.

These problems might suggest that the utility of the 'Equilibrium Model' might be limited to "ideal" enzyme reactions. However, a solution to these problems is to use only initial rate data.

By reducing the substrate concentration below the level at which it inhibits activity, the lag phase that usually occurs with relief of the inhibition can be eliminated and the initial, linear, rate of the reaction determined, by drawing a tangent to the early, linear, part of the progress curve or more correctly, by using a nonlinear regression method [15].

At very short times, the effect of product inhibition or the position of the equilibrium on activity should not be significant. If one measures the initial rate of the reaction, and the period of linearity is prolonged by slowing the rate of product formation (by decreasing the enzyme concentration), the effect on the rate of enzyme-catalysed reaction may, to all intents and purposes, be eliminated.

Determination of initial rates means that time-dependent thermal denaturation under assay conditions is not determined and therefore the 3-D analysis of data to determine T_{eq} is impossible.

However, using only the estimates of $\Delta G^{\ddagger}_{cat}$, ΔH_{eq} and T_{eq}, it is possible to fit the experimental data for "zero time" using Equation 3.5 with time (t) set to zero

(Equation 4.1), to determine the presence of a temperature optimum in the absence of thermal denaturation.

$$\text{At } t = 0, \qquad V_{\max} = \frac{k_B T \cdot e^{\left(-\frac{\Delta G^{\ddagger}_{cat}}{RT}\right)} \cdot E_0}{h\left(1 + e^{\left(\frac{\Delta H_{eq}\left(\frac{1}{T_{eq}} - \frac{1}{T}\right)}{R}\right)}\right)} \qquad \textbf{Equation 4.1}$$

To illustrate the determination of T_{eq} for an enzyme that operates under "non-ideal" conditions, initial rates of reaction were collected for the enzyme, malate dehydrogenase. This enzyme catalyses the reduction of oxaloacetate to malate with concomitant oxidation of NADH, and under typical assay conditions, the reaction strongly favours malate formation. In this assay, the enzyme was run in the reverse direction, (oxidation of malate to oxaloacetate), under assay conditions that put the reaction close to the equilibrium position.

Three progress curves (absorbance versus time) at each temperature were generated in triplicate. The initial rate for each of the progress curves was determined using a logarithmic approximation [15].

The initial rates for each temperature were then fitted to the modified, "zero-time" version of the 'Equilibrium Model' using the Scientist® software as described previously.

Table 7 gives the parameters for fitting the initial rate data for the enzyme, malate dehydrogenase, to the "zero-time" 'Equilibrium Model'.

Table 7 Parameters for fitting initial rate data to the "zero-time" Equilibrium Model

Parameter values are quoted ± 1 standard deviation

Parameter	*Value*
$\Delta G^{\ddagger}_{cat}$ ($kJ \cdot mol^{-1}$)	52.2±0.1
ΔH_{eq} ($kJ \cdot mol^{-1}$)	383±48
T_{eq} (K)	341±1
E_0 (M)	6.4×10^{-6}

The errors on each parameter determined using the "zero-time" method are similar to those expected using the "complete" method, suggesting that this manner of determination is as good as the "complete" method for the determination of $\Delta G^{\ddagger}_{cat}$, ΔH_{eq} and T_{eq}. This observation is consistent with results obtained when the parameters from data that has been fitted to the 'Equilibrium Model' using the "complete" method are compared to those parameters obtained when the same data set is re-analysed (initial rates determined via logarithmic approximation) and fitted using the "zero-time" method (data not shown).

This result is further confirmed by visual comparison of the experimentally determined data with the data generated by the Model (Figure 6).

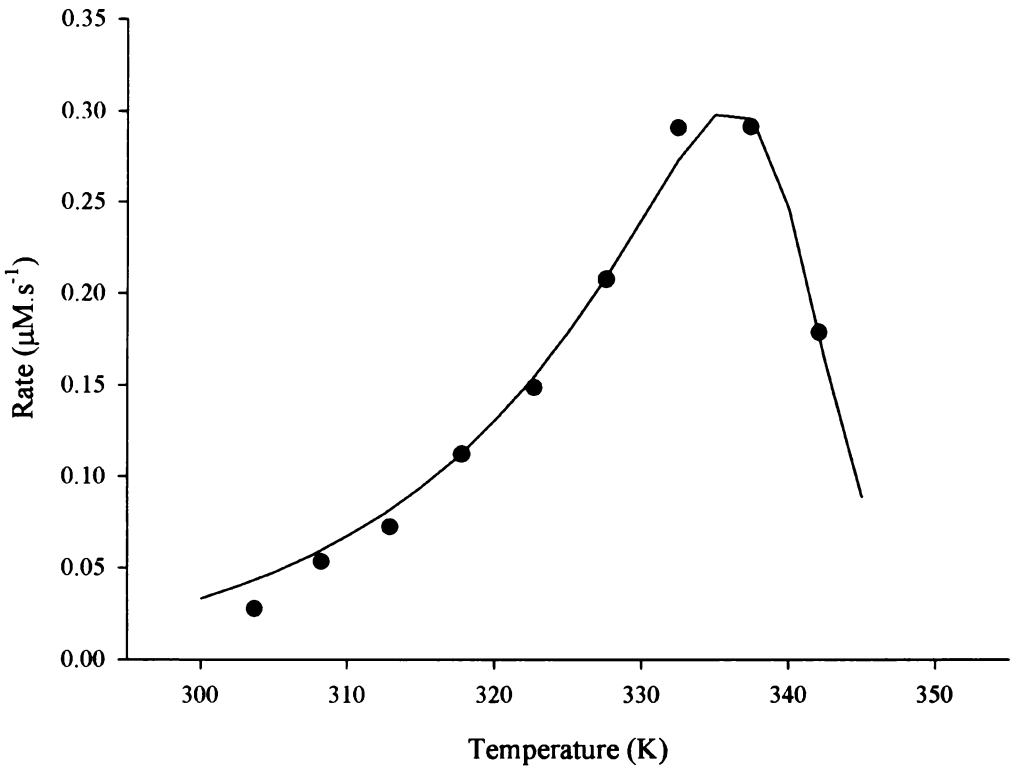

Figure 6 **The temperature dependence of malate dehydrogenase activity at time zero**

The *solid line* is the result of fitting the experimental data (solid points) to the "zero-time" version of the 'Equilibrium Model'.

Fitting "Progress Curves" Directly to the Equilibrium Model

There are two ways in which data can be fitted to the 'Equilibrium Model'. In all determinations of T_{eq} and the associated parameters to date, the experimental data fitted to the 'Equilibrium Model' has been expressed as catalytic rates (in $M \cdot s^{-1}$), calculated at 1 second time intervals along each progress curve (expressed as absolute absorbance versus time) at each temperature.

The alternative, and more correct method, is to fit progress curves (expressed as product concentration (in M) versus time) directly to the Model. This initially involves numerical differentiation of each complete reaction curve so that the amount of product formed by the reaction at any time can be calculated. The results of the differentiation of all the progress curves are then fitted to an adapted 'Equilibrium Model' equation and the parameters derived. However, it must be noted that due to program limitations, entire data sets can not be fitted using the progress curve method. Additionally, when compared to the time required for processing the data to be fitted using the catalytic rate method, manipulating the raw data into a form suitable for fitting to the Model using the progress curve method is far more time consuming.

While fitting the progress curves directly to the 'Equilibrium Model' is potentially more accurate, very similar results are obtained using the catalytic rate method. To illustrate, data for β-lactamase was treated in both manners and the results tabulated for comparison (Table 8). The fitting using the progress curve method was performed using nine temperature points, the temperature sampling limit

established above, and compared with the values derived from the fitting using the catalytic rate method using nine temperature points.

The results indicate that the use of the catalytic rate method for fitting experimental data to the 'Equilibrium Model' poses no compromise to the accuracy of the derived parameters, when compared to the parameters derived when using the potentially more accurate method of fitting using progress curves.

Table 8 Comparison of fitting techniques

Parameter values are quoted ± 1 standard deviation

	Catalytic rate analysis	*Progress curve analysis*
$\Delta G^{\ddagger}_{cat}$ ($kJ \cdot mol^{-1}$)	68.9±0.1	69.0±0.1
$\Delta G^{\ddagger}_{inact}$ ($kJ \cdot mol^{-1}$)	93.7±0.1	93.4±0.1
ΔH_{eq} ($kJ \cdot mol^{-1}$)	146±3	149±1
T_{eq} (K)	326±1	326±1

Conclusions

To date, determination of the parameters associated with the 'Equilibrium Model' for individual enzymes has involved continuous assays with collection of data at one second intervals over 5 min periods at 2-3°C temperature intervals over at least a 40°C range, with each temperature run being carried out in triplicate; i.e., processing about 15,000 data points gathered in about 50 experimental runs.

Here, the minimum assay parameters are described, in terms of sampling rate and temperature range, necessary for the determination of the parameters associated with the 'Equilibrium Model'. This has enabled more efficient and accurate determination of $\Delta G^{\ddagger}_{cat}$, $\Delta G^{\ddagger}_{inact}$, ΔH_{eq} and T_{eq} and led us to understand to what extent data collection (and thus labour) can be reduced without compromising the accuracy of the derived parameters.

With the minimum assay parameters in mind, we have demonstrated that determining T_{eq} and the associated thermodynamic parameters is not limited to those enzymes using a continuous assay. $\Delta G^{\ddagger}_{cat}$, $\Delta G^{\ddagger}_{inact}$, ΔH_{eq} and T_{eq} have been determined for an enzyme using a "stopped" enzyme assay. Establishing that this can be achieved is important, as future work might like to include the determination of T_{eq} of enzymes from extreme thermophiles, assays for which will likely be performed above 100°C and will have to be discontinuous [11].

Additionally, we have demonstrated the use of zero-time rates that enables the ready determination of the 'Equilibrium Model' parameters (except $\Delta G^{\ddagger}_{inact}$) of enzymes which are "non-ideal", for example are substrate or product inhibited, or are close to equilibrium.

Finally, we have established that our technique of fitting the raw data is robust and provides results of an acceptable accuracy, when compared to the more correct method of fitting progress curves directly to the 'Equilibrium Model'.

References

1. Daniel, R.M., Danson, M.J. & Eisenthal, R. (2001) The temperature optima of enzymes: a new perspective on an old phenomenon. *Trends in Biochemical Sciences*, **26**(4), 223 – 225.

2. Peterson, M.E., Eisenthal, R., Danson, M.J., Spence, A. & Daniel, R.M. (2004) A new, intrinsic, thermal parameter for enzymes reveals true temperature optima. *The Journal of Biological Chemistry*, **279**, 20717 – 20722.

3. Chapter 6, pg 166.

4. Daniel, R.M. & Danson, M.J. (2001) Assaying Activity and Assessing Thermostability of Hyperthermophilic Enzymes. *Methods in Enzymology*, **334**, 283 – 293.

5. Tipton, K.F. (1992) Principles of enzymes assays and kinetic studies, in *Enzyme Assays, a Practical Approach* (ed. Eisenthal, R. & Danson, M.J.) p1-58. Oxford University Press, Oxford, UK.

6. John, R.A. (1992) Photometric Assays, in *Enzyme Assays, a Practical Approach* (ed. Eisenthal, R. & Danson, M.J.) p59-92. Oxford University Press, Oxford, UK.

7. Hammond, P. M., Price, C. P. and Scawen, M. D. (1983) Purification and properties of aryl acylamidase from Pseudomonas fluorescens ATCC 39004. *European Journal of Biochemistry*, **132**, 651-655.

8. Hollander, V. P. (1971) Acid Phosphatases, in *The Enzymes*, Vol. 4 (ed. Boyer, P. D.) 449-498 (Academic Press, New York)

9. O'Callaghan, C. H., Morris, A., Kirby, S. M. and Shingler, A. H. (1972) Novel method for detection of beta-lactamases by using a chromogenic cephalosporin substrate. *Antimicrobial Agents and Chemotherapy,*. **1**, 283 – 288.

10. Wynne, S.A., Nicholls, D.J., Scawen, M.D. & Sundaram, T.K. (1996) Tetrameric malate dehydrogenase from a thermophilic *Bacillus*: cloning, sequence and overexpresssion of the gene encoding the enzyme and isolation and characterization of the recombinant enzyme. *Biochemical Journal*, **317**, 235-245.

11. Scopes, R. K. (1994) in *Protein Purification: Principles and Practice*, 3rd Edition, (ed. Cantor, C. R.) pp44-50 (Springer Verlag: San Diego)

12. Deming, S.N. & Morgan, S.L. (1973) Simplex Optimization of Variables in Analytical Chemistry. *Analytical Chemistry*, **45**, 278A – 283A.

13. Caceci, M.S. & Cacheris, W.P. (1984) Fitting Curves to Data. *Byte*, **May**, 340 – 362.

14. Powell, M.J.D. (1970) In *Numerical Methods for Nonlinear Algebraic Equations*, (ed. Robinowitz, P.) Chapter 7. Gordon & Breach Science Publishers, New York.

15. Cleveland, W. S. (1993) *Visualizing Data.* Hobart Press, New Jersey, USA.

16. Lu, W & Fei, L. (2003) A logarithmic approximation to initial rates of enzyme reactions. *Analytical Biochemistry*, **316**, 58 – 65.

Chapter Five

Factors affecting T_{eq}

This chapter deals with the collection and analysis of experimental data that examines the effect of substrate and of additives to an assay, on the position of the temperature equilibrium (T_{eq}) of enzymes.

Preliminary work in this area (in particular, the collection of the ampicillin, benzylpenicillin and urea data for β-lactamase) was performed by Kirsti Johanssen, a project student in the Thermophile Research Unit. My contribution to this work involved collection of all the other experimental data presented here, data analysis and, thus far, preparation of the manuscript.

This work forms part of a Research Article to be submitted to the Journal of Biological Chemistry and is therefore presented in the appropriate manuscript format.

The effect of varying assay conditions on the Temperature Equilibrium (T_{eq}) of enzymes

Michelle E. Peterson*, Robert Eisenthal†, Michael J. Danson††, and Roy M. Daniel*

* Department of Biological Sciences, University of Waikato, Private Bag 3105, Hamilton, New Zealand.

† Department of Biology and Biochemistry, University of Bath, Bath, BA2 7AY, UK.

†† Centre for Extremophile Research, Department of Biology and Biochemistry, University of Bath, Bath, BA2 7AY, UK.

Key words: temperature, thermostability, stability, substrate, optimum, enzyme, T_{eq}, catalysis

Corresponding Author: Professor Roy Daniel, Department of Biological Sciences, University of Waikato, Private Bag 3105, Hamilton, New Zealand

Tel: +64-7-8384213

Fax: +64-7-8384324

Email: r.daniel@waikato.ac.nz

Running Title: Factors affecting the T_{eq} of enzymes

Summary

To account for observed anomalies in the temperature-dependent behaviour of enzymes, a new model for the temperature dependence of enzyme behaviour has been developed and validated. This model (the 'Equilibrium Model') describes a reversible, temperature dependent equilibrium between the active form of the enzyme (E_{act}) and an inactive form (E_{inact}), where it is the inactive form that undergoes irreversible thermal inactivation to the thermally denatured state. The temperature dependence of the equilibrium constant that describes this equilibrium can be quantified in terms of the enthalpy of the equilibrium, ΔH_{eq}, and T_{eq}, the temperature at which E_{act} and E_{inact} are in equal concentrations.

At temperatures above its optimum, the decrease in enzyme activity arising from the temperature-dependent shift in this equilibrium is up to two orders of magnitude greater than occurs through thermal denaturation. Given this time frame, it has been hypothesised that E_{inact} is unlikely to be significantly unfolded. A reversible, local conformational change at or near the active site of the enzyme is most likely; the equilibrium between E_{act} and E_{inact} will therefore be relatively independent of the global conformational change associated with thermal denaturation. If this hypothesis is correct, then agents that affect stability but not activity should have no effect on the equilibrium (and therefore on the values of ΔH_{eq} and T_{eq}), and vice versa.

This paper describes some of the factors affecting the temperature equilibrium of enzymes, and offers evidence that the E_{act}/E_{inact} equilibrium is an active site phenomenon and somewhat independent of thermal denaturation.

Introduction

The temperature dependence of enzyme activity has previously been described by two parameters; the temperature coefficient of the catalytic rate (as defined by the Arrhenius activation energy) and thermal stability. To account for observed anomalies in the variation of enzyme activity with temperature (1-5), a new model describing the temperature dependence of enzyme activity has been developed (6). In this model (The 'Equilibrium Model'), the active form of the enzyme (E_{act}) is in reversible equilibrium with an inactive form (E_{inact}) and it is the inactive form that undergoes irreversible thermal inactivation to the thermally-denatured state (X):

$$E_{act} \leftrightarrows E_{inact} \rightarrow X$$

The variation in the equilibrium constant between active and inactive forms of the enzyme, K_{eq}, with temperature is given by:

$$\ln K_{eq} = \frac{\Delta H_{eq}}{R}\left[\frac{1}{T_{eq}} - \frac{1}{T}\right]$$

where ΔH_{eq} is the enthalpic change associated with the conversion of active to inactive enzyme, and T_{eq} is the temperature at which the E_{act} and E_{inact} are in equilibrium (i.e. the temperature at which $K_{eq} = 1$).

Data collected (7) support the 'Equilibrium Model' hypothesis, where the temperature-dependent behaviour of an enzyme can be explained only by involving K_{eq} as an intrinsic, temperature-dependent property of enzymes. The consequence is that, in such cases, T_{eq} must now be considered as a new thermal

parameter that is a characteristic of any particular enzyme and which gives rise to a true temperature optimum.

Currently, there is no evidence regarding the molecular basis of the equilibrium between E_{act} and E_{inact}, although it is clearly a fast process relative to thermal denaturation. It has been illustrated that all the variation of activity with temperature at zero time occurs as a result of changes in the E_{act}/E_{inact} equilibrium, and is thus attained over timescales shorter than the mixing process, say less than 1 second, whereas the measured rate of irreversible thermal inactivation (conversion from E_{inact} to denatured state) is at least two orders of magnitude slower over the same temperature range (7).

This paper examines the effect of altering enzyme reaction conditions on the temperature dependent equilibrium described by the 'Equilibrium Model'. Given the time frame involved, it has been hypothesised that E_{inact} is unlikely to be significantly unfolded and that a reversible conformational change is more likely; the equilibrium between E_{act} and E_{inact} will therefore be relatively independent of thermal denaturation. The enzyme reactions were altered in two ways, the first, using agents that are known to cause a local and specific effect on the active site, such as substrates; the second, using agents that are known to cause a global and non-specific effect, such as stabilising and destabilising agents.

The data presented in this paper lend support to the notion that the E_{act}/E_{inact} transition, and therefore T_{eq}, is independent of thermal denaturation. Additionally, the data show that T_{eq} is affected by factors affecting the active site.

Experimental Procedures

Enzymes and reagents

β-lactamase from *Bacillus cereus*, aryl acylamidase from *Pseudomonas fluorescens* and α-amylase from porcine pancreas were purchased from Sigma-Aldrich Inc. (St. Louis, MO., USA).

Reagents for the determination of activity of these enzymes were purchased from Sigma-Aldrich, Diagnostic Chemicals Ltd (Prince Edward Island, Canada), Oxoid Ltd (Basingstoke, UK) and Merck KGaA (Darmstadt, Germany). Betaine, EGTA and BSA were obtained from Sigma-Aldrich. All other chemicals used (sodium dodecylsulfate, deoxycholic acid, guanidium hydrochloride, cetyltrimethylammonium chloride, urea, sorbitol and glycerol) were of analytical grade. Buffers were adjusted to the appropriate pH value at the temperature of use, using a combination electrode calibrated at this temperature.

Enzyme Assays

β-lactamase [E.C. 3.5.2.6; β-lactamhydrolase] activity was measured by four methods:

a) following the increase in absorbance at 485nm ($\Delta\varepsilon_{485}$ = 20500 $M^{-1}cm^{-1}$) associated with the hydrolysis of the β-lactam ring of nitrocefin (8). Reaction mixtures contained 0.05 M sodium phosphate pH 7.0, 0.1 mM nitrocefin and 0.003 U of enzyme plus the appropriate amount of effector. One unit is defined as that which will hydrolyse the β-lactam ring of one μmole of cephaloridine per minute at 25°C;

b) following the increase in absorbance at 320nm ($\Delta\varepsilon_{320}$ = 1067 $M^{-1}cm^{-1}$) associated with the hydrolysis of the β-lactam ring of cefazolin (9). Reaction mixtures contained 0.05 M sodium phosphate pH 7.0, 2 mM cefazolin and 0.005 U of enzyme. One unit is defined as that which will hydrolyse the β-lactam ring of one μmole of cephaloridine per minute at 25°C;

c) following the decrease in absorbance at 240nm ($\Delta\varepsilon_{240}$ = 820 $M^{-1}cm^{-1}$) associated with the hydrolysis of the β-lactam ring of benzylpenicillin (10). Reaction mixtures contained 0.05 M sodium phosphate pH 7.0, 1.5 mM benzylpenicillin and 1 x 10^{-6} U of enzyme. One unit is defined as that which will hydrolyse the β-lactam ring of one μmole of benzylpenicillin per minute at 25°C;

d) following the decrease in absorbance at 240nm ($\Delta\varepsilon_{240}$ = 700 $M^{-1}cm^{-1}$) associated with the hydrolysis of the β-lactam ring of ampicillin (11). Reaction mixtures contained 0.05 M sodium phosphate pH 7.0, 1.5 mM ampicillin and 1 x 10^{-6} U of enzyme. One unit is defined as that which will hydrolyse the β-lactam ring of one μmole of benzylpenicillin per minute at 25°C.

Aryl acylamidase [E.C. 3.5.1.13; aryl-acylamide amidohydrolyase] activity was measured by following the increase in absorbance at 382nm ($\Delta\varepsilon_{382}$ = 18.4 $mM^{-1}\cdot cm^{-1}$ corresponding to the release of *p*-nitroaniline from the *p*-nitroacetanilide (*p*NAA) (12). Reaction mixtures contained 0.1 M Tris/HCl pH 8.6, 0.75 mM *p*NAA and 0.018 units of enzyme plus the appropriate concentration of effector. One unit is defined as the amount of enzyme required to catalyse the hydrolysis of one μmole of *p*NAA per minute at 37°C. Aryl acylamidase activity was also

determined at pH 7.02 in a similar manner ($\Delta\varepsilon_{382}$ = 13.27 $mM^{-1}\cdot cm^{-1}$; see appendix C)

Data collection

All enzymic activities were measured using a Thermospectronic™ Helios γ-spectrophotometer equipped with a Thermospectronic™ single cell peltier-effect cuvette holder. This system was networked to a computer installed with Vision32™ (Version 1.25, Unicam Ltd) software including the Vision Enhanced Rate Programme capable of recording absorbance changes over time intervals down to 0.125 seconds.

The temperature of each assay was recorded directly, using a Cole-Parmer Digi-Sense® thermocouple thermometer accurate to ± 0.1% of the reading and calibrated using a Cole-Parmer NIST-traceable high-resolution glass thermometer. The temperature probe was placed inside the cuvette adjacent to the light path during temperature equilibration prior to the initiation of the reaction and again immediately after completion of each enzyme reaction. Measurements of temperature were also taken at the top and bottom of the cuvette to check for temperature gradients. Where the temperature measured before and after the reaction differed by more than 0.1°C, the reaction was repeated.

Buffers were adjusted to the appropriate pH value at the assay temperature, using a combination electrode calibrated at this temperature.

Substrate concentrations were maintained at ~10 times K_M to minimise the effects of any increases in K_M with temperature and to ensure that the enzyme remains saturated with substrate for the entire assay duration. Where these concentrations

could not be maintained (e.g. because of substrate solubility), tests were conducted to confirm that there was no decrease in rate over the assay period arising from substrate depletion.

Assays reactions were initiated by the addition of microlitre amounts of enzyme (less than 2% of the total assay volume) that had no significant effect on the temperature of the solution inside the cuvette.

Three progress curves were collected at each temperature - where the slope for these triplicates deviated by more than 10%, the reactions were repeated.

Data analysis

Using the values for $\Delta G^{\ddagger}_{cat,}$ $\Delta G^{\ddagger}_{inact}$, ΔH_{eq} and T_{eq} described in the original paper (1) as initial parameter estimates and the concentration of protein in each assay (expressed in mol $\cdot$ L^{-1}), the experimental data (expressed as rates, in mol $\cdot$ L^{-1} $\cdot$ s^{-1}) was fitted to the 'Equilibrium Model' using MicroMath® Scientist® for Windows™ (Version 2.01, MicroMath Scientific Software, Inc.) software.

The values for each parameter were first "improved" by Simplex searching (13, 14). The experimental data was then fitted to the 'Equilibrium Model' using the parameters derived from the Simplex search, employing a re-iterative, non-linear minimisation of the least squares function of the analytical rate equation. This minimisation utilises Powell's algorithm (15), to find a local minimum, possibly a global minimum, of the sum of squared deviations between the experimental data and the model calculations.

In each case, the fitting routine was set to take minimum and maximum iterative step-sizes of 1 $x10^{-12}$ and 1, respectively. The sum of squares goal – the termination criterion for the fitting routine – was set to 1 x 10^{-12}.

The "fit" of the raw data to the 'Equilibrium Model' was then verified by visual means, by comparing the 3D plot of rate (in $\mu M \cdot s^{-1}$) versus temperature (in Kelvin) versus time (in seconds) of the smoothed raw data (generated by SigmaPlot® 2001 for Windows (Version 7.101, SPSS Inc.) applying a Loess algorithm (16) (a curve-fitting technique based on local regression that applies a tricube weight function to elicit trends from noisy data) to the 3D plot generated in Scientist® by the 'Equilibrium Model'.

Protein determination

The protein concentrations (determined by Biuret) claimed by the manufacturers were checked using the far UV method of Scopes (17).

Results

The effect of substrate on T_{eq}

Reaction rate versus temperature versus time data were collected for the enzyme, β-lactamase, against four different antibiotic substrates. The four substrates are representatives of two of the four classes of β-lactam antibiotics; benzyl penicillin and ampicillin representing the penicillins and nitrocefin and cefazolin representing the cephalosporins. Figure 1 shows the structure of each substrate.

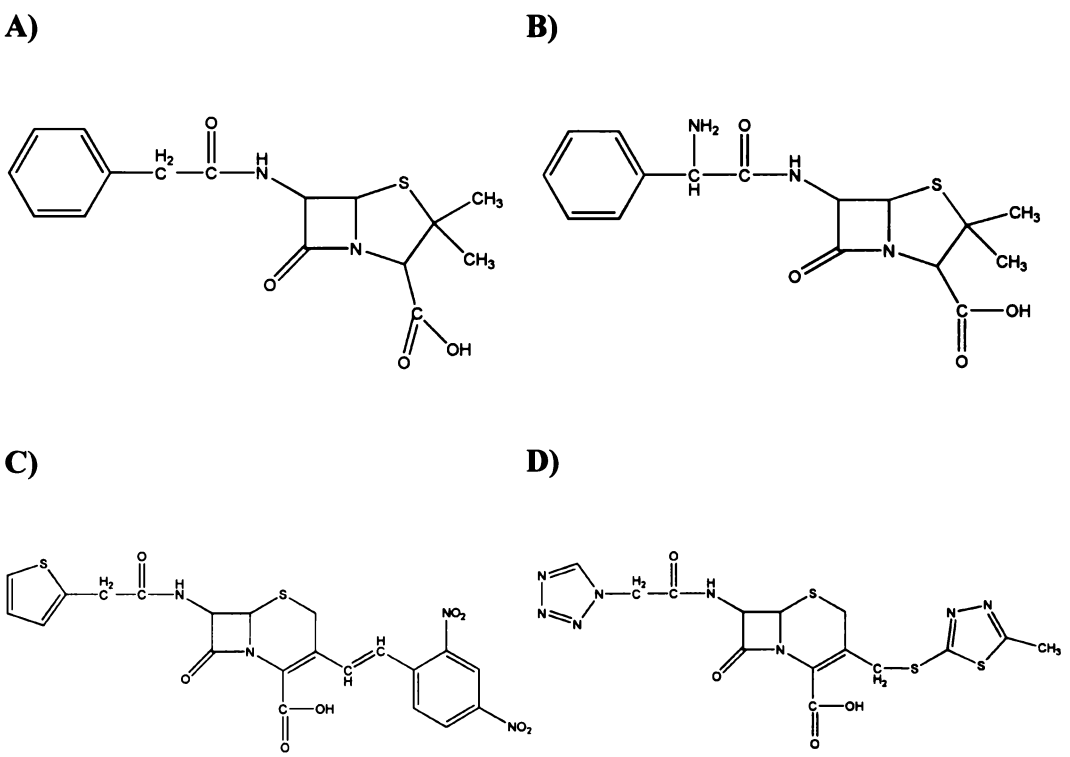

Figure 1 Chemical structure of the four antibiotic substrates tested against β-lactamase

A) benzyl penicillin, **B)** ampicillin, **C)** nitrocefin, **D)** cefazolin

The data collected for β-lactamase against each substrate was fitted to the 'Equilibrium Model' and values for $\Delta G^{\ddagger}_{cat}$, $\Delta G^{\ddagger}_{inact}$, ΔH_{eq} and T_{eq} derived (Table I).

For the penicillin class substrates, where the representatives differ only by a single amine group, the difference in the values for each thermodynamic parameter is insignificant (within errors).

For the cephalosporin class substrates, T_{eq} and T_{opt} occur at higher temperatures and an increase in the value of ΔH_{eq} is observed in comparison to the penicillin class substrates.

The cephalosporin substrate, nitrocefin ($t_{½}$ = 206 s at 320 K), appears to slightly destabilise β-lactamase in comparison to ampicillin and benzyl penicillin ($t_{½}$ = 311 s and 288 s at 320 K, respectively) while the saturation of the active site with cefazolin appears to have a marked stabilising effect ($t_{½}$ = 1296 s at 320 K). This is particularly interesting, since despite the difference in stability conferred by cefazolin compared with the relatively structurally similar nitrocefin, the values for T_{eq} for each cephalosporin substrate are similar if compared with the values determined for the penicillin substrates. Additionally, the values of ΔH_{eq} determined for both cephalosporin substrates are somewhat similar despite the differences in $\Delta G^{\ddagger}_{cat}$.

Interestingly, the 3D plots resulting from the fit of the experimental data to the 'Equilibrium Model' are very similar in shape (particularly around T_{opt}) within classes of antibiotic substrate, yet are somewhat different between the classes of antibiotic substrates (Figure 2).

Table I The effect of substrate on T_{eq}

Parameters for $\Delta G^{\ddagger}_{cat}$, $\Delta G^{\ddagger}_{inact}$, ΔH_{eq} and T_{eq} were determined by fitting the data to the 'Equilibrium Model'. T_{opt} is defined as the temperature at which maximum velocity is attained at zero time and was determined by fitting the data to the Model with time (t) set to zero.

	$\Delta G^{\ddagger}_{cat}$	$\Delta G^{\ddagger}_{inact}$	ΔH_{eq}	T_{eq}	T_{opt}	E_0
	($kJ \cdot mol^{-1}$)	($kJ \cdot mol^{-1}$)	($kJ \cdot mol^{-1}$)	(K)	(K)	(M)
Benzylpenicillin	65.7±0.1	94.6±0.4	111±4	304±1	308	$7.8x10^{-8}$
Ampicillin	65.4±0.1	94.8±0.4	114±4	304±1	307	$7.8x10^{-8}$
Nitrocefin	68.9±0.1	93.7±0.1	146±2	326±1	326	$5.5x10^{-9}$
Cefazolin	76.5±0.1	98.6±0.2	152±3	331±1	332	$6.3x10^{-7}$

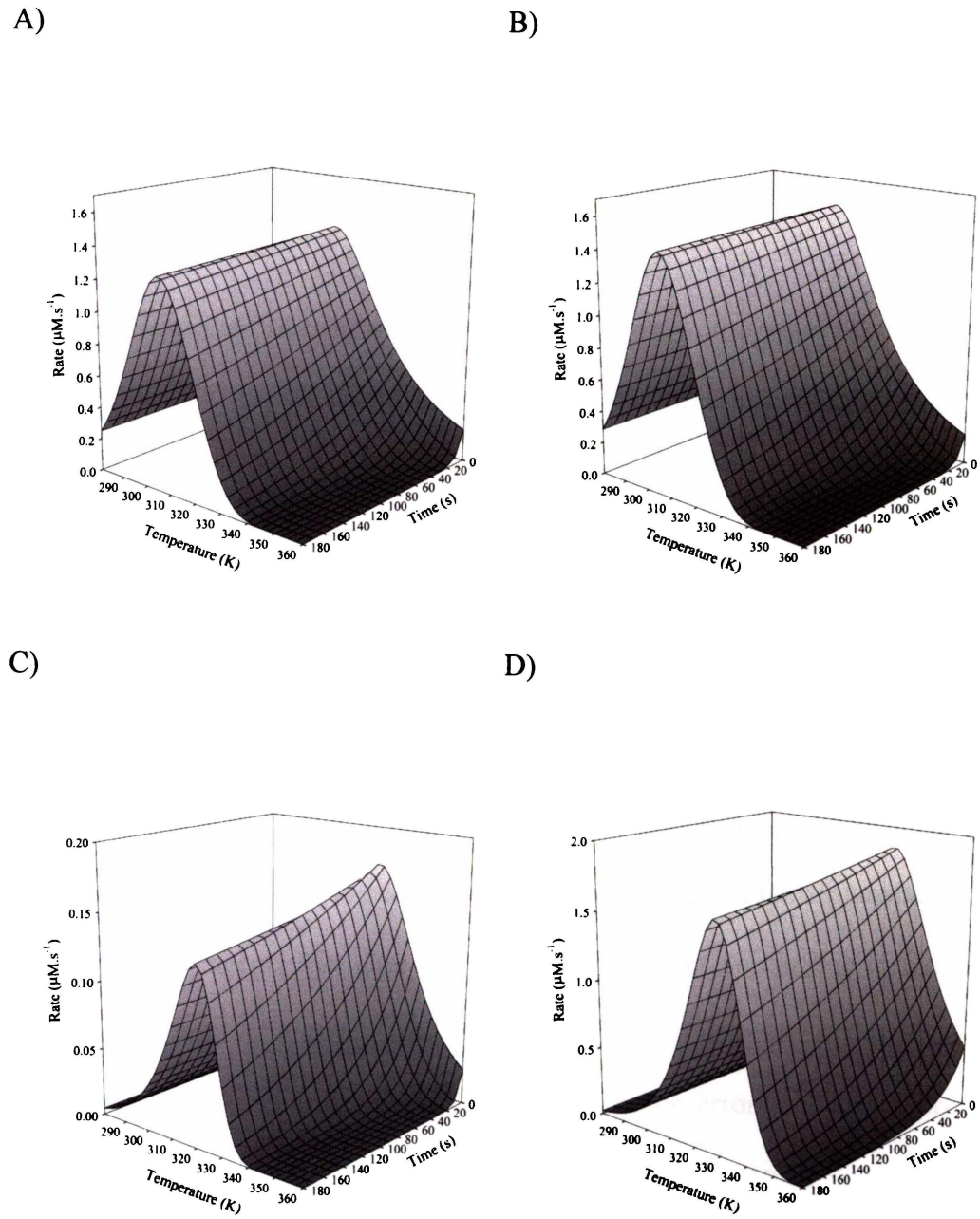

Figure 2 The effect of substrate on the shape of the 3D plot resulting from the fit of experimental data to the 'Equilibrium Model'

A) benzylpenicillin; B) ampicillin; C) nitrocefin; D) cefazolin

The effect of stabilising and destabilising agents on T_{eq}

Data on the effect of time and temperature on reaction rate were collected for β-lactamase and aryl acylamidase, in the presence of a number of agents that are known to affect their stability. The data collected in the presence of each agent were fitted to the 'Equilibrium Model' and values for $\Delta G^{\ddagger}_{cat}$, $\Delta G^{\ddagger}_{inact}$, ΔH_{eq} and T_{eq} determined (Table II).

It was not expected that the addition of these agents to the assay solution would have an effect on the way the reaction rate increases with temperature. Accordingly, $\Delta G^{\ddagger}_{cat}$ was fairly well conserved.

Consistent with previous knowledge of the effect of these agents on the stability of enzymes (18-23), differences in the thermal stability (expressed here as $\Delta G^{\ddagger}_{inact}$ and $t_{½}$) of the enzyme in the presence of these agents were observed.

Given the notion that the E_{act}/E_{inact} transition, and therefore T_{eq}, is independent of thermal denaturation, it is expected that the value of T_{eq} will remain unaffected by the addition of agents that alter the thermal stability of an enzyme to the assay solution. Indeed, T_{eq} and T_{opt} are fairly well conserved; in general, the values are scattered about the control values and are within the errors calculated on each fitting of the data to the 'Equilibrium Model' when compared with the control assay conditions. Comparison of the zero time plots for the enzymes in the presence of the effects further confirms this observation (Figures 5.3 & 5.4).

Aryl acylamidase in the presence of 20% glycerol produces the only value for T_{eq} well outside the calculated errors; while it was not evident under the conditions

specified here, a reduction in rate has been observed with increasing concentrations of glycerol, suggesting some non-specific inhibition (24). The anomalous value of T_{eq} determined for aryl acylamidase in the presence of 20% glycerol might be attributed to this observation.

A variation in ΔH_{eq} is observed, consistent with other results that suggest that the value of ΔH_{eq} is much more sensitive to experimental error than the other parameters (25); this is not surprising since ΔH_{eq} arises in the 'Equilibrium Model' from an exponential function raised to an exponential function.

Table II The effect of stabilising and destabilising agents on T_{eq}

Parameters for $\Delta G^{\ddagger}_{cat}$, $\Delta G^{\ddagger}_{inact}$, ΔH_{eq} and T_{eq} were determined by fitting the data to the 'Equilibrium Model'. Parameter values are quoted ± 1 standard deviation. T_{opt} is defined as the temperature at which maximum velocity is attained at zero time and was determined by fitting the data to the Model with time (t) set to zero. Half-life ($t_{½}$) was determined at 315 K.

	$\Delta G^{\ddagger}_{cat}$ (kJ·mol^{-1})	$\Delta G^{\ddagger}_{inact}$ (kJ·mol^{-1})	ΔH_{eq} (kJ·mol^{-1})	T_{eq} (K)	T_{opt} (K)	$t_{½}$ (s)
β-lactamase						
Nitrocefin	68.9±0.1	93.7±0.1	146±2	326±1	326	365
+ 0.1 M urea	68.9±0.1	92.3±0.1	150±2	325±1	325	214
+ 4mg.mL^{-1} BSA	69.7±0.1	94.2±0.1	202±3	328±1	326	442
+ 2.5 M sorbitol	68.9±0.1	95.9±0.1	135±2	329±1	330	846
Aryl acylamidase						
p-nitroacetanilide	74.4±0.1	92.4±0.1	133±2	310±1	312	222
+ 0.005% SDS	76.6±0.1	91.2±0.3	135±6	309±1	312	141
+ 0.2 mM deoxycholic acid	75.4±0.1	91.8±0.4	143±5	310±1	311	177
+ 0.00005% CTAB	75.1±0.1	91.8±0.1	160±3	313±1	313	177
+ 0.1 M guanidium HCl	74.8±0.1	90.1±0.1	137±3	309±1	310	92
+ 0.1 M betaine	75.0±0.1	93.0±0.1	142±3	313±1	314	280
+ 20% glycerol	75.0±0.1	95.3±0.3	162±3	316±1	316	673

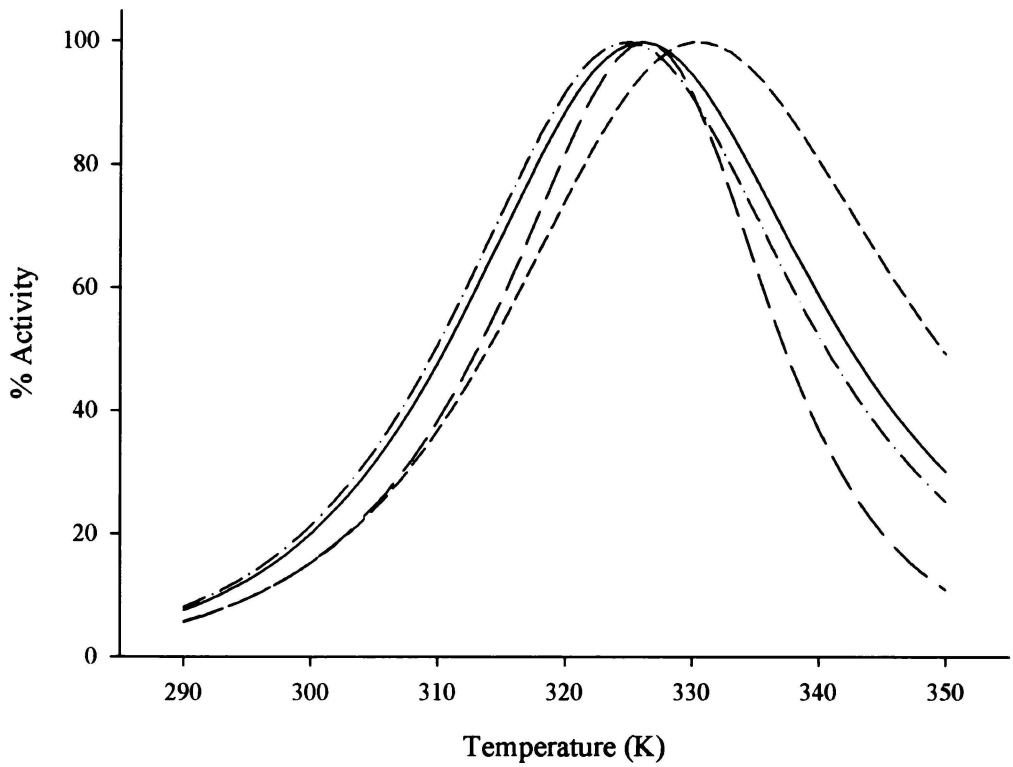

Figure 3 Temperature dependence of enzymic activity at time zero for β-lactamase in the presence of stabilising and destabilising agents

Enzymic activities at time zero were plotted against temperature to demonstrate the independence of enzymic activity at zero time on the presence of agents that affect thermal inactivation. The activity data for each enzyme are scaled from 5-100% relative to the maximum activity for that enzyme. β-lactamase (solid line); β-lactamase + BSA (– – – –); β-lactamase + sorbitol (-------); β-lactamase + urea (· – · –).

A)

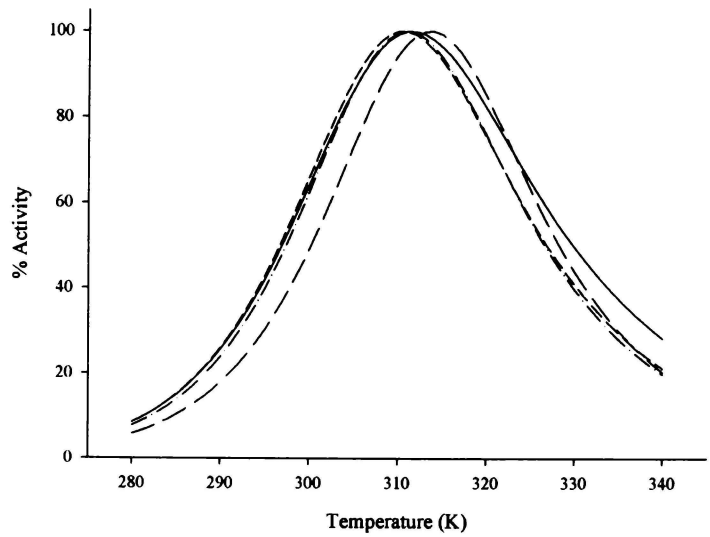

B)

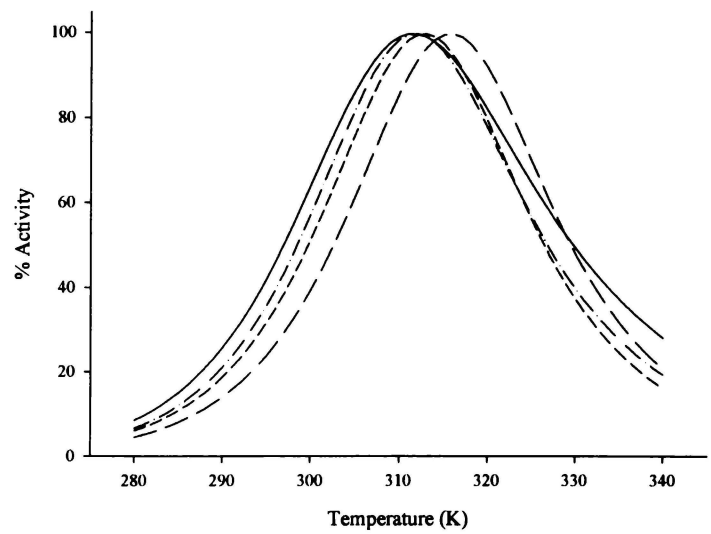

Figure 4 Temperature dependence of enzymic activity at time zero for aryl acylamidase in the presence of stabilising and destabilising agents

Enzymic activities at time zero were plotted against temperature to demonstrate the independence of enzymic activity at zero time on the presence of agents that affect thermal inactivation. The activity data for each enzyme are scaled from 5-100% relative to the maximum activity for that enzyme. **A)** aryl acylamidase (solid line); aryl acylamidase + betaine (– – – –); aryl acylamidase + guanidium hydrochloride (-------); aryl acylamidase + deoxycholic acid (· – · –); **B)** aryl acylamidase (solid line); aryl acylamidase + glycerol (– – – –); aryl acylamidase + CTAB (-------); aryl acylamidase +SDS (· – · –)

Discussion

It has previously been shown that the temperature dependent interconversion of E_{act} and E_{inact} is a fast process relative to thermal denaturation. The variation of activity with temperature at zero time occurs as a result of changes in the E_{act}/E_{inact} equilibrium, and is attained over timescales shorter than or equal to that of the mixing process. Comparatively, the measured rate of irreversible thermal inactivation (conversion from E_{inact} to denatured state) is at least two orders of magnitude slower over the same temperature range (7).

Given this observation, and the fact that the Native/Denatured transition is generally a two-state process for single-domain proteins (26), it seems unlikely that E_{inact} is significantly unfolded. A reversible conformational change is most likely, and as T_{eq} is unaffected by denaturing or stabilising agents, but is affected when the enzyme-substrate interaction is altered (by the use of different substrates), the transition from E_{act} to E_{inact} is likely to be local (probably at the active site) and, unlike stability, not a global feature of the enzyme.

This observation is not unexpected. Arnott *et al* (5) engineered chimeric citrate synthases where the large (inter-subunit contact) and small (catalytic) domains of *Thermoplasma acidophilum* (optimal growth at 55°C) and *Pyrococcus furiosus* (optimal growth at 100°C) were swapped. A comparison of the thermal inactivation data with the dependence of catalytic activity on temperature of the assay shows that when the small domain from the *Thermoplasma* citrate synthase is combined with the *Pyrococcus* large domain, the thermostability of the chimeric protein is enhanced with respect to the native *Thermoplasma* enzyme, but it retains the same T_{opt}. This partial independence of thermostability and

thermoactivity has also been reported for mesophilic and thermophilic phosphoglycerate kinases (3) and for a hyperthermophilic 2-keto-3-deoxygluconate aldolase (4).

Furthermore, there is evidence for a reduction in catalytic rate before there is any effect of irreversible denaturation due to localised unfolding of the protein active site. Shoichet *et al* (27), on examining the structure and function of T4 lyzozyme, concluded that catalytic residues within the enzyme were not optimised for protein stability and that this was a general property of enzyme active sites. Enzyme active sites are, therefore, more susceptible to unfolding than the rest of the protein molecule due to increased flexibility required for catalytic function. This has been observed for a number of proteins both in the presence of chemical denaturants (28-30), and during thermal denaturation (31-33). The conclusion is that enzymes unfold in a sequential process, the first stage of which is the localised, reversible unfolding of the active site, followed by the unfolding of the whole protein (3).

With the support of these findings, the 'Equilibrium Model' indicates that engineering an increase in thermostability alone will not necessarily lead to enhanced activity at high temperatures unless T_{eq} is also shifted to higher temperatures. It is possible that T_{eq} could be increased by mutations that increase ΔH_{eq} and/or decrease ΔS_{eq}. The former might be easier to achieve through the introduction of stabilising interactions at the active site, which might reduce the protein's flexibility and hence its tendency to deform as the temperature is raised (34). A comparison of the effect of substrate on T_{eq} indicates that the incorporation of large bulky substrates into the active site (thus reducing the

flexibility of the active site) results in an increase in ΔH_{eq} and T_{eq}. There are a number of theories to support this observation; that the incorporation of larger substrates into the active site results in the reduction of peptide loop movement about the active site, producing a more 'closed' and hence more thermostable conformation (35, 36), and that the closure of the peptide loops restricts access of solvent water to hydrogen bonding sites within the enzyme (37).

The evidence for the theory that active sites are more susceptible to temperature than the protein as a whole, and the results presented here (that agents that affect the active site alter ΔH_{eq} and T_{eq}) further supports the notion that the transition from E_{act} to E_{inact} is likely to be local conformational change, rather than a global effect.

To conclusively confirm what is thus far anecdotal evidence, a direct physical determination of the conformational state of E_{act} and E_{inact} is required. The temperature-linked response of fluorescent groups or labels at the active site, and elsewhere on the enzyme, may be a useful tool to distinguish between the active and the inactive form (38, 39). If successful, this work should offer the most unequivocal answer to whether T_{eq} depends upon local and/or global conformational changes. However, this technique is not without its pitfalls; fluorescence itself is temperature dependent (40), but the main problem will arise if the enzyme in both the active and inactive forms populates a number of conformational states (41-44), and especially if intermediate states with partial activity are present, in which case any difference may be hard to see. In the case that this technique fails to answer the question regarding the molecular basis of the E_{act}/E_{inact} transitions, other methods, particularly the use of NMR to measure

short-term hydrogen-deuterium exchange to examine dynamics changes at specific sites in an NMR-characterised enzyme, will be considered (45).

Acknowledgements

We thank Kirsti Johanssen for her assistance in the collection some of the β-lactamase data presented in this paper. This work was partially supported by the Royal Society of New Zealand's International Science and Technology Linkages Fund.

References

1. Daniel, R.M., Danson, M.J. & Eisenthal, R. (2001) The temperature optima of enzymes: a new perspective on an old phenomenon. *Trends in Biochemical Sciences*, **26**(4), 223 – 225.

2. Gerike, U., Danson, M.J., Russell, N.J & Hough, D.W. (1997) Sequencing and expression of the gene encoding a cold-active citrate synthase from an Antarctic bacterium, strain DS2-3R. *European Journal of Biochemistry*, **248**, 49 – 57.

3. Thomas, T.M. & Scopes, R.K. (1998) The effects of temperature on the kinetics and stability of mesophilic and thermophilic 3-phosphogylcerate kinases. *Biochemical Journal*, **330**, 1087 – 1095.

4. Buchanan, C.L, Connaris, H., Danson, M.J., Reeve, C.D., & Hough, D.W. (1999) An extremely thermostable aldolase from *Sulfolobus solfataricus* with specificity for non-phosphorylated substrates. *Biochemical Journal*, **343**, 563 – 570.

5. Arnott, M.A., Michael, R.A., Thompson, C.R., Hough, D.W. & Danson, M.J. (2000) Thermostability and Thermoactivity of Citrate Synthases from the Thermophilic and Hyperthermophilic Archaea, *Thermoplasma acidophilum* and *Pyrococcus furiosus*. *Journal of Molecular Biology*, **304**, 657 – 668.

6. Medina, D.C., Hanna, E., MacRae, I.J., Fisher, A.J., & Segel, I.H. (2001) Temperature Effects on the Allosteric Transition of ATP Sulfurylase from

Penicillium chrysogenum. Archives of Biochemistry and Biophysics, **393**(1), 51 – 60.

7. Peterson, M.E., Eisenthal, R., Danson, M.J., Spence, A. & Daniel, R.M. (2004) A new, intrinsic, thermal parameter for enzymes reveals true temperature optima. *The Journal of Biological Chemistry*, **279**, 20717 – 20722.

8. O'Callaghan, C. H., Morris, A., Kirby, S. M. and Shingler, A. H. (1972) Novel method for detection of beta-lactamases by using a chromogenic cephalosporin substrate. *Antimicrobial Agents and Chemotherapy*, **1**, 283 – 288.

9. Trépanier, S., Knox, J.R., Clairoux, N., Sanschagrin, F., Levesque, R.C. & Huletsky, A. (1999) Structure-Function Studies of Ser-289 in the Class C β-Lactamase from *Enterobacter cloacae* P99. *Antimicrobial Agents and Chemotherapy*, **43**, 543 – 548.

10. Jansson, J.A. (1965) A Direct Spectrophotometric Assay for Pencillin Beta-Lactamase (Penicillinase). *Biochimica et Biophysica Acta*, **99**, 171 – 172.

11. Waley, S. G. (1974) A spectrophotometric assay of β-lactamase action on penicillins. *Biochemical Journal*, **139,** 789 – 790.

12. Hammond, P. M., Price, C. P. and Scawen, M. D. (1983) Purification and properties of aryl acylamidase from Pseudomonas fluorescens ATCC 39004. *European Journal of Biochemistry*, **132**, 651-655.

13. Deming, S.N. & Morgan, S.L. (1973) Simplex Optimization of Variables in Analytical Chemistry. *Analytical Chemistry*, **45**, 278A – 283A.

14. Caceci, M.S. & Cacheris, W.P. (1984) Fitting Curves to Data. *Byte*, **May**, 340 – 362.

15. Powell, M.J.D. (1970) In *Numerical Methods for Nonlinear Algebraic Equations*, (ed. Robinowitz, P.) Chapter 7. Gordon & Breach Science Publishers, New York.

16. Cleveland, W. S. (1993) *Visualizing Data.* Hobart Press, New Jersey, USA.

17. Scopes, R. K. (1994) in *Protein Purification: Principles and Practice*, 3rd Edition, (ed. Cantor, C. R.), pp44 – 50, Springer Verlag: San Diego, USA.

18. Volkin, D.B. & Klibanov, A.M. (1984) in *Protein function: A practical approach*, (ed. Creighton, T.E.) pp6 – 8, IRL Press, Oxford, England.

19. Arakawa T. & Timasheff, S.N. (1985) The stabilization of proteins by osmolytes. *Biophysical Journal*, **47**, 411 – 414.

20. Santoro, M.M., Liu, Y., Khan, S.M., Hou, L.X. & Bolen, D.W. (1992) Increased thermal stability of proteins in the presence of naturally occurring osmolytes. *Biochemistry*, **31**, 5278 – 5283.

21. Knapp, S., Ladenstein, R. & Galinski, E.A. (1999) Extrinsic protein stabilization by the naturally occurring osmolytes beta-hydroxyectoine and betaine. *Extremophiles*, **3**, 191 – 198.

22. Chang, B.S. & Mahoney, R.R. (1995) Enzyme thermostabilization by bovine serum albumin and other proteins: evidence for hydrophobic interactions. *Biotechnology and Applied Biochemistry*, **22**, 203 – 214.

23. Schellman JA. (2003) Protein stability in mixed solvents: a balance of contact interaction and excluded volume. *Biophysical Journal*, 85(1):108 – 125.

24. Stein, R.L. (2002) Enzymatic Hydrolysis of *p*-Nitroacetanilide: Mechanistic Studies of the Aryl Acylamidase from *Pseudomonas flourescens*. *Biochemisty*, **41**, 991 – 1000.

25. Peterson, M.E., Eisenthal, R., Danson, M.J. & Daniel, R.M. (2005) The determination of T_{eq}, the new and fundamental third thermal parameter of enzymes. *In progress*.

26. Creighton, T. E. (1993) *Proteins*, 2nd Edition, W H Freeman, New York.

27. Shoichet, B.K., Baase, W.A., Kuroki, R.& Matthews, B.W. (1995) A relationship between protein stability and protein function. *Proceedings of the National Academy of Sciences of the United States of America*, **92**, 452 – 456.

28. Yao, Q.Z., Tian, M. & Tsou, C.L. (1984) Comparison of the rates of inactivation and conformational changes of creatine kinase during urea denaturation. *Biochemistry*, **23**, 2740 – 2744.

29. Zhou, H.M., Zhang, X.H., Yin, Y. & Tsou, C.L. (1993) Conformational changes at the active site of creatine kinase at low concentrations of guanidinium chloride. *Biochemical Journal*, **291**, 103 – 107.

30. Jiang, R.F. & Tsou, C.L. (1994) Inactivation precedes changes in allosteric properties and conformation of D-glyceraldehyde-3-phosphate dehydrogenase and fructose-1,6-bisphosphatase during denaturation by guanidinium chloride. *Biochemical Journal*, **303**, 241 – 245.

31. Edwards, R.A., Jacobson, A.L. & Huber, R.E. (1990) Thermal denaturation of beta-galactosidase and of two site-specific mutants. *Biochemistry*, **29**, 11001 – 11008.

32. Lin, Y.Z., Liang, S.J., Zhou, J.M., Tsou, C.L., Wu, P.Q. & Zhou, Z.K. (1990) Comparison of inactivation and conformational changes of D-glyceraldehyde-3-phosphate dehydrogenase during thermal denaturation. *Biochimica et Biophysica Acta*, **1038**, 247 – 252.

33. Zhang, Y.L., Zhou, J.M. & Tsou, C.L. (1993) Inactivation precedes conformation change during thermal denaturation of adenylate kinase. *Biochimica et Biophysica Acta*, **1164**, 61 – 67.

34. Eisenthal, R., Peterson, M.E., Daniel, R.M. & Danson, M.J. (2005) The Thermal Behaviour of Enzymes: Implications for Biotechnology. Submitted to *Nature: Biotechnology*.

35. Jaenicke, R. & Bohm, G.(1998) The stability of proteins in extreme environments. *Current Opinion in Structural Biology*, **8**, 738 – 748.

36. Brewer, J.M. & Wampler, J.E. (2001) A differential scanning calorimetric study of the effects of metal ions, substrate/product, substrate analogues and chaotropic anions on the thermal denaturation of yeast enolase 1. *International Journal of Biological Macromolecules*, **28**, 213 – 218.

37. Brewer, J.M., Glover, C.V.C., Holland, M.J. & Lebioda, L. (1998) Significance of the enzymatic properties of yeast S39A enolase to the catalytic mechanism. *Biochimica et Biophysica Act,* **1383**, 351 – 355.

38. Anderson, E. & Britt, B.M. (2002) The stability curve of bovine adenosine deaminase is bimodal. *Journal of Biomolecular Structure and Dynamics,* **20**, 375 – 380.

39. Porumb, H., Zargarian, L., Merad, H., Maroun, R., Mauffret, O., Troalen, F. & Fermandjian, S. (2004) Circular dichroism and fluorescence of a tyrosine side-chain residue monitors the concentration-dependent equilibrium between U-shaped and coiled-coil conformations of a peptide derived from the catalytic core of HIV-1 integrase. *Biochimica et Biophysica Acta,* **1699**, 77 – 86.

40. Bismuto, E., Martelli, P.L., De Maio, A., Mita, D.G., Irace, G. & Casadio, R. (2002) Effect of molecular confinement on internal enzyme dynamics: Frequency domain fluorometry and molecular dynamics simulation studies. *Biopolymers*, **67**, 85 – 95.

41. Brooks, C. L., Karplus, M. and Pettitt, B. M. (1988) *Proteins*, John Wiley, New York.

42. Svensson, A-K.E., O'Neill, J.C. and Matthews, C.R. (2003) The coordination of the isomerization of a conserved non-prolyl cis peptide bond with the rate-limiting steps in the folding of dihydrofolate reductase. *Journal of Molecular Biology*, **326**, 569 – 583.

43. Wintrode, P.L., Zhang, D., Vaidehi, N., Arnold, F.H. and Goddard III, W.A. (2003) Protein dynamics in a family of laboratory evolved thermophilic enzymes. *Journal of Molecular Biology*, **327**, 745 – 757.

44. James, L.C. & Tawfik, D.S. (2003) Conformational diversity and protein evolution – a 60-year-old hypothesis revisited. *Trends in Biochemical Sciences*, **28**, 361 – 368.

45. Hammes, G.G. (2002) Multiple conformational changes in enzyme catalysis. *Biochemistry*, **41,** 8221 – 8228.

Chapter Six

The Implications of T_{eq} for Biotechnology

This chapter consists of the draft manuscript of a paper that has been submitted to Nature - Biotechnology, detailing the implications of the Equilibrium Model in at least three biotechnological areas: enzyme engineering, enzyme reactor operation, and the selection/screening of useful enzymes from the environment.

My contribution to this work involved any experimental work detailed, and preparation of figures for the manuscript.

The Thermal Behaviour of Enzymes: Implications for Biotechnology

[1]Robert Eisenthal, [2]Michelle E. Peterson, [2]Roy M. Daniel and [3]Michael J. Danson

[1] Department of Biology and Biochemistry, University of Bath, Bath, BA2 7AY, UK.

[2] Department of Biological Sciences, University of Waikato, Private Bag 3105, Hamilton, New Zealand.

[3] Centre for Extremophile Research, Department of Biology and Biochemistry, University of Bath, Bath, BA2 7AY, UK.

All correspondence should be addressed to Danson, M.J. [Email: m.j.danson@bath.ac.uk].

The increased availability of complete genomes, coupled with the ready resolution of enzyme structures and the ability to manipulate them at will, has provided the biotechnologist with the potential to obtain enzymes designed for individual applications. Enzymes with increased stability are still a prime target for biotechnology, both for their prolonged shelf life and for the need in some situations to employ them under extreme conditions, such as high temperatures. In this communication, we explore the implications of our recent description of a new model for the thermal behaviour of enzymes[1], applicable to their engineering and use.

Traditionally, the dependence of enzyme activity on temperature has been described by a model (the "Classical Model") consisting of two processes: the catalytic reaction defined by k_{cat}, and irreversible inactivation defined by k_{inact}. The temperature dependence of these rate constants is characterised respectively by the catalytic activation energy $\Delta G^{\ddagger}_{cat}$, and the activation energy for the thermal inactivation reaction $\Delta G^{\ddagger}_{inact}$. As a consequence, if the rate of enzyme activity over a fixed assay time is plotted against temperature, these two parameters will lead to a temperature optimum that is dependent on the assay duration; that is, since thermal denaturation is time dependent, changing the assay duration changes the apparent optimum temperature, T_{opt}[2, 3].

Recent observations show that in some enzymes less activity is observed at high temperatures than can be accounted for by thermal denaturation[4, 5]. In response to these anomalies, we have hypothesised that the temperature dependence of enzyme activity is reversible, at least in part, and have developed and validated a model that incorporates the features of both reversibility and time-dependent

inactivation[1, 6]. This model (the "Equilibrium Model") includes an inactive form of the enzyme (E_{inact}) that is in reversible equilibrium with the active form (E_{act}); it is the inactive form that undergoes irreversible thermal inactivation to the thermally denatured state (X):

$$E_{act} \leftrightarrows E_{inact} \rightarrow X$$

The equilibrium is described by an equilibrium constant (K_{eq}), whose temperature dependence is characterised in terms of the enthalpy of the equilibrium, ΔH_{eq}, and a new thermal parameter, T_{eq}, which is the temperature at which the concentrations of E_{act} and E_{inact} are equal. Thus, $T_{eq} = \Delta H_{eq}/\Delta S_{eq}$, the enthalpic and entropic changes associated with the interconversion of E_{act} and E_{inact}. A useful characteristic of this model is that it "buffers" the enzyme against irreversible inactivation, because only a fraction of the total native enzyme is susceptible to inactivation at any time[1].

The effect of incorporating an additional inactive species of the enzyme in reversible equilibrium with the active form is most evident from a plot of enzyme activity vs. temperature vs. time [Fig. 1a]. This shows a temperature optimum at zero time, which is not seen in the Classical Model [Fig. 1b]. At any temperature above the maximal enzyme activity, the loss of activity due to the shift in the E_{act}/E_{inact} equilibrium is effectively instantaneous (<1s)[7] and at least two orders of magnitude faster than denaturation at temperatures above the maximal enzyme activity[6]. Furthermore, T_{eq} is essentially unaffected by agents such as betaine and guanidium hydrochloride at concentrations that respectively enhance and lower the stability of the enzyme (Fig. 2); this shows that T_{eq} is independent of thermostability.

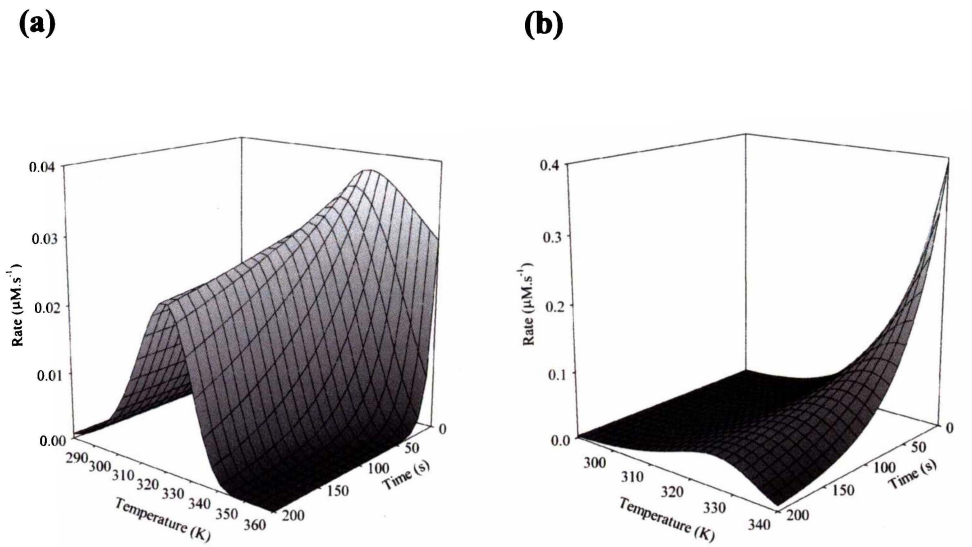

Figure 1 Comparison of the Equilibrium (a) and Classical (b) models of temperature dependence of enzyme activity[1].

The data were simulated using parameter values: **A)** $\Delta G^{\ddagger}_{cat}$ = 80 kJ ·mol^{-1}, $\Delta G^{\ddagger}_{inact}$ = 95 kJ ·mol^{-1}, ΔH_{eq} = 100 kJ ·mol^{-1}, T_{eq} = 320 K; **B)** $\Delta G^{\ddagger}_{cat}$ = 80 kJ ·mol^{-1}, $\Delta G^{\ddagger}_{inact}$ = 95 kJ ·mol^{-1}. Note the absence of a temperature optimum at zero time in the Classical model.

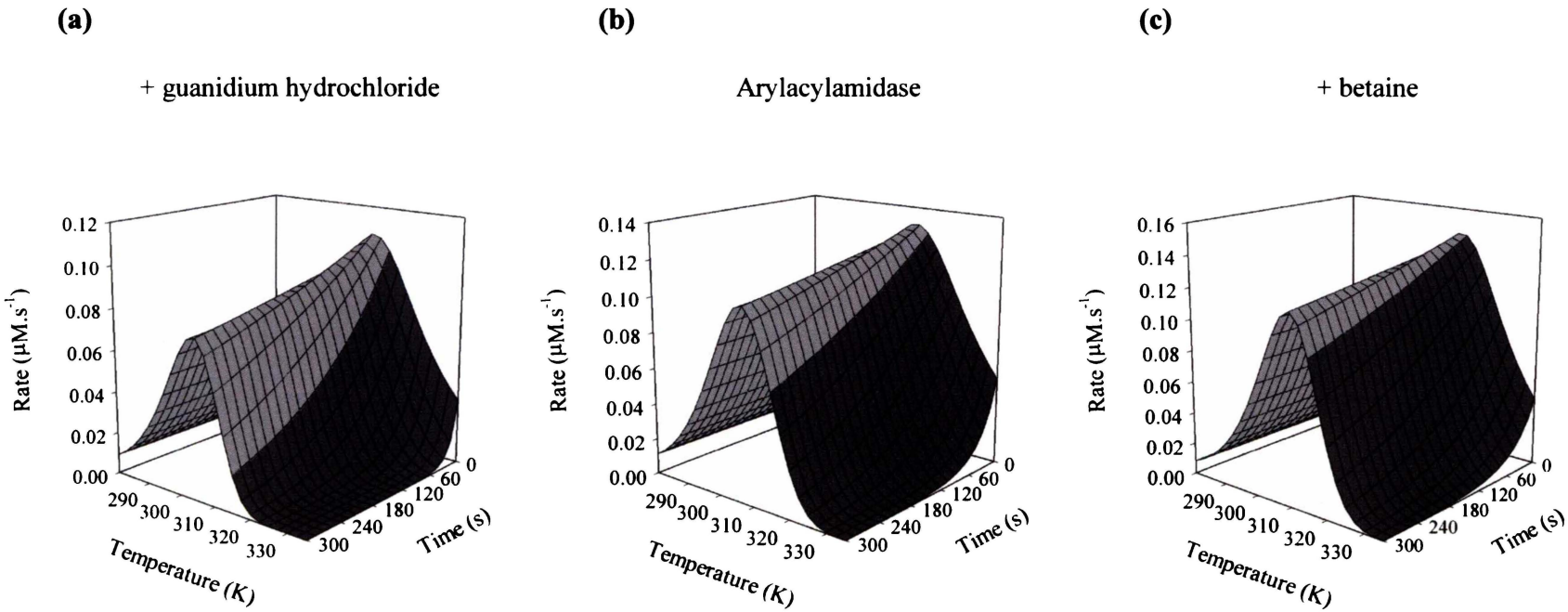

Figure 2 Experimentally-determined temperature/time profiles of the enzymic activity of aryl acylamidase [E.C. 3.5.1.13] in the presence of (a) 0.1 M guanidium hydrochloride; (b) no addition; and (c) 0.1 M betaine.

The enzyme was assayed as described in Peterson *et al* [6]. The curve traced by the border between the shaded areas represents the progress curve of irreversible inactivation at 315 K, to highlight the differences in the rates of inactivation under the different conditions.

The idea of a temperature-dependent reversible equilibrium between active and inactive forms of an enzyme was proposed in 1944 by Sizer[8], but Sizer's model did not include the possibility of time-dependent, irreversible inactivation. Time-dependent inactivation was considered by Wright and Schomaker[9] who studied the inactivation of diphtheria antitoxin by heat. They proposed a model that comprised two interconvertible forms of active antibody, one susceptible to irreversible inactivation, and the other protected. They made no assumption of a rapid equilibrium, and treated the system as one consisting of three first-order reactions. They recognised that the model provided a reservoir of native antibody during a significant fraction of the time course. However, their model differs from the Equilibrium Model in assuming that the "activity" (which was based on a bioassay) is independent of temperature and also that both non-denatured forms are active.

What are the biotechnological implications of the Equilibrium Model of the thermal behaviour of enzymes? Below we describe three areas, enzyme engineering, enzyme reactor operation, and the selection/screening of useful enzymes from the environment, where knowledge of T_{eq} may be essential to understanding the temperature dependence of enzyme activity.

[1] Enzyme engineering

The Equilibrium Model introduces an additional and separate factor, T_{eq}, to be considered when trying to enhance enzyme activity at high temperatures. The model tells us that engineering an increase in thermostability alone will not necessarily lead to enhanced activity at high temperatures unless the temperature of the equilibrium mid-point between the active and inactive forms, T_{eq}, is also

shifted to higher temperatures. Moreover, if the T_{eq} of the engineered enzyme is unaffected or lowered, and thermostability is assessed by a high-temperature enzyme assay, increased stability may not be detected upon the screening of mutants. This phenomenon is clearly demonstrated in Fig. 2, which shows the effect of agents that increase or decrease the thermal stability of aryl acylamidase. Note that, although the rate of irreversible inactivation is affected by the presence of guanidine (a denaturing agent) and betaine (a stabilising agent), the shape of the temperature/activity profile at time zero is virtually identical to that of the enzyme in buffer alone. The activity of the enzyme at the temperature optimum at time zero is similarly unaffected.

The molecular basis of the equilibrium described by T_{eq} has not been defined, but since it is unaffected by denaturing or stabilising agents it is likely to be local (probably at the active site) and, unlike stability, not a global feature of the enzyme. It will therefore be important when assessing the effect of engineered mutations on enzymes to determine the effect on stability and on activity separately. This may necessarily involve a compromise - clearly, T_{eq} can be increased by mutations that increase ΔH_{eq} and/or decrease ΔS_{eq}. The former might be easier to achieve through the introduction of stabilising interactions at the active site, which might reduce the protein's flexibility and hence its tendency to deform as the temperature is raised. However, given that conformational flexibility is often required for efficient catalysis, it may turn out to be difficult to alter T_{eq} by such a mutational strategy without adversely affecting the *k*cat value of the enzyme.

[2] Enzyme reactors

Maximising the output of enzyme reactors requires a very careful balance of the effects of temperature upon enzyme stability and upon activity. Predictions of the output of product with time and temperature based upon the Classical Model can be quite different from those derived from the Equilibrium Model.

When using an enzyme in a batch reactor for chemical synthesis, intuition would predict that the higher the operating temperature, the faster the catalysed reaction, but also the less stable the enzyme. In fact, this is only generally true if T_{eq} exceeds the working temperature of the reactor. If T_{eq} is less than the working temperature, the reverse is true (compare Figs. 3a & 3b). A typical temperature/time profile predicted by the Classical Model (which will never show the effect seen in Fig. 3a) is shown in Fig. 3c for comparison.

[3] Enzyme screening and selecting for applications

Enzyme screening or selection for particular thermal properties is normally carried out to obtain good activity and/or resistance to denaturation at a particular temperature. Enzyme thermal stability is usually correlated with the growth temperature of the source organism: enzymes from thermophiles are generally more thermally stable than those from mesophiles, while those from psychrophiles are relatively less stable. Exceptions to this are known, although we would expect T_{eq} to be even more closely associated with the cell's growth temperature than thermal stability.

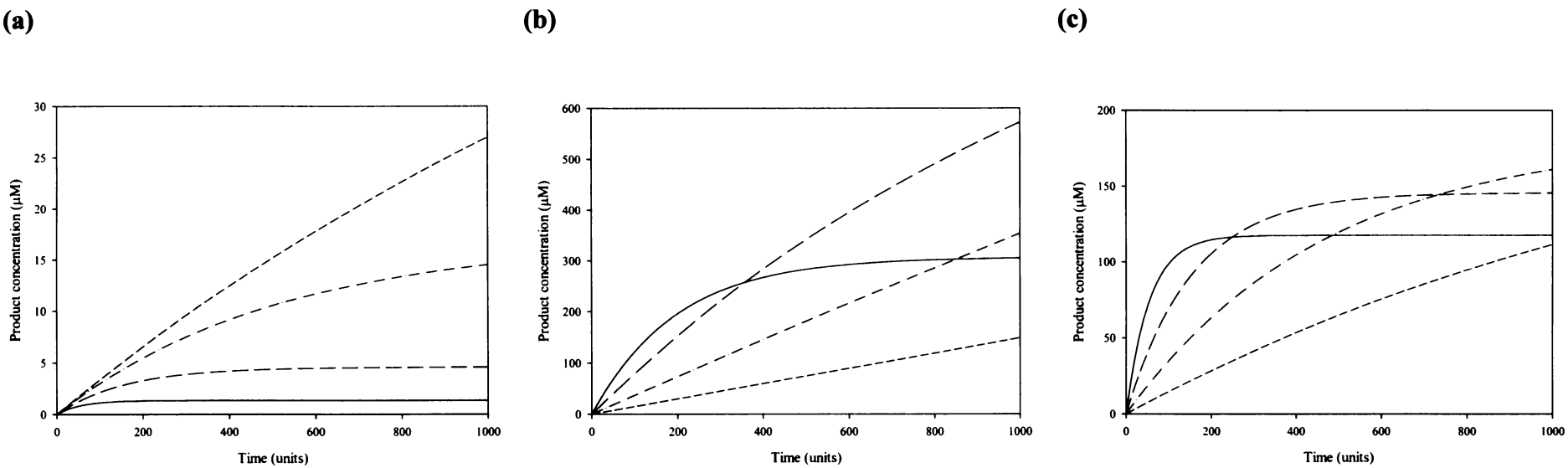

Figure 3 **Effect of T_{eq} on time courses of product concentration simulated at various temperatures.**

310 K (-------); 320 K (· – · –); 330 K (– – – –); 340 K (———). **(a)** Equilibrium Model with T_{eq} = 300 K; **(b)** Equilibrium Model with T_{eq} = 350 K; **(c)** Classical Model for comparison. Parameter values: Equilibrium Model, $\Delta G^{\ddagger}_{cat}$ = 75 kJ ·mol^{-1}, $\Delta G^{\ddagger}_{inact}$ = 95 kJ ·mol^{-1}, ΔH_{eq} = 95 kJ ·mol^{-1}; Classical model, $\Delta G^{\ddagger}_{cat}$ = 75 kJ ·mol^{-1}, $\Delta G^{\ddagger}_{inact}$ = 95 kJ ·mol^{-1}.

The simple Classical Model for the thermal behaviour of enzymes suggests that both activity and resistance to denaturation can be achieved by assessment of thermal stability alone. The Equilibrium Model shows that reduction of activity as the temperature is raised may not be due to irreversible thermal inactivation -- stability is necessary for activity, but does not guarantee it. Therefore, to gain the full benefit from screening, both stability and T_{eq} must be sought or selected separately. In short, successful selection from the environment of thermally stable/active enzymes will depend upon making a clear distinction between activity at high temperatures (determined by T_{eq}) and thermal stability.

Acknowledgements

We are grateful to the New Zealand ISAT Linkages Fund for travel support.

References

[1] Daniel, R.M., Danson, M. J. & Eisenthal, R. *Trends Biochem. Sci.* 26, 223-225 (2001).

[2] Daniel, R.M. & Danson, M.J. *Methods Enzymol.* 334, 283-293 (2000).

[3] Cornish-Bowden, A. In "*Fundamentals of Enzyme Kinetics*" (3rd Edn) Portland Press Ltd., London, UK. (2004).

[4] Thomas, T.M. & Scopes, R.K. *Biochem. J.* 330, 1087-1095 (1998).

[5] Gerike, U., Russell, N.J., Danson, M.J. & Hough, D.W. *Eur. J. Biochem.* 248, 49-57 (1997).

[6] Peterson M. E., Eisenthal, R., Danson, M. J., Spence, A. and Daniel R.M. *J. Biol. Chem.* 279, 20717-20722 (2003).

[7] Tsou, C.L. *Biochim. Biophys. Acta* 1253, 151-162 (1995).

[8] Sizer, I.W. *J. Biol. Chem.* 154, 461-473 (1944).

[9] Wright, G.G. & Schomaker, V. *J. Amer. Chem. Soc.* 70, 356-364 (1948).

Chapter Seven

Characterisation of 3-isopropylmalate dehydrogenase from various sources

---

This work contributed to a collaborative effort to provide empirical data regarding the thermal habitat of the ancestors of extant mesophiles and thermophiles, by attempting to reconstruct ancient genes via computational phylogenetic inference. It is hoped that this information may provide a test for the hypothesis that the Last Common Ancestor of living organisms was a thermophile or hyperthermophile.

While I was not involved in the conception of this project, my specific contribution included experimental design, and providing technical expertise and assistance in the collection of data for the determination of the kinetic and thermal parameters of nine enzymes. This also included the use of methods I have developed for the accumulation and processing of data for the determination of the parameters associated with the 'Equilibrium Model' and the subsequent interpretation of the results.

7.1 Introduction

The overall aim of this research is to deduce the ancestral state of one gene and to synthesise the gene using assembly PCR. This ancestral gene will then be expressed, purified and characterised in the hope that this information will indicate the optimal growth conditions of the ancestral organism that may have possessed this gene.

The credibility of the phylogenetic tree is essential to the success of the predicted sequence. The deeper the branches in the tree, the less reliable the predicted ancestral sequence becomes. Therefore, an appropriate gene and lineages are necessary for building well supported trees and for determining reliable ancestral states. The family of interest is the low GC content, gram positive *Bacillus* genus as they have a range of species, which consist of psychrophiles, mesophiles and thermophiles. The target organisms were selected for their sequence availability and range of growth temperatures.

The target gene selected for this study is the *leuB* gene, which encodes for the enzyme 3-isopropylmalate dehydrogenase (IPMDH) [E.C. 1.1.1.85; 3-carboxy-2-hydroxy-4-methylpentanoate:NAD oxidoreductase]. This was chosen for a number of reasons:

- *leuB* and IPMDH are highly conserved with high levels of homology between prokaryotes and eukaryotes.

- It is present in Bacteria, Archaea and fungal and plant members of the Eukarya as it is crucial to biosynthesis of the amino acid leucine.

- The gene is approximately 1kb long, which is an acceptable size for *de novo* gene synthesis.

- The quaternary structure of IPMDH is homodimeric, there are no prosthetic groups and it has a relatively simple conformation.

- There is a large amount of data currently available for IPMDH genes in the form of sequence and structural information from organisms from a range of growth temperatures, as well as kinetic information.

- The enzyme has a relatively simple assay.

IPMDH catalyses the third step in the biosynthesis of the amino acid, leucine. The reaction involves a dehydrogenation and subsequent decarboxylation of *threo*-D-3-isopropylmalate to 2-oxoisocaproate with concomitant reduction of NAD^+.

For this study, four "ancestral" IPMDH genes were designed, constructed and the protein product of each expressed, purified and characterised. The first gene was designed at the node indicated in Figure 7.1, using only the sequences of the species detailed in this figure. Once it was established that the protein product of this gene was functional, three additional "ancestral" genes were designed, using additional and higher quality sequence information, at the nodes indicated on Figure 7.2. For comparison, the IPMDH gene was cloned from five *Bacillus* species - two psychrophilic, two mesophilic and one thermophilic. The protein products were expressed, purified, and the results of the characterisation compared with those determined for the "ancestral" IPMDH's.

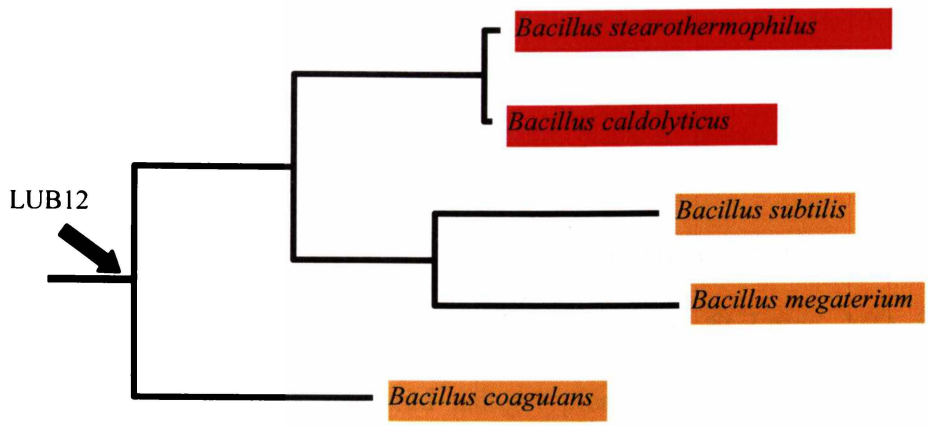

Figure 7.1 Phylogenetic tree used in ancestral gene design pilot study.

The ancestral gene, LUB12, was designed at the node indicated, using the IPMDH gene sequence data of these five *Bacillus* species.

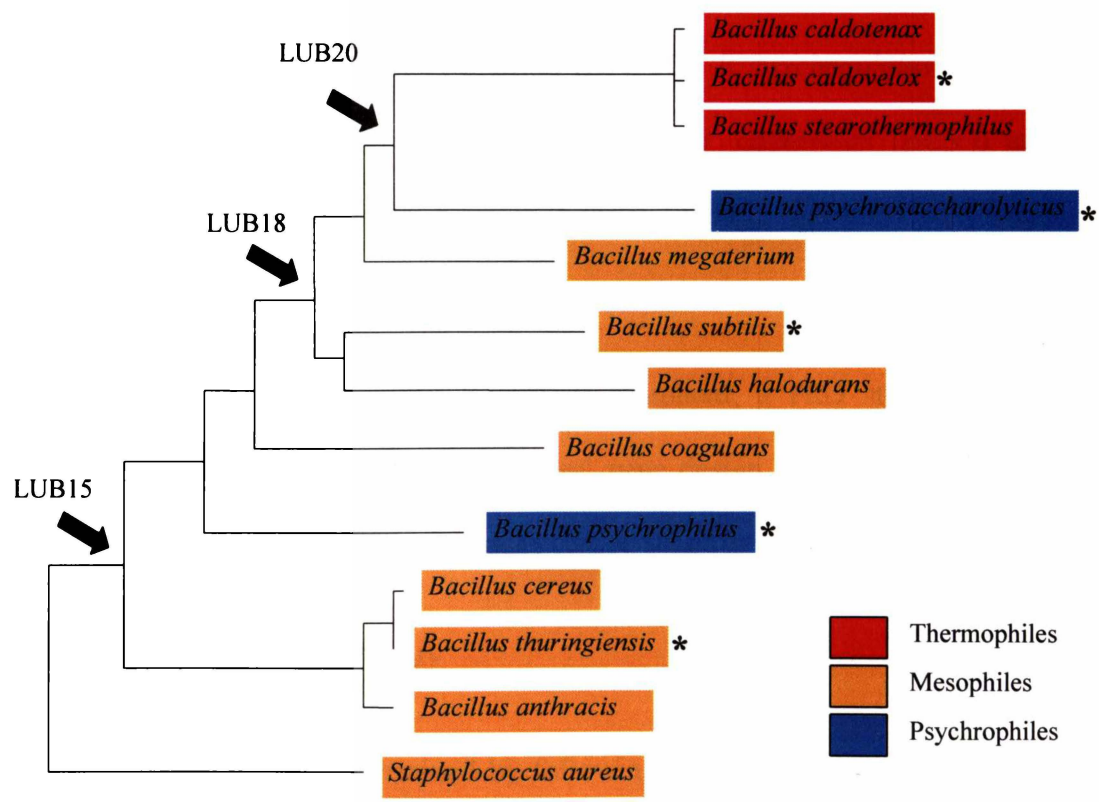

Figure 7.2 IMPDH gene tree used for further ancestral gene design.

Arrows indicate the nodes at which further ancestral genes were designed. Species marked with an asterix indicate organisms from which the IPMDH gene was cloned and protein characterized.

7.2 Materials and Methods

7.2.1 Materials

Threo-D,L-3-isopropylmalic acid was purchased from Wako Chemical Company, Tokyo, Japan. NAD was obtained from Sigma-Aldrich, St Louis, MO, USA. Buffers and co-factors were prepared using typical analytical grade materials. Buffers were adjusted to the appropriate pH value at the assay temperature, using a combination electrode calibrated at this temperature.

7.2.2 Source of Enzyme

IPMDH was purified from *E. coli* clones containing the *leuB* genes from five *Bacillus* species (*B. psychrosaccharolyticus* (BPSYC), *B. psychrophilus* (BPSY), *B. subtilis* (BSUBT), *B. thuringiensis* (BTK) *and B. caldovelox* (BCV)) and containing the four ancestral *leuB* genes (termed LUB12, LUB15, LUB18 and LUB20).

All nine enzymes were prepared by Charis Shepherd, a PhD student at the University of Auckland. Details of ancestral gene design, cloning, sequencing, expression and purification of the enzymes can be found in Appendix D.

7.2.3 Enzyme Activity Assay

The enzyme activity was determined by following the increase in absorbance at 340nm using a Thermospectronic™ Helios γ-spectrophotometer equipped with a Thermospectronic™ single cell peltier-effect cuvette holder. The standard assay mixture consisted of the appropriate buffer at a concentration of 20 mM containing 0.3 M KCl, 0.2 mM $MnCl_2$, 1 mM NAD^+ and 1 mM *threo*-D,L-3-

isopropylmalic acid (IPM), and appropriately diluted enzyme preparation in the appropriate buffer in a final volume of 1 mL. Assay reactions were initiated by the addition of microlitre amounts of enzyme that had no significant effect on the temperature. One unit of activity is defined as the amount of enzyme that reduces one μmol of NAD^+ per minute, using a molar absorption coefficient for NADH at 340 nm of 6.22×10^3 $M^{-1}.cm^{-1}$. The specific activity is defined as units per milligram of protein.

7.3 Results and Discussion

7.3.1 Functionality of the Gene Products

IPMDH purified from the five representatives of the *Bacillus* species were all functional, as were the enzyme products of ancestral gene constructs LUB12, LUB18 and LUB20. Activity could not be detected for the enzyme product of ancestral gene construct LUB15 when tested over a range of assay conditions (temperature, pH, substrate concentration, co-factor concentration and enzyme concentration).

7.3.2 Effect of pH on Catalytic Activity

The effect of pH was studied over a relatively narrow range (between pH 6.0 and pH 9.5) using 20 mM potassium phosphate buffer and 20 mM potassium carbonate buffer. Buffer species did not appear to have a significant effect on catalytic activity. Table 7.1 summarises the pH optima for each enzyme. The range of pH optima by the eight active enzymes was well within the range of pH optima displayed by other IPMDH's under similar assay conditions[1-7].

7.3.3 Determination of Kinetic Constants

Kinetic constants were determined at the respective standard conditions (temperature and pH) for each enzyme, as detailed in Table 7.1. A curve from the Henri-Michaelis-Menten equation was fitted through IPMDH initial rate data using parameters calculated by the Marquardt-Levenberg method of nonlinear least squares regression [SigmaPlot® 2001 for Windows™, Version 7.101, SPSS Inc.].

Direct Linear Plots were graphed using the same initial rate data and the values derived from these plots were found to be in good agreement (i.e. within errors) with the values calculated from the Henri-Michaelis-Menten fit (Table 7.1).

The values of K_M and specific activity for the eight enzymes characterised were all within the range of values determined from the characterisation of other IPMDH's[1-7].

All K_M's for the ancestral enzymes were at or above the upper end of the range found for the wild-type *Bacillus* enzymes; interestingly, so were the values of specific activity. However, the V_{max}/ K_M ratio (i.e. the enzyme efficiency[8]) values for the ancestral enzymes were typical of those found for the wild-type *Bacillus* IPMDH's, suggesting that the ancestral gene design process has correctly produced enzymes with characteristics that mirror those of enzymes produced by extant organisms.

Table 7.1 Kinetic parameters for the nine IPMDH's against IPM

Values determined via Direct-Linear Plot are distinguished from those determined via fitting to the Henri-Michaelis-Menten Model by an asterix (*). ND = not determined.

Enzyme	pH optimum	Temperature (°C)	K_M (μM)	V_{max} (U/mg protein)	V_{max}/K_M (U/mg protein/M)
B. psychrophilus	9	15	7 ± 3* 9 ± 2	1.7 ± 0.5* 1.8 ±0.1	2.4 x 10^5
B. psychrosacchrolyticus	9.5	25	37 ± 10 * 29 ± 8	2.7 ± 2.0* 2.7 ± 0.2	0.7 x 10^5
B. subtilis	9.5	30	16 ± 2* 15 ± 1	2.5 ± 0.2* 2.5 ± 0.1	1.6 x 10^5
B. thuringienesis	8.5	30	50 ± 11* 40 ± 4	2.6 ± 1.9* 2.5 ± 0.1	0.5 x 10^5
B. caldovelox	8.0	55	66 ± 9* 69 ± 5	9.0 ± 1.2* 8.9 ± 0.2	1.4 x 10^5
LUB12	7.6	50	92 ± 19* 78 ± 8	10.2 ± 5.8* 9.6 ± 0.3	1.1 x 10^5
LUB15	ND	ND	ND* ND	ND* ND	ND
LUB18	8	50	68 ± 6* 50 ± 7	16.0 ± 2.0* 15.0 ± 0.7	2.4 x 10^5
LUB20	9.5	60	516 ± 94* 389 ± 140	60 ± 26* 52 ± 12	1.3 x 10^5

7.3.4 The Effect of Temperature on IPMDH Activity

The effect of temperature on the activity of the eight functional IPMDH's was experimentally determined as previously described[9].

All eight sets of data were fitted to the 'Equilibrium Model' and values for $\Delta G^{\ddagger}_{cat}$, $\Delta G^{\ddagger}_{inact}$, ΔH_{eq}, T_{eq} and T_{opt} (at zero time) calculated. Table 7.2 summarises the results of each fit.

The values of $\Delta G^{\ddagger}_{cat}$ for the five *Bacillus* representatives and the three functional "ancestral" gene products compare favourably with published values of 68 and 71 kJ · mol^{-1} for *Escherichia coli* and *Thermus thermophilus* IPMDH respectively[6]. This result may be seen as an indication that the cloning and over-expression of the *leuB* gene in *E. coli* has not in any way affected the activity of the enzyme which it encodes, and that the construction of the ancestral genes is near perfect, as confirmed by the specificity results.

It is widely accepted that thermal stability (expressed here as $\Delta G^{\ddagger}_{inact}$, and $t_{½}$) is a satisfactory indicator of the temperature from which an organism is sourced. Indeed, the values for $\Delta G^{\ddagger}_{inact}$ reported here are consistent with the growth temperature regime of each *Bacillus* species, except for *B. psychrophilus*, a psychrotrophic organism which appears to have produced a very thermostable IPMDH ($t_{½}$ @ 330 K = 693 seconds).

However, it appears that T_{eq} and ΔH_{eq} might be a better expression of how environmental temperature affects the way an enzyme behaves with temperature[10].

With the exception of *B. psychrophilus*, T_{eq} appears to increase with increasing growth temperature, and as noted by Thomas and Scopes[11] and by Peterson *et al*[10], for the psychrophilic and mesophilic enzymes, the T_{opt} is approximately 20-40°C above the optimum growth temperature of the source organism. As also noted by Thomas and Scopes[11] and by Lee *et al*[12], T_{opt} for thermophilic enzymes is very close to the optimum growth temperature.

It appears that those enzymes with a low ΔH_{eq} (such as those purified from the psychrophilic *Bacilli*) have a broad "zero-time" plot (Figure 7.3) compared to those with higher ΔH_{eq} values (e.g. *B. caldovelox*, Figure 7.4). This observation appears to correlate with the growth temperature range of the organism, where it is seen that the psychrophilic and mesophilic organisms have growth temperature ranges of 35°C to 40°C, and low values of ΔH_{eq} (120 kJ · mol^{-1} to 270 kJ · mol^{-1}), while the thermophilic organism has a growth temperature range of only 10°C and a high value of ΔH_{eq} (573 kJ · mol^{-1}) (Table 7.2). It might be suggested that the value of ΔH_{eq} best reflects the growth temperature range of the organism and therefore the nature of the thermal environment from which it was sourced.

If it is assumed that the correlations above hold for all proteins, then the results of fitting experimental data for the "wild-type" *Bacillus* IPMDH's to the 'Equilibrium Model' can be used to predict the thermal habitat of the source organism of the ancestral IPMDH's.

The values of T_{eq} calculated for LUB12 and LUB18 (67.2°C and 68.9°C, respectively) might suggest that the source organisms of these enzymes originate at the lower end of thermophily, possibly on the border of mesophily. Accordingly, it might be suggested that LUB20 is certainly thermophilic (T_{eq} =

83.3°C), a conclusion that could be seen to be confirmed by the value of $\Delta G^{\ddagger}_{inact}$ (98.5 kJ · mol^{-1}).

According to the values of ΔH_{eq}, we might expect then that the temperature regime of the ancestral organisms that yield LUB12 and LUB20 to be eurythermal, i.e. with a growth temperature range of 30 – 40°C, an adaptation that reflects the fluctuating nature of the organism's thermal environment. However, LUB18, which has a relatively high ΔH_{eq} (416 kJ · mol^{-1}) we would expect to originate from a source organism that inhabits a much narrower, more uniform thermal environment, similar to that of *B. caldovelox* (ΔH_{eq} = 573 kJ · mol^{-1}).

Table 7.2 The Effect of Temperature on IPMDH Activity

	BPSY	*BPSYC*	*BSUBT*	*BTK*	*BCV*	*LUB12*	*LUB18*	*LUB20*
$\Delta G^{\ddagger}_{cat}$ ($J \cdot mol^{-1}$)	71.9 ± 0.1	71.9 ± 0.1	73.4 ± 0.1	73.7 ± 0.1	75.7 ± 0.1	71.1 ± 0.1	72.6 ± 0.1	74.4 ± 0.1
$\Delta G^{\ddagger}_{inact}$ ($J \cdot mol^{-1}$)	99.9 ± 0.2	86.1 ± 0.1	93.5 ± 0.2	98.7 ± 0.2	101.2 ± 1.6	96.4 ± 0.1	96.0 ± 0.2	98.5 ± 0.2
ΔH_{eq} ($J \cdot mol^{-1}$)	123 ± 3	138 ± 2	255 ± 5	269 ± 4	573 ± 23	299 ± 4	416 ± 10	228 ± 9
T_{eq} (°C)	56.5 ± 0.4	41.2 ± 0.2	52.6 ± 0.1	64.5 ± 0.1	63.7 ± 0.2	67.2 ± 0.1	68.9 ± 0.1	83.3 ± 0.3
T_{opt} (°C)	60	42.5	50	61.5	60	64.5	65	80
$T_{opt\ growth}$ * (°C)	20	20	30	30	70			
$T_{growth\ range}$ (°C)	-5 – 30	0 – 35	10 – 50	10 – 50	60 – 70			
E_0 (M)	4.72×10^{-5}	2.4×10^{-4}	1.22×10^{-4}	4.67×10^{-5}	4.44×10^{-5}	1.63×10^{-5}	1.85×10^{-5}	1.32×10^{-5}
$t_{½}$ @ 330K (s)	693	4.4	69	433	1050	182	158	407

* As defined by DSMZ

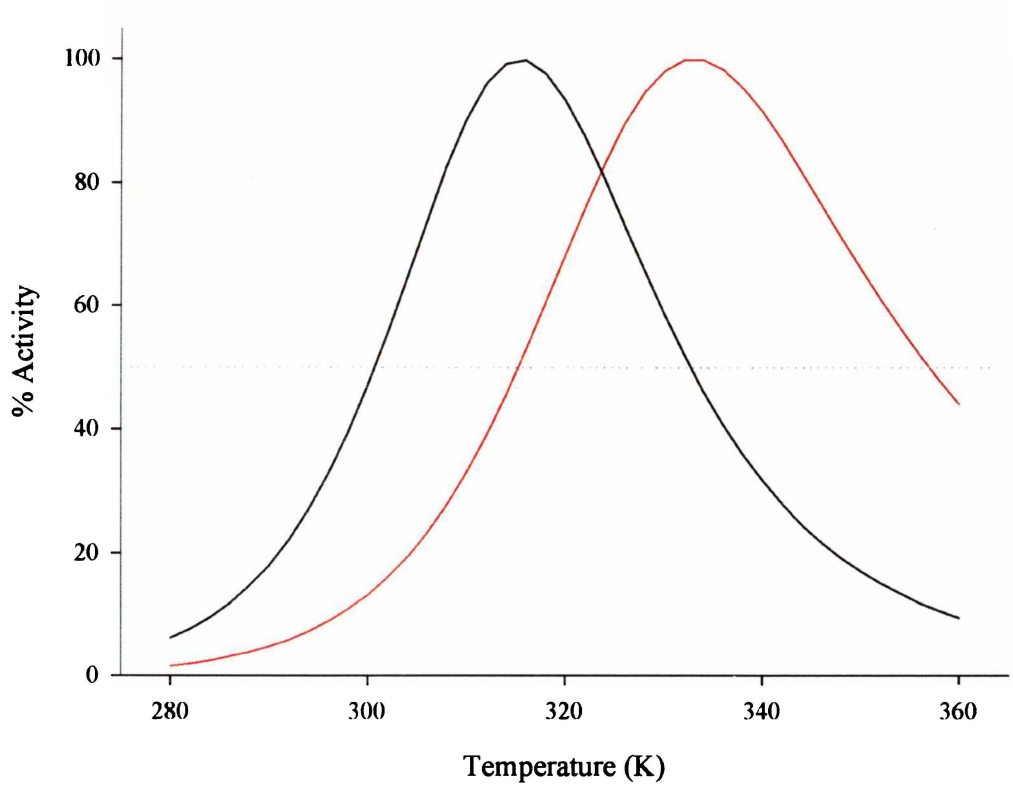

Figure 7.3 The effect of temperature on activity of wild-type psychrophilic *Bacillus* IPMDH's at zero-time.

Zero time activity was simulated by the Equilibrium Model with time (t) set to zero, using parameters derived from fitting the experimental data (Table 7.2). The activity data for each enzyme are scaled from 0–100% relative to the maximum activity for that enzyme. *B. psychrosaccharolyticus* (black), *B. psychrophilus* (red).

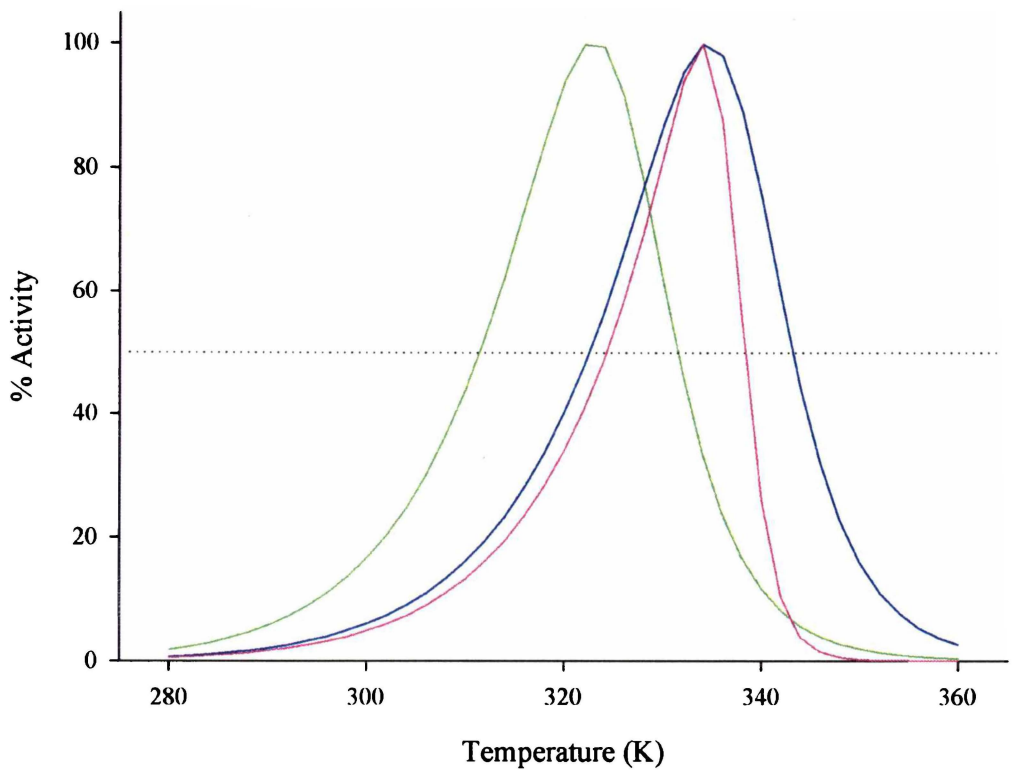

Figure 7.4 The effect of temperature on activity of wild-type mesophilic and thermophilic *Bacillus* IPMDH's at zero-time.

Zero time activity was simulated by the Equilibrium Model with time (t) set to zero, using parameters derived from fitting the experimental data (Table 7.2). The activity data for each enzyme are scaled from 0–100% relative to the maximum activity for that enzyme. *B. subtilis* (green), *B. thuringiensis* (blue), *B. caldovelox* (pink).

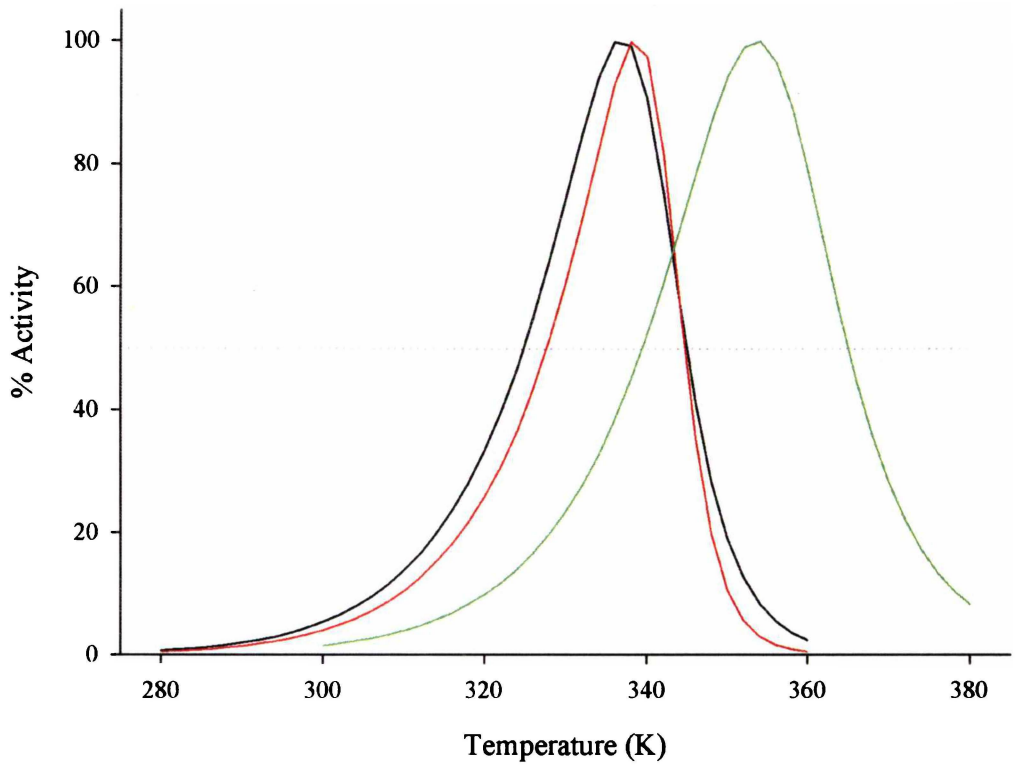

Figure 7.5 The effect of temperature on activity of ancestral *Bacillus* IPMDH's at zero-time.

Zero time activity was simulated by the Equilibrium Model with time (t) set to zero, using parameters derived from fitting the experimental data (Table 7.2). The activity data for each enzyme are scaled from 0–100% relative to the maximum activity for that enzyme. LUB12 (black), LUB18 (red), LUB20 (green).

7.4 Conclusions

The *leuB* gene was designed for four "ancestors" of the *Bacillus* genus, and the protein product of each was expressed, purified and assayed for activity, in an attempt to provide empirical data regarding the thermal habitat of the ancestors of extant psychrophiles, mesophiles and thermophiles. Three functional enzymes were obtained; these were characterised, and results compared to those from the characterisation of five "wild-type" *Bacillus* enzymes. This characterisation included fitting experimental data to the 'Equilibrium Model' to derive values for $\Delta G^{\ddagger}_{cat}$, $\Delta G^{\ddagger}_{inact}$, ΔH_{eq} and T_{eq}.

Any correlation between the Arrhenius activation energy (which has been expressed here as $\Delta G^{\ddagger}_{cat}$) of an enzyme to its thermal environment is uncertain and at best very loose[12-17] and although there is a strong correlation between thermal stability ($\Delta G^{\ddagger}_{inact}$) and the environmental temperature of the source organism, it is known that enzyme thermal stability also reflects resistance to other cellular conditions such as the action of proteases[18]. It has been predicted that T_{eq} will be a better expression of the effect of environmental temperature on the evolution of the enzyme than thermal stability and that the value of ΔH_{eq} might best describe the fit of an enzyme to its thermal environment[10]. Indeed, the results of fitting the experimental data of the five "wild-type" *Bacillus* IPMDH's to the 'Equilibrium Model' show a loose correlation between T_{eq} and growth temperature, and between ΔH_{eq} and the temperature range over which the organism grows.

Assuming that these correlations can be extrapolated to all proteins, then the values of T_{eq} and ΔH_{eq} derived from fitting the experimental data of the three "ancestral" *Bacillus* IPMDH's to the "Equilibrium Model' lead us to speculate that the "ancestral" enzymes are thermophilic, a premise that is lent credence by the values of $\Delta G^{\ddagger}_{inact}$ determined for these enzymes. These observations lend evidence to the hypothesis that the Last Common Ancestor of living organisms may have been a thermophile or hyperthermophile.

7.5 References

1. Hsu, Y.P. & Kohlhaw, G.B. (1980) Leucine biosynthesis in *Saccharomyces cerevisiae*. Purification and characterization of beta-isopropylmalate dehydrogenase. *Journal of Biological Chemistry*, **255**, 7255-7260.

2. Burns, R.O., Umbarger, H.E. & Gross, S.R. (1963) The biosynthesis of leucine. III. The conversation of alpha-hydroxy-beta-carboxyisocaproate to alpha-ketoisocaproate. *Biochemistry,* **2**, 1053-1058.

3. Sekiguchi, T., Harada, Y., Shishido, K. & Nosoh, Y. (1984) Cloning of beta-isopropylmalate dehydrogenase gene from *Bacillus coagulans* in *Escherichia coli* and purification and properties of the enzyme. *Biochimica et Biophysica Acta*, **788**, 267-273.

4. Yamada, T., Akutsu, N., Miyazaki, K., Kakinuma, K., Yoshida, M. & Oshima, T. (1990) Purification, catalytic properties, and thermal stability of threo-Ds-3-isopropylmalate dehydrogenase coded by leuB gene from an extreme thermophile, *Thermus thermophilus* strain HB8. *Journal of Biochemistry*, **108**, 449-456.

5. Kawaguchi, H., Inagaki, K., Kuwata, Y., Tanaka, H. & Tano, T. (1993) 3-Isopropylmalate dehydrogenase from chemolithoautotroph *Thiobacillus ferrooxidans*: DNA sequence, enzyme purification, and characterization. *Journal of Biochemistry*, **114**, 370-377.

6. Wallon, G., Yamamoto, K., Kirono, H., Yamagashi, A., Lovett, S.T., Petsko, G.A. & Oshima, T. (1997) Purification, catalytic properties and

thermostability of 3-isopropylmalate dehydrogenase from *Escherichia coli*. *Biochimica et Biophysica Acta*, **1337**, 105-112.

7. Yoda, E., Anraku, Y., Kirino, H., Wakagi, T. & Oshima, T. (1995) Purification and characterization of 3-isopropylmalate dehydrogenase from a thermoacidophilic archaebacterium *Sulfolobus* sp. strain 7. *FEMS Microbiology Letters*, **131**, 243-247.

8. Matthews, C.K., van Holde, K.E. & Ahern, K.G. (2000) In *Biochemistry*, 3rd Edition. Benjamin Cummings, Oregon State University, Corvallis, USA.

9. Peterson, M.E., Eisenthal, R., Danson, M.J. & Daniel, R.M. (2005) The determination of T_{eq}, the new and fundamental third thermal parameter of enzymes. *In Progress*.

10. Peterson, M.E., Eisenthal, R., Danson, M.J., Spence, A. & Daniel, R.M. (2004) A new, intrinsic, thermal parameter for enzymes reveals true temperature optima. *The Journal of Biological Chemistry*, **279**, 20717 – 20722.

11. Thomas, T.M. & Scopes, R.K. (1998) The effects of temperature on the kinetics and stability of mesophilic and thermophilic 3-phosphogylcerate kinases. *Biochemical Journal*, **330**, 1087 – 1095.

12. Lee, C.K., Peterson, M.E., Eisenthal, R., Danson, M.J., Cary, S.C. & Daniel, R.M. (2005) Growth temperature correlates with T_{eq}, a new intrinsic thermal property of enzymes. *In Progress.*

13. Georlette, D., Blaise, V., Collins, T., D'Amico, S., Gratia, E., Hoyoux, A.. Marx, J.-C., Sonan, G., Feller, G. & Gerday, C. (2004) Some like it cold: biocatalysis at low temperatures. *FEMS Microbiology Reviews*, **28**, 25 – 42.

14. Feller, G. (2003) Molecular adaptations to cold in psychrophilic enzymes. *Cellular and Molecular Life Science*, **60**, 648 – 662.

15. Feller, G. & Gerday, C. (2003) Psychrophilic enzymes: hot topics in cold adaptation. *Nature Reviews Microbiology*, **1**, 200 – 208.

16. D'Amico, S., Claverie, P., Collins, T., Georlette, D., Gratia, E., Hoyoux, A., Meuwis, M-A., Feller, G. & Gerday, C. (2002) Molecular basis of cold adaptation. *Philosophical Transactions of the Royal Society B*, **357**, 917 – 925.

17. Lonhienne, T., Gerday, C. & Feller, G. (2000) Psychrophilic enzymes: revisiting the thermodynamic parameters of activation may explain local flexibility. *Biochimica et Biophysica Acta,* **1543**, 1 – 10.

18. Daniel, R.M. Dines, M. & Petach, H.H. (1996) The denaturation and degradation of stable enzymes at high temperatures. *Biochemical Journal*, **317**, 1 – 11.

Chapter Eight

Final Discussion & Conclusions

A new proposal for the way in which enzyme activity is described with respect to temperature gives rise to a new thermal parameter for enzymes, T_{eq}[1]. The aim of this work has been to test the proposal, and determine the role of T_{eq} in describing the behaviour of an enzyme catalysed reaction with regards to temperature.

8.1 Testing the Theory

To test the proposal for this new thermal parameter, five enzymes from a variety of sources were initially assayed for activity at different temperatures, using continuous assays to allow the simultaneous measurement of activity and thermal stability in the same cuvette, and therefore under identical conditions. By comparing 3D plots (expressed as rate versus temperature versus time) of the outputs predicted by both the 'Classical' and the 'Equilibrium Model' with a 3D plot generated from the experimental data, it could be seen that all of the enzymes studied conformed to the 'Equilibrium Model'; that is, they displayed clear temperature optima at zero time. The data was then fitted to the Model to give values for $\Delta G^{\ddagger}_{cat}$, $\Delta G^{\ddagger}_{inact}$, ΔH_{eq} and T_{eq} for each enzyme. These results substantiate the claim that this third thermal parameter is required to wholly explain experimental enzymic rate data as a function of temperature[2].

Upwards of twenty enzymes have now been examined[2-4] and all have behaved as predicted by the 'Equilibrium Model'. This behaviour was also observed when a number of these enzymes were examined under altered assay conditions, for

example, running the reaction in the reverse direction, using different substrates, and with the addition of stabilising and destabilising agents to the assay.

Nevertheless, enzyme selection has been biased towards hydrolases and dehydrogenases, and given the overall variety of enzymes available; the number surveyed thus far is very few. To establish if the Equilibrium Model is truly a universal phenomenon, the number of enzymes surveyed will need to be extended to include representatives of all enzyme classes, from all three kingdoms (Eukarya, Bacteria, Archaea), and originating from organisms growing at a variety of temperatures and temperature regimes (psychrophilic versus mesophilic versus thermophilic; stenothermal versus eurythermal).

8.2 Molecular Aspects

The results from the analysis of the experimental data collected for the five enzymes initially tested show that the temperature dependent interconversion of E_{act} and E_{inact} is a fast process relative to thermal denaturation[5].

Assuming the 'Equilibrium Model, all of the variation of activity with temperature at zero time occurs as a result of changes in the E_{act}/E_{inact} equilibrium, and, given that the reaction is initiated by the addition of microlitre amounts of ice-cold enzyme (so all as E_{act}), any change in this equilibrium occurs over timescales shorter than that of the mixing process (equal to or less than one second). Comparatively, the measured rate of irreversible thermal inactivation (conversion from E_{inact} to denatured state) is at least two orders of magnitude slower at temperatures above T_{eq}.

Considering the time frame involved, it seems unlikely that E_{inact} is significantly unfolded and more likely that the transition from E_{act} to E_{inact} involves only a local (reversible) conformational change, possibly near or at the active site, in contrast to the largely irreversible (under assay conditions) global conformational changes associated with thermal denaturation.

Given that the E_{act}/E_{inact} transition appears to be a separate process to the process of thermal denaturation, it was thought that the hypothesis that the reversible conformational change associated with T_{eq} is at or near the active site could be tested, albeit indirectly, by altering assay conditions to change the E_{act}/E_{inact} equilibrium.

If the transition were an active site phenomenon, agents known to cause a local and specific effect on the active site, such as substrates, would have an effect on the E_{act}/E_{inact} equilibrium and therefore, on T_{eq}. Conversely, it was expected that the addition of agents to the assay that are known to cause a global and non-specific effect, such as stabilising and destabilising agents, would only affect the thermal stability of the enzyme (expressed as $\Delta G^{\ddagger}_{inact}$) and have not affect on the E_{act}/E_{inact} equilibrium (T_{eq} remains unaffected). The results offer some support for the hypothesis that the E_{act}/E_{inact} conformational change is at or near the active-site and that it is process separate to denaturation. T_{eq} was affected when the enzyme-substrate interaction was altered[6] (by the use of different substrates) but was, in general, unaffected by denaturing or stabilising agents. There was one exception to this rule[7]; aryl acylamidase in the presence of 20% glycerol produced the only value for T_{eq} well outside the calculated errors and while it was not apparent under the conditions specified here, there is evidence to suggest that this agent produces

a non-specific inhibition[8]. This has not been investigated further but it is possible that this agent alters the enzyme-substrate interaction in addition to having a global effect on stability, consequently causing the anomaly observed.

Only a direct comparison of the conformation of E_{act} and E_{inact} can provide an unequivocal answer to the question regarding the molecular basis of the E_{act}/E_{inact} equilibrium. This will not be easy to achieve. While denaturation is relatively slow at T_{eq}, if a larger population of enzyme as E_{inact} is required (say, 80%), in most cases, at the temperature required to achieve this percentage more than 30% will be denatured per minute. It will be difficult to achieve a high proportion of the inactive form without significant "contamination" by the denatured form, so the technique used to compare the conformations must be able to make observations over timescales of ten seconds or less.

A comparison of the temperature-linked response of fluorescent groups or labels at the active site, and elsewhere on the enzyme, between the active and the inactive (but not denatured) form has the potential to offer a definitive answer to the question of the molecular basis of the E_{act}/E_{inact} equilibrium. This technique maybe prove difficult to implement as fluorescence itself is temperature dependent[9], but the main problem will be if the enzyme, in both the active and inactive forms, populates a number of conformational states and especially if intermediate states with partial activity are present, in which case the discrete differences between E_{act} and E_{inact} will be difficult to ascertain.

8.3 Methodology

Much of the experimental work described here used methods for the determination of the 'Equilibrium Model' parameters that are relatively laborious. Determination of $\Delta G^{\ddagger}_{cat}$, $\Delta G^{\ddagger}_{inact}$, ΔH_{eq} and T_{eq} involved the use of continuous assays, with the collection of data at one second intervals over five minute periods at 2-3°C temperature intervals over at least a 40°C range, with each temperature run being performed in triplicate; i.e. processing about 15000 data points gathered in about 50 experimental runs.

To enable more straightforward determinations of $\Delta G^{\ddagger}_{cat}$, $\Delta G^{\ddagger}_{inact}$, ΔH_{eq} and T_{eq}, minimum assay parameters were determined, in terms of sampling rate and temperature range, establishing to what extent data collection (and thus labour) could be reduced without compromising the accuracy of the derived parameters.

In terms of sampling rate, it was established[10] that the accuracy of these parameters is not dominated by a requirement for "early" data, taken very soon after zero time, and that the collection of data at 60 second intervals potentially gives quite accurate results. This result implies that adequate data might be obtained from a discontinuous assay that is "stopped" at 60 second time intervals. The confirmation of this result widens the potential utility of determining T_{eq} as future work will possibly include the determination of T_{eq} of enzymes from extreme thermophiles, assays for which will likely be performed above 100°C and may have to be discontinuous[11].

To collect progress curves, continuously or by "stopped" means, over an extended period of time for fitting to the 'Equilibrium Model' requires that any decrease in

activity observed is due solely to thermal inactivation and not some other process. This requires that the enzyme and the reaction it catalyses be "ideal"; that is, that the enzyme is neither product nor substrate inhibited, the reaction is essentially irreversible (far from equilibrium) and the enzyme operates at V_{max}. This suggests that the utility of the 'Equilibrium Model' might be limited to "ideal" enzyme reactions. However, by altering the assay conditions to prolong the initial rate of reaction, data collected (as initial rates, therefore essentially zero time data) can be fitted to the 'Equilibrium Model' equation with time (t) set to zero[12]. This has enabled the determination of the 'Equilibrium Model' parameters (with the exception of $\Delta G^{\ddagger}_{inact}$) of an enzyme that was assayed in the reverse direction and near to the reaction equilibrium position. This result indicates that determining T_{eq} is not limited to "ideal" situations and that equally accurate results can be obtained when assaying "non-ideal" enzymes, further extending the potential utility of determining T_{eq}.

8.4 Biotechnological implications

In terms of protein engineering, the results presented here indicate that engineering an increase in thermostability alone will not necessarily lead to enhanced activity at high temperatures unless the equilibrium mid-point between the active and inactive forms, T_{eq}, is also shifted to higher temperatures.

The increases in T_{eq} and ΔH_{eq} observed when the flexibility of the active site is decreased (by the incorporation of large bulky substrates into the active site)[13-16], suggests that engineering bonds in or around active site might increase T_{eq}. However, given that conformational flexibility is often required for efficient catalysis, it is possible that this mutational strategy will affect K_M and k_{cat}. It

might be a better approach then when screening enzymes for biotechnological use to select for T_{eq} rather than thermal stability. If engineering an increase in T_{eq} turns out to be too difficult, it might be possible to select among enzymes with a high T_{eq} then engineer an increase in the thermal stability of the selected enzyme.

An additional biotechnological implication of this new model for the thermal behaviour of enzymes is its effect on enzyme reactor performance. Maximising the output of enzyme reactors requires a very careful balance of the effects of temperature upon enzyme stability and upon activity, and now must take into account the influence of T_{eq}. Predictions of the output of product with time and temperature based upon the traditional Classical Model are quite different from those derived from the Equilibrium Model[17], and suggests that the use of the Equilibrium Model might enable better predictions than the Classical Model for the output of enzyme reactors.

Using a simple stirred tank reactor and provided the substrate and product are stable under reactor conditions, a comparison of experimental results with predicted results from both the Equilibrium and the Classical Model should be possible.

8.5 Environmental and Ecological Implications

Any correlation between the Arrhenius activation energy of an enzyme to its thermal environment is uncertain and at best very loose[18-22], and although there is a strong correlation between thermal stability and the environmental temperature of the source organism, it is known that enzyme thermal stability also reflects resistance to other cellular conditions such as the action of proteases[23, 24]. It has

been predicted that T_{eq} will be a better expression of the effect of environmental temperature on the evolution of the enzyme than thermal stability; and that the overall shape of the zero time T_{opt} curve will describe the fit of an enzyme to its thermal environment, T_{eq} thus providing an important new parameter in matching an enzyme's properties to its cellular and environmental function.

The data collected here provides evidence of the relationship between T_{eq} and growth temperature (compared with $\Delta G^{\ddagger}_{inact}$) and potentially its evolutionary significance. Although the sample population is rather small, results from the assay of three enzymes, one each from a psychrophilic, mesophilic and thermophilic source, indicate that there is a correlation between T_{eq} and growth temperature; that T_{eq} is a better indication of the source temperature of the enzyme than $\Delta G^{\ddagger}_{inact}$; and that ΔH_{eq} correlates with the shape of the zero time T_{opt} curve, which in turn correlates with the growth temperature range of the organism and reflects the thermal environment from which the enzyme was sourced (i.e. stenothermal versus eurythermal). These observations have allowed the tentative prediction of the thermal habitat of three ancestors of the *Bacillus* genus by characterisation of the enzyme products of ancient genes reconstructed using computational phylogenetic inference.

The results of this work are such that T_{eq} can now be considered a fundamental thermal parameter of enzymes alongside Arrhenius activation energy and thermal stability. The concept of true temperature optima described by the 'Equilibrium Model' and characterised by the values of ΔH_{eq} and T_{eq}, has already earned a mention in a major enzyme kinetics text[25] and as it is the temperature at which the

concentrations of E_{act} and E_{inact} are equal (i.e. where the enzyme is 50% "active"), T_{eq} might be referred to as the thermal equivalent of K_M. This suggests that T_{eq} may rank alongside K_M as a parameter to determine in the characterisation of a novel enzyme.

8.6 References

1. Daniel, R.M., Danson, M.J. & Eisenthal, R. (2001) The temperature optima of enzymes: a new perspective on an old phenomenon. *Trends in Biochemical Sciences*, **26**(4), 223 – 225.

2. Chapter 3, 77 – 82.

3. Chapter 7, 180 – 186.

4. Lee, C.K., Peterson, M.E., Eisenthal, R., Danson, M.J., Cary, S.C. & Daniel, R.M. (2005) Growth temperature correlates with T_{eq}, a new intrinsic thermal property of enzymes. *In Progress.*

5. Chapter 3, 83.

6. Chapter 5, 40 – 42.

7. Chapter 5, 43 – 44.

8. Stein, R.L. (2002) Enzymatic Hydrolysis of *p*-Nitroacetanilide: Mechanistic Studies of the Aryl Acylamidase from *Pseudomonas flourescens*. *Biochemisty*, **41**, 991 – 1000.

9. Bismuto, E., Martelli, P.L., De Maio, A., Mita, D.G., Irace, G. & Casadio, R. (2002) Effect of molecular confinement on internal enzyme dynamics: Frequency domain fluorometry and molecular dynamics simulation studies. *Biopolymers*, **67**, 85 – 95.

10. Chapter 4, 106 – 108.

11. Daniel, R.M. & Danson, M.J. (2001) Assaying Activity and Assessing Thermostability of Hyperthermophilic Enzymes. *Methods in Enzymology*, **334**, 283 – 293.

12. Chapter 4, 119 – 122.

13. Jaenicke, R. & Bohm, G. (1998) The stability of proteins in extreme environments. *Current Opinion in Structural Biology*, **8**, 738 – 748.

14. Brewer, J.M. & Wampler, J.E. (2001) A differential scanning calorimetric study of the effects of metal ions, substrate/product, substrate analogues and chaotropic anions on the thermal denaturation of yeast enolase 1. *International Journal of Biological Macromolecules*, **28**, 213 – 218.

15. Brewer, J.M., Glover, C.V.C., Holland, M.J. & Lebioda, L. (1998) Significance of the enzymatic properties of yeast S39A enolase to the catalytic mechanism. *Biochimica et Biophysica Act,* **1383**, 351 – 355.

16. Chapter 5, 139 – 141.

17. Chapter 6, 168.

18. Georlette, D., Blaise, V., Collins, T., D'Amico, S., Gratia, E., Hoyoux, A.. Marx, J.-C., Sonan, G., Feller, G. & Gerday, C. (2004) Some like it cold: biocatalysis at low temperatures. *FEMS Microbiology Reviews*, **28**, 25 – 42.

19. Feller, G. (2003) Molecular adaptations to cold in psychrophilic enzymes. *Cellular and Molecular Life Science*, **60**, 648 – 662.

20. Feller, G. & Gerday, C. (2003) Psychrophilic enzymes: hot topics in cold adaptation. *Nature Reviews Microbiology*, **1**, 200 – 208.

21. D'Amico, S., Claverie, P., Collins, T., Georlette, D., Gratia, E., Hoyoux, A., Meuwis, M-A., Feller, G. & Gerday, C. (2002) Molecular basis of cold adaptation. *Philosophical Transactions of the Royal Society B*, **357**, 917 – 925.

22. Lonhienne, T., Gerday, C. & Feller, G. (2000) Psychrophilic enzymes: revisiting the thermodynamic parameters of activation may explain local flexibility. *Biochimica et Biophysica Acta,* **1543**, 1 – 10.

23. Daniel, R.M., Cowan, D.A., Morgan, H.W. & Curran, M.P. (1982) A correlation between protein thermostability and resistance to proteolysis. *Biochemical Journal*, **207**, 641 – 644.

24. Daniel, R.M. Dines, M. & Petach, H.H. (1996) The denaturation and degradation of stable enzymes at high temperatures. *Biochemical Journal*, **317**, 1 – 11.

25. Cornish-Bowden, A. (2004) In "*Fundamentals of Enzyme Kinetics*" (3rd Edn) Portland Press Ltd., London, UK.

Appendix A

The temperature optima of enzymes: a new perspective on an old phenomenon

Opinion TRENDS in Biochemical Sciences Vol.26 No.4 April 2001 223

The temperature optima of enzymes: a new perspective on an old phenomenon

Roy M. Daniel, Michael J. Danson and Robert Eisenthal

Careful analysis of the dependence of enzyme activity on assay temperature has revealed that some enzymes might have real temperature optima in which the decrease in catalytic rate at temperatures above the optimum is not primarily a result of irreversible thermal inactivation. The 'equilibrium model' has been formulated to describe genuine temperature optima, and to suggest a simple experimental method by which to distinguish these cases from those in which enzyme instability is the major determinant of temperature optima.

Roy M. Daniel†
Dept of Biological Sciences, University of Waikato, Hamilton, New Zealand.

Michael J. Danson*†
Centre for Extremophile Research, Dept of Biology and Biochemistry, University of Bath, Bath, UK BA2 7AY.
*e-mail: m.j.danson@bath.ac.uk

Robert Eisenthal†
Dept of Biology and Biochemistry, University of Bath, Bath, UK BA2 7AY.

If enzymes were to have 'real' temperature optima, this would have more than academic significance. For instance, engineering an enzyme to operate at high temperatures would necessitate that attention be paid to activity as well as to stability, and the temperature optimum (T_{opt}) would be as important to the user as would specific activity and the pH optimum. However, as an intrinsic property of an enzyme, the temperature optimum has been regarded as a discredited concept[1,2]. That is, it is thought to be of dubious validity and limited value because the apparent optimum temperature arises from an unknown mixture of thermal stability and temperature coefficient, and is dependent upon assay duration. Thus, the ascending limb of an 'enzyme activity versus temperature' plot arises from the temperature coefficient of the catalytic rate (as defined by the Arrhenius activation energy) until the point at which denaturation becomes significant; the descending limb of the plot consists of a combination of this and thermal stability. Because the contribution of denaturation is time dependent as well as temperature dependent, the apparent optimum is shifted to lower temperatures for longer assays. In this situation, which we term the 'classical model', the variation in enzyme activity with temperature and time of assay can be described as in Eqn 1:

$$V_{max} = k_{cat} \cdot [E]_0 \, e^{-k_{inact} \cdot t} \quad [1]$$

where V_{max} = maximum enzyme velocity; k_{cat} = catalytic constant of the enzyme; $[E]_0$ = total enzyme concentration; k_{inact} = thermal inactivation rate constant; and t = assay duration.

The variation of the two rate constants in Eqn [1] with temperature is given by Eqns 2 and 3:

$$k_{cat} = \frac{k_B T}{h} \cdot e^{-(\Delta G^{\ddagger}_{cat}/RT)} \quad [2]$$

and

$$k_{inact} = \frac{k_B T}{h} \cdot e^{-(\Delta G^{\ddagger}_{inact}/RT)} \quad [3]$$

where k_B = Boltzmann's constant; R = gas constant; T = absolute temperature; h = Planck's constant; $\Delta G^{\ddagger}_{cat}$ = activation energy of the catalysed reaction; and $\Delta G^{\ddagger}_{inact}$ = activation energy of the thermal inactivation process. Note that for simplicity, the above situation assumes that the enzyme remains saturated with substrate during the assay. The variation in enzyme activity with temperature and time is displayed graphically in Fig. 1, in which it can be seen that the apparent temperature optimum decreases with increasing time during the assay.

Although the term is no longer found widely in biochemistry undergraduate textbooks, 'temperature optima' of enzymes continue to be reported, particularly in some journals concerned with enzyme technology or the field of extremophile microbiology. Until recently, the use of this term could be regarded merely as sloppy thinking, but was defended on the grounds that it was a useful shorthand way of comparing enzymes with respect to their potential technical use at elevated temperatures. However, a recent paper by Thomas and Scopes[3] suggests that at least some enzymes do have genuine temperature optima; that is, above a certain temperature the enzyme becomes (reversibly) less active. In this paper, the authors describe the kinetic and stability properties of the monomeric enzyme phosphoglycerate kinase from mesophilic and thermophilic sources. In all cases, a comparison of these properties shows a lower activity at high temperatures than can be accounted for by irreversible denaturation. At the same time, studies in our own laboratories have confirmed that these are not isolated examples[4–6]. We emphasize that the behaviour we are describing here is qualitatively different from the experimentally observed loss of activity that results from denaturation, which is almost invariably irreversible under assay conditions.

To describe a true temperature optimum, we have formulated a model, the 'equilibrium model', wherein the active enzyme (E_{act}) is in equilibrium with an inactive form (E_{inact}), and it is the inactive form that undergoes irreversible thermal inactivation to the thermally-denatured state (X; Eqn 4):

$$E_{act} \rightleftharpoons E_{inact} \longrightarrow X \quad [4]$$

In this case, the dependence of enzyme activity on temperature has an additional component, namely

http://tibs.trends.com 0968-0004/01/$ - see front matter PII: S0968-0004(01)01803-5

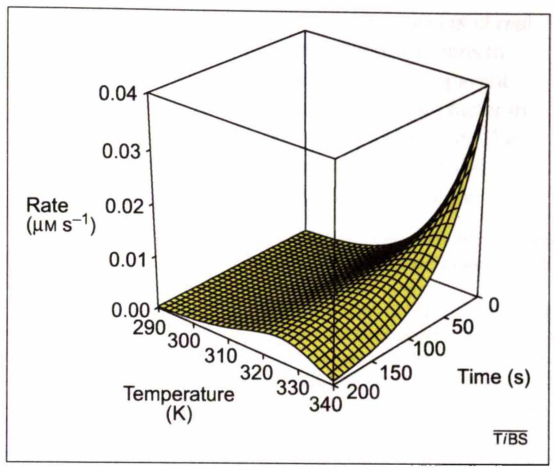

Fig. 1. Temperature dependence of enzyme activity: the classical model. The variation of enzyme activity with temperature (290–340 K) and time (0–200 s) during the assay was simulated using Eqns 1–3 with the following parameter values: ΔG^{*}_{cat} = 80 KJ mol^{-1}; ΔG^{*}_{inact} = 95 KJ mol^{-1}; total enzyme concentration = 100 nM.

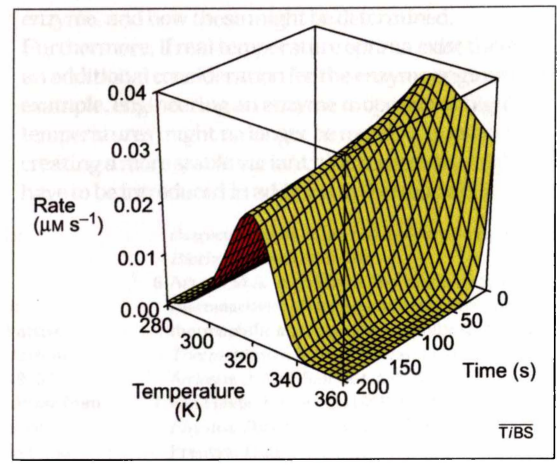

Fig. 2. Temperature dependence of enzyme activity: the equilibrium model. The variation of enzyme activity with temperature (280–360 K) and time (0–200 s) during the assay was simulated using Eqns 4–7 with the following parameter values: ΔG^{*}_{cat} = 80 KJ mol^{-1}; ΔG^{*}_{inact} = 95 KJ mol^{-1}; total enzyme concentration = 100 nM; ΔH_{eq} = 100 KJ mol^{-1}; T_m = 320 K.

the effect of temperature on the equilibrium position between active and inactive forms of the protein (Eqn 5):

$$V_{max} = k_{cat} \cdot [E_{act}] \quad [5]$$

where the dependence of k_{cat} on temperature remains as defined in Eqn [2], but the concentration of active enzyme at any time point is defined by Eqn 6:

$$[E_{act}] = \frac{[E_0] - [X]}{1 + K_{eq}} \quad [6]$$

where K_{eq} is the equilibrium constant between active and inactive forms of the enzyme $\{K_{eq} = [E_{inact}] / [E_{act}]\}$, and the rate of appearance of X is given by Eqn 7:

$$\frac{d[X]}{dt} = k_{inact}\{[E_0] - [E_{act}] - [X]\} \quad [7]$$

The variation of K_{eq} with temperature is given by Eqn 8:

$$\ln(K_{eq}) = \frac{\Delta H_{eq}}{R}\left[\frac{1}{T_m} - \frac{1}{T}\right] \quad [8]$$

where ΔH_{eq} is the enthalpic change associated with the conversion of active to inactive enzyme, and T_m is the temperature at the mid-point of transition between the two forms[7].

The variation of enzymic rate with temperature and time during assay in the equilibrium model is shown in Fig. 2. It is obvious that, even at time zero when no thermal inactivation can have taken place, the enzyme shows a temperature optimum (cf. the classical model in Fig. 1). Moreover, depending on the value of T_m with respect to the temperatures at which significant inactivation is observed during the time course of the assay, there is a much smaller change in the apparent temperature optimum with time in the equilibrium model than in the classical model. In effect, the equilibrium model provides a 'thermal buffer' that protects the enzyme from thermal inactivation.

It is interesting to note that this effect is seen even if the equilibrium model is generalized to allow for the possibility of E_{act} also undergoing thermal denaturation. If, for example, both E_{act} and E_{inact} lose activity irreversibly, each with a rate constant equal to k_{inact}, the rate–temperature–time profile looks much like that depicted in Fig. 2. At the lower range of temperatures, the generalized model gives somewhat lower catalytic rates, but at higher temperatures most of the enzyme is in the inactive state, and the two plots are virtually identical.

It remains to be determined how widespread are genuine temperature optima for enzymes, compared with the 'classical' behaviour, although our own experience inclines us to the view that it might turn out to be relatively common. Therefore, although we are not proposing that the classical model should be discarded, we are suggesting that, for some enzymes, the equilibrium model could give a better representation of the observations. In any event, when genuine optima are present, the phenomenon provides enzymologists with an additional intrinsic property by which an enzyme can be characterized and matched to its physiological role. The detection of true optima has not been entirely straightforward: stability must be determined under the same conditions as activity (i.e. in the presence of substrates and any cofactors, and ideally at comparable protein concentrations) and, because the effects are not necessarily large, careful attention must be paid to the statistical errors of both determinations. However, we have shown that simulated progress curves for an enzyme-catalysed reaction (concentration of product formed with time), generated by the equilibrium model at a series of temperatures, cannot then be fitted to the classical model, nor vice versa. Therefore, an experimental distinction can be made as to which of the two models fits any particular enzyme simply by collecting such progress curves at a variety of temperatures, thereby obviating the need to perform separate activity and stability measurements. Analysis of these curves should provide estimates of T_m and ΔH_{eq}, as well as the activation energies of the catalytic reaction (ΔG^{*}_{cat}) and the thermal inactivation process (ΔG^{*}_{inact}).

†Acknowledgements
We are indebted to the Biotechnological and Biological Sciences Research Council, UK (M.J.D. and R.E.), and to the Marsden Fund, New Zealand (R.M.D.) for financial support. We also thank Frances H. Arnold (CalTech, USA) for useful suggestions.

In conclusion, we have described the concept of real temperature optima for enzymes, and the means to distinguish the phenomenon from cases of apparent optima in which protein instability is a major factor in the temperature-dependence of enzyme activity. The question now is about the nature of the structural changes between active and inactive forms of the enzyme, and how these might be determined. Furthermore, if real temperature optima exist there is an additional consideration for the enzyme engineer; for example, engineering an enzyme to operate at high temperatures might no longer be merely a question of creating a more stable variant: thermoactivity might have to be introduced in addition to thermostability.

References

1 Cornish-Bowden, A. (1995) In *Fundamentals of Enzyme Kinetics*, pp. 193–197, Portland Press Ltd, London, UK
2 Daniel, R.M. and Danson, M.J. Assaying activity and assessing thermostability of hyperthermophilic enzymes. *Methods Enzymol.* (in press)
3 Thomas, T.M. and Scopes, R.K. (1998) The effects of temperature on the kinetics and stability of mesophilic and thermophilic 3-phosphoglycerate kinase. *Biochem. J.* 330, 1087–1095
4 Gerike, U. *et al.* (1997) Sequencing and expression of the gene encoding a cold-active citrate synthase from an antarctic bacterium, strain DS2-3R. *Eur. J. Biochem.* 248, 49–57
5 Buchanan, C.L. *et al.* (1999) A novel aldolase from the hyperthermophilic Archaeon *Sulfolobus solfataricus*: gene cloning and expression, and characterisation of the recombinant enzyme. *Biochem. J.* 343, 563–570
6 Arnott, M.A. *et al.* (2000) Thermostability and thermoactivity of citrate synthases from the thermophilic and hyperthermophilic Archaea, *Thermoplasma acidophilum* and *Pyrococcus furiosus*. *J. Mol. Biol.* 304, 655–666
7 van Holde, K.E. *et al.* (1998) In *Principles of Physical Biochemistry*, pp. 158–159, Prentice-Hall

Translation control: bridging the gap between genomics and proteomics?

Bérengère Pradet-Balade, Florence Boulmé, Hartmut Beug, Ernst W. Müllner and Jose A. Garcia-Sanz

mRNA profiling enables the expression levels of thousands of transcripts in a cell to be monitored simultaneously. Nevertheless, analyses in yeast and mammalian cells have demonstrated that mRNA levels alone are unreliable indicators of the corresponding protein abundances. This discrepancy between mRNA and protein levels argues for the relevance of additional control mechanisms besides transcription. As translational control is a major mechanism regulating gene expression, the use of translated mRNA in profiling experiments might depict the proteome more closely than does the use of total mRNA. This would combine the technical potential of genomics with the physiological relevance of proteomics.

Proteins, rather than genes or mRNAs, represent the key players in the cell. The proteome (i.e. the complete set of proteins encoded by the genome[1]) determines the cellular phenotype and its plasticity in response to external signals. Expression levels of a protein depend not only on transcription rates of the gene, but also on additional control mechanisms, such as nuclear export and mRNA localization[2], transcript stability[3], translational regulation[4] and protein degradation[5–7]. Moreover, both the activity and the function of proteins can be altered, mainly through post-translational modifications (e.g. glycosylation and phosphorylation) or proteolytic cleavage[8]. Transcriptional and post-translational regulation have attracted much attention, whereas the regulation of protein levels by translational control has often been either neglected or underestimated[9]. However, in recent years, interest in the mechanisms controlling the activity of the translation machinery – during development, in response to extracellular stimuli, following viral infections or in disease – has notably increased[10]. The best-understood mechanisms controlling translational efficiency are those that act at the level of initiation, which involve structural elements within particular mRNAs, modifications of components of the initiation machinery or the regulated association of the initiation machinery with other proteins that affect the activity of the complex[11]. Indeed, rather than influencing a few individual mRNAs, translational control is a widespread mechanism for regulating gene expression. This was first demonstrated upon oocyte fertilization[12,13] and reticulocyte maturation[14]. More recently, it has been shown that translational control affects ~20% of the genes regulated upon T-cell activation[15]. Thus, an idea is emerging that the relevance of mRNA profiling data might be improved if the level of translational regulation is also taken into account.

Do mRNA expression levels faithfully reflect protein abundance?

A recurring criticism to the use of mRNA expression profiling in characterizing cellular phenotypes has been that the transcriptome does not faithfully represent the proteome[16]. A limited number of reports have compared the steady-state levels of proteins with those of their corresponding mRNAs. Results from these studies have suggested that mRNA abundance is a poor indicator of the levels of the corresponding protein[17–20]. As it is the proteome that determines cell phenotype, this disparity between protein and transcript levels might lead to misinterpretation of mRNA profiling results.

To date, the two most extensive analyses correlating mRNA and protein expression levels have both been

http://tibs.trends.com 0968-0004/01/$ – see front matter PII: S0968-0004(00)01776-X

Appendix B

Loess smoothing

Adapted from the *National Institute of Standards and Technology/SEMATECH e-Handbook of Statistical Methods*, http://www.itl.nist.gov/div898/handbook/, 15-11-2004

B.1 Introduction

LOESS is one of many "modern" modelling methods that build on "classical" methods, such as linear and nonlinear least squares regression. Modern regression methods are designed to address situations in which the classical procedures do not perform well or cannot be effectively applied without undue labour. LOESS combines much of the simplicity of linear least squares regression with the flexibility of nonlinear regression. It does this by fitting simple models to localized subsets of the data to build up a function that describes the deterministic part of the variation in the data, point by point. In fact, one of the chief attractions of this method is that the data analyst is not required to specify a global function of any form to fit a model to the data, only to fit segments of the data.

The trade-off for these features is increased computation. Because it is so computationally intensive, LOESS would have been practically impossible to use in the era when least squares regression was being developed. Most other modern methods for process modelling are similar to LOESS in this respect. These methods have been consciously designed to use our current computational ability

to the fullest possible advantage to achieve goals not easily achieved by traditional approaches.

B.2 Definition of a LOESS Model

LOESS, originally proposed by Cleveland[1] and further developed by Cleveland and Devlin[2], specifically denotes a method that is (somewhat) more descriptively known as locally weighted polynomial regression. At each point in the data set a low-degree polynomial is fit to a subset of the data, with explanatory variable values near the point whose response is being estimated. The polynomial is fit using weighted least squares, giving more weight to points near the point whose response is being estimated and less weight to points further away. The value of the regression function for the point is then obtained by evaluating the local polynomial using the explanatory variable values for that data point. The LOESS fit is complete after regression function values have been computed for each of the n data points. Many of the details of this method, such as the degree of the polynomial model and the weights, are flexible. The range of choices for each part of the method and typical defaults are briefly discussed next.

B.2.1 Localized Subsets of Data

The subsets of data used for each weighted least squares fit in LOESS are determined by a nearest neighbours algorithm. A user-specified input to the procedure called the "bandwidth" or "smoothing parameter" determines how much of the data is used to fit each local polynomial. The smoothing parameter, q, is a number between $(d+1)/n$ and 1, with d denoting the degree of the local polynomial. The value of q is the proportion of data used in each fit. The subset

of data used in each weighted least squares fit is comprised of the nq (rounded to the next largest integer) points whose explanatory variables values are closest to the point at which the response is being estimated.

q is called the smoothing parameter because it controls the flexibility of the LOESS regression function. Large values of q produce the smoothest functions that wiggle the least in response to fluctuations in the data. The smaller q is, the closer the regression function will conform to the data. Using too small a value of the smoothing parameter is not desirable, however, since the regression function will eventually start to capture the random error in the data. Useful values of the smoothing parameter typically lie in the range 0.25 to 0.5 for most LOESS applications.

B.2.2 Degree of Local Polynomials

The local polynomials fit to each subset of the data are almost always of first or second degree; that is, either locally linear (in the straight line sense) or locally quadratic. Using a zero degree polynomial turns LOESS into a weighted moving average. Such a simple local model might work well for some situations, but may not always approximate the underlying function well enough. Higher-degree polynomials would work in theory, but yield models that are not really in the spirit of LOESS. LOESS is based on the ideas that any function can be well approximated in a small neighbourhood by a low-order polynomial and that simple models can be fit to data easily. High-degree polynomials would tend to over-fit the data in each subset and are numerically unstable, making accurate computations difficult.

B.2.3 Weight Function

As mentioned above, the weight function gives the most weight to the data points nearest the point of estimation and the least weight to the data points that are furthest away. The use of the weights is based on the idea that points near each other in the explanatory variable space are more likely to be related to each other in a simple way than points that are further apart. Following this logic, points that are likely to follow the local model best influence the local model parameter estimates the most. Points that are less likely to actually conform to the local model have less influence on the local model parameter estimates.

The traditional weight function used for LOESS is the tri-cube weight function,

$$w(x) = \begin{cases} (1 - |x|^3)^3 & \text{for } |x| < 1 \\ 0 & \text{for } |x| \geq 1 \end{cases}$$

However, any other weight function that satisfies the properties listed in Cleveland[1] could also be used. The weight for a specific point in any localized subset of data is obtained by evaluating the weight function at the distance between that point and the point of estimation, after scaling the distance so that the maximum absolute distance over all of the points in the subset of data is exactly one.

B.3 Advantages of LOESS

As discussed above, the biggest advantage LOESS has over many other methods is the fact that it does not require the specification of a function to fit a model to all of the data in the sample. Instead the analyst only has to provide a smoothing parameter value and the degree of the local polynomial. In addition, LOESS is

very flexible, making it ideal for modelling complex processes for which no theoretical models exist. These two advantages, combined with the simplicity of the method, make LOESS one of the most attractive of the modern regression methods for applications that fit the general framework of least squares regression but which have a complex deterministic structure.

Although it is less obvious than for some of the other methods related to linear least squares regression, LOESS also accrues most of the benefits typically shared by those procedures. The most important of those is the theory for computing uncertainties for prediction and calibration. Many other tests and procedures used for validation of least squares models can also be extended to LOESS models.

B.4 Disadvantages of LOESS

Although LOESS does share many of the best features of other least squares methods, efficient use of data is one advantage that LOESS doesn't share. LOESS requires fairly large, densely sampled data sets in order to produce good models. This is not really surprising, however, since LOESS needs good empirical information on the local structure of the process in order perform the local fitting. In fact, given the results it provides, LOESS could arguably be more efficient overall than other methods like nonlinear least squares. It may simply frontload the costs of an experiment in data collection but then reduce analysis costs.

Another disadvantage of LOESS is the fact that it does not produce a regression function that is easily represented by a mathematical formula. This can make it difficult to transfer the results of an analysis to other people. In order to transfer the regression function to another person, they would need the data set and

software for LOESS calculations. In nonlinear regression, on the other hand, it is only necessary to write down a functional form in order to provide estimates of the unknown parameters and the estimated uncertainty. Depending on the application, this could be either a major or a minor drawback to using LOESS.

Finally, as discussed above, LOESS is a computational intensive method. This is not usually a problem in our current computing environment, however, unless the data sets being used are very large. LOESS is also prone to the effects of outliers in the data set, like other least squares methods. There is an iterative, robust version of LOESS[1] that can be used to reduce LOESS' sensitivity to outliers, but extreme outliers can still overcome even the robust method.

B.5 References

1. Cleveland, W.S. (1979) Robust Locally Weighted Regression and Smoothing Scatterplots. *Journal of the American Statistical Association*, **74**, 829-836.

2. Cleveland, W.S. and Devlin, S.J. (1988) Locally Weighted Regression: An Approach to Regression Analysis by Local Fitting. *Journal of the American Statistical Association*, **83**, 596-610.

Appendix C

Equilibrium model rate equations

C.1 The numerically integrated rate equation

$$\text{Rate} \longleftarrow E_{act} \rightleftharpoons E_{inact} \longrightarrow X$$

$$K_{eq} = \frac{E_{inact}}{E_{act}}$$

$$E_{inact} = K_{eq} E_{act}$$

$$E_0 = E_{act} + E_{inact} + X$$

$$E_0 = E_{act} + K_{eq} E_{act} + X$$

$$E_{act} + K_{eq} E_{act} = E_0 - X$$

$$E_{act} = \frac{E_0 - X}{1 + K_{eq}} \qquad [1]$$

$$\frac{dX}{dt} = k_{inact} E_{inact} \qquad \text{where} \qquad E_{inact} = E_0 - E_{act} - X$$

$$\frac{dX}{dt} = k_{inact}\left(E_0 - E_{act} - X\right)$$

At this point, this equation is numerically integrated (using the EPISODE package for stiff equations), and related through [1] to give the rate via the equation

$$\text{Rate} = k_{\text{cat}} \cdot \text{E}_{\text{act}}$$

Where

$$k_{cat} = \frac{k_B T}{h} e^{-\frac{\Delta G^{*}_{cat}}{RT}}$$

$$k_{inact} = \frac{k_B T}{h} e^{-\frac{\Delta G^{*}_{inact}}{RT}}$$

$$K_{eq} = e^{\frac{\Delta H_{eq}}{R}\left(\frac{1}{T_{eq}} - \frac{1}{T}\right)}$$

C.2 Derivation of the analytic solution to the Equilibrium model rate equation

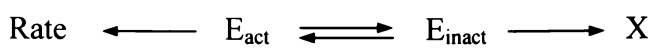

$$K_{eq} = \frac{E_{inact}}{E_{act}}$$

$$E_{inact} = K_{eq} E_{act}$$

$$E_0 = E_{act} + E_{inact} + X$$

$$E_0 = E_{act} + K_{eq} E_{act} + X$$

$$E_{act} + K_{eq} E_{act} = E_0 - X$$

$$E_{act} = \frac{E_0 - X}{1 + K_{eq}} \qquad [1]$$

$$\frac{dX}{dt} = k_{inact} E_{inact} \qquad \text{where} \qquad E_{inact} = E_0 - E_{act} - X$$

$$\frac{dX}{dt} = k_{inact} \left(E_0 - E_{act} - X\right)$$

Substituting from [1]

$$\frac{dX}{dt} = k_{inact}\left(E_0 - \left(\frac{E_0 - X}{1 + K_{eq}}\right) - X\right)$$

$$\frac{dX}{dt} = k_{inact}\left(\frac{E_0 + k_{eq}E_0 - E_0 + X - X - K_{eq}X}{1 + K_{eq}}\right)$$

$$\frac{dX}{dt} = k_{inact}\left(\frac{K_{eq}E_0}{1 + K_{eq}} - \frac{K_{eq}X}{1 + K_{eq}}\right)$$

$$\frac{dX}{\frac{K_{eq}E_0}{1 + K_{eq}} - \frac{K_{eq}X}{1 + K_{eq}}} = k_{inact}\,dt$$

which is of the form: $$\int_0^x \frac{dX}{A + BX} = \int_0^t k_{inact}\,dt$$

where: $$A = \frac{K_{eq}E_0}{1 + K_{eq}} \quad \text{and} \quad B = \frac{-K_{eq}}{1 + K_{eq}} \qquad [2]$$

integral of $$\frac{dX}{A + Bx} = \frac{1}{B}\ln(A + Bx) + \alpha = k_{inact}t \quad [\alpha = \text{integration constant}]$$

at $t = 0, X = 0$ and therefore $$\frac{1}{B}\ln A + \alpha = 0 \text{ and } \alpha = -\frac{1}{B}\ln A$$

so $\frac{1}{B}\ln(A+BX)-\frac{1}{B}\ln A = k_{inact}t$ and $\ln\left(\frac{A+BX}{A}\right) = Bk_{inact}t$

taking exponentials:

$$\frac{A+BX}{A} = e^{Bk_{inact}t}$$

$$A+BX = Ae^{Bk_{inact}t}$$

$$BX = Ae^{Bk_{inact}t} - A$$

$$X = \frac{Ae^{Bk_{inact}t} - A}{B}$$

Substituting for A and B from [2]

$$X = \frac{\frac{K_{eq}E_0}{1+K_{eq}}e^{-\frac{k_{inact}K_{eq}t}{1+K_{eq}}} - \frac{K_{eq}E_0}{1+K_{eq}}}{\frac{-K_{eq}}{1+K_{eq}}}$$

$$x = E_0 - E_0 e^{-\frac{k_{inact}K_{eq}t}{1+K_{eq}}}$$

$$rate = k_{cat} E_{act} = k_{cat}\left(\frac{E_0 - X}{1 + K_{eq}}\right) = k_{cat}\left(\frac{E_0 - E_0 + E_0 e^{-\frac{k_{inact} K_{eq} t}{1 + K_{eq}}}}{1 + K_{eq}}\right)$$

$$\boxed{rate = \frac{k_{cat} E_0 e^{-\frac{k_{inact} K_{eq} t}{1 + K_{eq}}}}{1 + K_{eq}}}$$

This is the "analytical version" of the Equilibrium Model where:

$$k_{cat} = \frac{k_B T}{h} e^{-\frac{\Delta G^{\ddagger}_{cat}}{RT}}$$

$$k_{inact} = \frac{k_B T}{h} e^{-\frac{\Delta G^{\ddagger}_{inact}}{RT}}$$

$$K_{eq} = e^{\frac{\Delta H_{eq}}{R}\left(\frac{1}{T_{eq}} - \frac{1}{T}\right)}$$

$$V_{\max} = \frac{k_B T\, e^{-\left(\frac{\Delta G^{*}_{cat}}{RT}\right)} E_0\, e^{\left(-\frac{k_B T\, e^{-\left(\frac{\Delta G^{*}_{inact}}{RT}\right)} e^{\left(\frac{\Delta H_{eq}\left(\frac{1}{T_{eq}}-\frac{1}{T}\right)}{R}\right)}}{h\left(1+e^{\left(\frac{\Delta H_{eq}\left(\frac{1}{Teq}-\frac{1}{T}\right)}{R}\right)}\right)} t\right)}}{h\left(1+e^{\left(\frac{\Delta H_{eq}\left(\frac{1}{T_{eq}}-\frac{1}{T}\right)}{R}\right)}\right)}$$

Appendix D

Details of gene design, sequencing, cloning, expression and purification of IPMDH from *Bacillus* species

---

The experimental details described here are the work of Charis Shepherd, a PhD student at the University of Auckland. They are included here for completeness.

D.1 Cloning, expression and purification of "native" Bacillus IPMDH

IPMDH genes were cloned from number of different *Bacillus* strains using PCR based techniques using primers designed specifically for each organism. Psychrophilic IPMDH from *Bacillus psychrophilus* and *Bacillus psychrosaccharolyticus* were obtained using genomic walking PCR[1,2]. Restriction sites were designed into the primer sequences to allow for easy directional cloning into the ProEX™ HT expression vector (Life Technologies – now Invitrogen). The ProEX™ HT Prokaryotic Expression System incorporates a polyhistidine (6xHis) sequence at the amino terminus of the expressed protein. This 6xHis sequence has a strong affinity for Ni^{2+} nitrilo-tri-acetic acid (Ni-NTA) resin allowing for simple purification of the protein of interest.

Plasmids containing the IPMDH gene of interested were used to transform MAX EFFICIENCY® DH5α™ Competent Cells (Invitrogen). Transformed bacterial colonies were screened for the presence of the IPMDH insert using insert specific PCRs. Single colonies from the overnight agar plates were picked and used to

inoculate 150 μL of Luria Broth (ampicillin 100 μg/mL) and incubated overnight at 37°C. 100 μL of overnight culture was transferred into a new tube and glycerol added to a final concentration of 15%. These were frozen and used as glycerol stocks for future protein expression work. To the remaining 50 μL of culture, 50 μL of H_2O was added and cells lysed at 94°C for 30 minutes. Samples were snap-frozen at -20°C for 1hour. Samples were thawed and 1.5 μL of lysate used as template for a PCR with IPMDH insert specific primers. PCR products were run on a 1% agarose gel and the presence of a PCR product of the correct size used to indicate whether the insert was present.

In order to express recombinant IPMDH, 5 mL of Terrific Broth (ampicillin 100 μg/mL) was inoculated with 5 μL of glycerol stock of transformed *E. coli* containing the insert of interest, and the culture grown overnight at 37°C. The 5 mL overnight culture was used to inoculate a 500 mL culture of Terrific Broth (ampicillin 100 μg/mL) and culture was incubated at 37°C to an A_{600} of 0.5-1.0. IPTG was added to a final concentration of 0.5 mM and culture left for a minimum of 3 hours at 37°C with vigorous shaking. Inducement of protein from psychrophiles was performed at 18°C overnight as inducement at higher temperatures resulted in unfolded protein.

Protein was purified using Ni-NTA His-Bind® Superflow (QIAGEN) beads following manufacturer's instructions. Protein was concentrated in 10000 MW Viva spin concentrators (Vivascience) and centrifuged at 1500 g at 8 °C until protein solution was less than 1 mL. Protein quantification was performed using the colorimetric BIORAD DC Protein assay using kit instructions.

D.2 Ancestral Gene Design, Construction and Expression

Gene sequences for IPMDH (*leuB*) from the *Bacillus* family and an out group of *Staphylococcus aureus* were compiled from a range of sources including NCBI[3] and PSCB Databank. The organisms were selected for their sequence availability and range of growth temperatures.

The amino acid sequences for the IPMDH genes from *Bacillus* were aligned using ClustalX[4] and the alignment refined using MacClade v4.0[5]. The DNA alignment was edited in MacClade v4.0 to match the amino acid alignment. The amino acid alignment was used in PAUP[6] to create a phylogenetic tree (Figure 4.4).

Ancestral genes were designed for nodes 15, 18 and 20 as these seemed likely to be the most interesting for studying the evolution of IPMDH in *Bacillus*.

Ancestral sequences were inferred using six different methods as described by Shepherd[2]. It involved the use of Maximum Parsimony using PAUP[6] and Maximum Likelihood methods using PAML[7]. The results from each ancestral inference methods were aligned for each node to enable manual checking of the ancestral gene. Where all methods predicted the same amino acid this was accepted as the ancestral state. Conflicts between the ancestral states were solved using the a number of criteria including a majority rules consensus, weighting was towards codon and protein-derived choices using PAML methods, bias was towards a choice of amino acid that appeared in organisms from all temperature ranges and the JTT model of amino acid classification was also used as a guide[8].

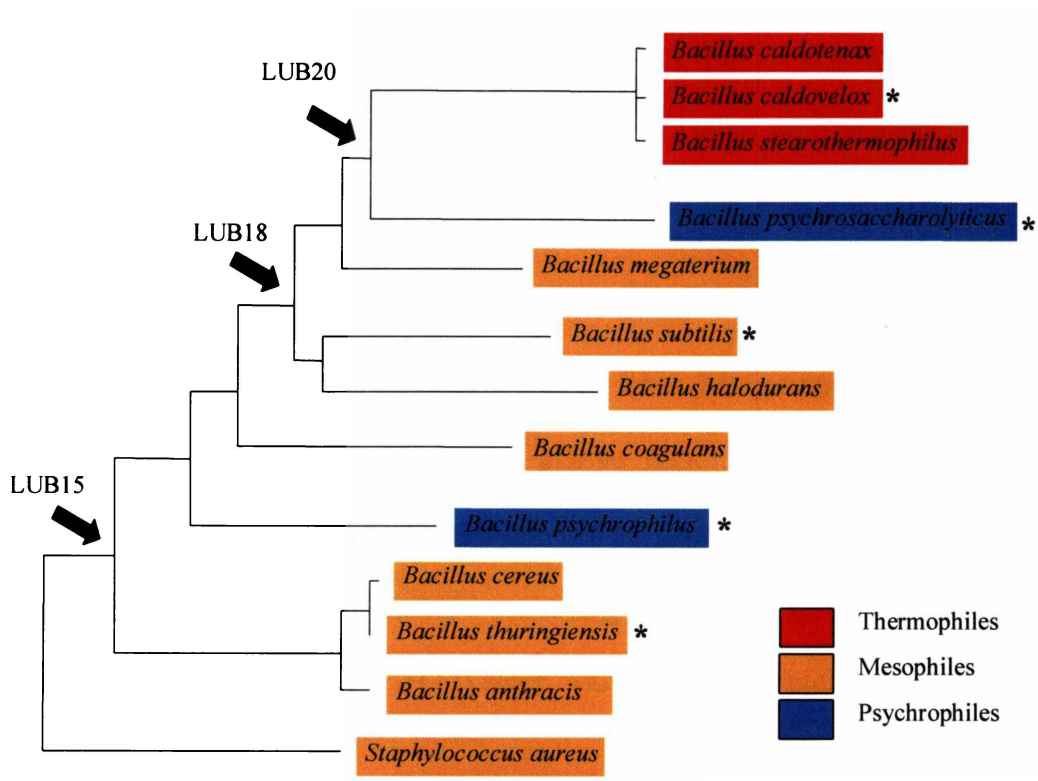

Figure D.1 IMPDH gene tree for Bacillus species

This tree was used to design ancestral IPMDH sequences for Nodes 15, 18 and 20 as indicated.

Once the ancestral amino acid sequences for each node were finalised, codon usage bias was optimized in order to achieve desired protein expression levels. The amino acid sequences were back translated using the *E.coli* codon preference table using the GCG program "backtranslate"[9]. Amino acid sequences were modified to allow the addition of restriction sites at the start and finish of the gene.

Synthetic ancestral genes were manufactured by DNA 2.0 California, USA. Genes were received inserted into the Qiagen pDrive vector. Ancestral genes were received as 5 μg lyophilized plasmid containing gene insert and as an *E. coli* culture stab transformed with plasmid containing constructed gene. The gene was transferred into the ProEX™ HT vector was used for protein expression as described in Section D.1.

D.3 References

1. Morris, D.D., Reeves, R.A., Gibbs, M.D., Saul, D.J., & Bergquist, P.L. (1995) Correction of the β-Mannanase Domain of the *celC* Psuedogene from *Caldocellulosiruptor saccharolyticus* and Activity of the Gene Product on Kraft Pulp, *Applied and Environmental Microbiology,* **61**, 2262 – 2269.

2. Shepherd, C. *et al* (2005) manuscript in progress

3. National Centre of Biotechnology, http://www.ncbi.nlm.nih.gov/.

4. Thompson, J.D., Gibson, T.J., Plewniak, F., Jeanmougin, F. & Higgins, D.G. (1997) The ClustalX windows interface: flexible strategies for

multiple sequence alignment aided by quality analysis tools, *Nucleic Acids Research*, **25**, 4876 – 4882.

5. Maddison, D. & Maddison, W. (2000) Analysis of Phylogeny and Character Evolution University of Arizona.

6. Swofford, D. L. (2003) PAUP*. Phylogenetic Analysis Using Parsimony (*and Other Methods). Version 4. Sinauer Associates, Sunderland, Massachusetts.

7. Yang, Z. (1997) PAML: a program package for phylogenetic analysis by maximum likelihood. CABIOS, **13**.

8. Taylor, W. R. (1986) The Classification of Amino Acid Conservation. *Journal of Theoretical Biology*, **119**, 205-218.

9. GCG Wisconsin Package Accerlys Software Inc. http://www.accelrys.com.

Complete reference list

Ahern, T.J. & Klibanov, A.M. (1985) The mechanisms of irreversible enzyme inactivation at 100°C. *Science*, **228**, 1280 – 1283.

Allison, R.D. (1996) Kinetic Assay Methods, in *Current Protocols in Protein Science*, (eds. Coligan, J.E., Dunn, B.M., Ploegh, H.L., Speicher, D.W. & Wingfield, P.T.), pp 3.5.4, John Wiley & Sons Inc., New York, New York, USA.

Anderson, E. & Britt, B.M. (2002) The stability curve of bovine adenosine deaminase is bimodal. *Journal of Biomolecular Structure and Dynamics,* **20**, 375 – 380.

Anson, M.L. (1938) The Estimation of Pepsin, Trypsin, Papain and Cathepsin with Hemoglobin. *Journal of General Physiology*, **22**, 79.

Arakawa T. & Timasheff, S.N. (1985) The stabilization of proteins by osmolytes. *Biophysical Journal*, **47**, 411 – 414.

Arnott, M.A., Michael, R.A., Thompson, C.R., Hough, D.W. & Danson, M.J. (2000) Thermostability and Thermoactivity of Citrate Synthases from the Thermophilic and Hyperthermophilic Archaea. *Thermoplasma acidophilum* and *Pyrococcus furiosus, Journal of Molecular Biology*, **304**, 657 – 668.

Arrhenius, S. (1889) On the Reaction Velocity of the Inversion of Cane Sugar by Acids. *Zeitschrift für physikalische Chemie,* **4**, 226ff.

Bailey, J.E. & Ollis, D.F. (1977) In *Biochemical Engineering Fundamentals*, pp132 – 134, McGraw-Hill, New York.

Bismuto, E., Martelli, P.L., De Maio, A., Mita, D.G., Irace, G. & Casadio, R. (2002) Effect of molecular confinement on internal enzyme dynamics: Frequency domain fluorometry and molecular dynamics simulation studies. *Biopolymers*, **67**, 85 – 95.

Brewer, J.M. & Wampler, J.E. (2001) A differential scanning calorimetric study of the effects of metal ions, substrate/product, substrate analogues and chaotropic anions on the thermal denaturation of yeast enolase 1. *International Journal of Biological Macromolecules*, **28**, 213 – 218.

Brewer, J.M., Glover, C.V.C., Holland, M.J. & Lebioda, L. (1998) Significance of the enzymatic properties of yeast S39A enolase to the catalytic mechanism. *Biochimica et Biophysica Act,* **1383**, 351 – 355.

Brooks, C. L., Karplus, M. & Pettitt, B. M. (1988) *Proteins*, John Wiley, New York.

Buchanan, C.L, Connaris, H., Danson, M.J., Reeve, C.D., & Hough, D.W. (1999) An extremely thermostable aldolase from *Sulfolobus solfataricus* with specificity for non-phosphorylated substrates. *Biochemical Journal*, **343**, 563 – 570.

Burns, R.O., Umbarger, H.E. & Gross, S.R. (1963) The biosynthesis of leucine. III. The conversation of alpha-hydroxy-beta-carboxyisocaproate to alpha-ketoisocaproate. *Biochemistry,* **2**, 1053-1058.

Caceci, M.S. & Cacheris, W.P. (1984) Fitting Curves to Data. *Byte*, **May**, 340 – 362.

Chang, B.S. & Mahoney, R.R. (1995) Enzyme thermostabilization by bovine serum albumin and other proteins: evidence for hydrophobic interactions. *Biotechnology and Applied Biochemistry*, **22**, 203 – 214.

Chang, R (1994) In *Chemistry*, 5th Edition, McGraw-Hill, Inc., New York.

Cleveland, W. S. (1993) *Visualizing Data*, Hobart Press, New Jersey.

Cornish-Bowden, A. (1976) In *Principles of Enzyme Kinetics*, Butterworth's, London, UK.

Cornish-Bowden, A. (1995) In *Fundamentals of Enzyme Kinetics*, pp 193 – 197, Portland Press Ltd, London, UK.

Cornish-Bowden, A. (2004) In "*Fundamentals of Enzyme Kinetics*" (3rd Edn) Portland Press Ltd., London, UK.

Cornish-Bowden, A. J. (1972) Analysis of progress curves in enzyme kinetics. *Biochemical Journal*, **130,** 637 – 639.

Creighton, T.E. (1993) In *Proteins*, 2nd Edition, W.H. Freeman & Co, New York.

D'Amico, S., Claverie, P., Collins, T., Georlette, D., Gratia, E., Hoyoux, A., Meuwis, M-A., Feller, G. & Gerday, C. (2002) Molecular basis of cold adaptation. *Philosophical Transactions of the Royal Society B*, **357**, 917 – 925.

Daniel, R.M. & Cowan, D.A. (2000) Biomolecular stability and life at high temperatures. *Cellular and Molecular Life Sciences*, **57**, 250 – 264.

Daniel, R.M. & Danson, M.J. (2001) Assaying Activity and Assessing Thermostability of Hyperthermophilic Enzymes. *Methods in Enzymology*, **334**, 283 – 293.

Daniel, R.M. Dines, M. & Petach, H.H. (1996) The denaturation and degradation of stable enzymes at high temperatures. *Biochemical Journal*, **317**, 1 – 11.

Daniel, R.M., Cowan, D.A., Morgan, H.W. & Curran, M.P. (1982) A correlation between protein thermostability and resistance to proteolysis. *Biochemical Journal*, **207**, 641 – 644.

Daniel, R.M., Danson, M.J. & Eisenthal, R. (2001) The temperature optima of enzymes: a new perspective on an old phenomenon. *Trends in Biochemical Sciences*, **26**(4), 223 – 225.

Deming, S.N. & Morgan, S.L. (1973) Simplex Optimization of Variables in Analytical Chemistry. *Analytical Chemistry*, **45**, 278A – 283A.

Dixon, M. & Webb, E.C. (1979) In *Enzymes*, 3rd Edition (assisted by Thorne, C.J.R. & Tipton, K.F.), p 170, Longman Group Ltd, London.

Edwards, R.A., Jacobson, A.L. & Huber, R.E. (1990) Thermal denaturation of beta-galactosidase and of two site-specific mutants. *Biochemistry*, **29**, 11001 – 11008.

Eisenthal, R., Peterson, M.E., Daniel, R.M. & Danson, M.J. (2005) The Thermal Behaviour of Enzymes: Implications for Biotechnology. Submitted to *Nature: Biotechnology*.

Erratum. *Trends in Biochemical Sciences*, Volume 26, Issue 6, 1 June 2001, Page 401.

Eyring, H. (1935) The activated complex in chemical reactions. *Journal of Chemical Physics*, **3**,107 – 115.

Feller, G. (2003) Molecular adaptations to cold in psychrophilic enzymes. *Cellular and Molecular Life Science*, **60**, 648 – 662.

Feller, G. & Gerday, C. (2003) Psychrophilic enzymes: hot topics in cold adaptation. *Nature Reviews Microbiology*, **1**, 200 – 208.

Fernley, H. N. (1971) in *The Enzymes*, Vol. 4 (ed. Boyer, P. D.) 417 – 447 (Academic Press, New York).

Fourage, L., Helbert, M., Nicholet, P. & Colas, B. (1999) Temperature Dependence of the Ultraviolet–Visible Spectra of Ionized and Un-ionized Forms of Nitrophenol: Consequence for the Determination of Enzymatic Activities Using Nitrophenyl Derivatives – A Warning. *Analytical Biochemistry*, **270**, 184 – 185.

Garcia-Viloca, M., Gao, J., Karplus, M. & Truhlar, D.G. (2004) How Enzymes Work: Analysis by Modern Rate Theory and Computer Simulations. *Science*, **303**, 186 – 195.

Georlette, D., Blaise, V., Collins, T., D'Amico, S., Gratia, E., Hoyoux, A.. Marx, J.-C., Sonan, G., Feller, G. & Gerday, C. (2004) Some like it cold: biocatalysis at low temperatures. *FEMS Microbiology Reviews*, **28**, 25 – 42.

Gerike, U., Danson, M.J., Russell, N.J & Hough, D.W. (1997) Sequencing and expression of the gene encoding a cold-active citrate synthase from an Antarctic bacterium, strain DS2-3R. *European Journal of Biochemistry*, **248**, 49 – 57.

Gilbert, H. F. (1990) Molecular and cellular aspects of thiol-disulfide exchange. *Advances in enzymology & related areas of molecular biology*, **63**, 69 – 172.

Goldfarb, A.R. & Saidel, L.J. (1951) Ultraviolet absorption spectra of proteins. *Science*, **114**,156 – 157.

Goldfarb, A.R., Saidel, L.J., Mosovich, E. (1951) The ultraviolet absorption spectra of proteins. *Journal of Biological Chemistry*, **193**, 397 – 404.

Guldberg, C. M. & Waage, P. (1879) Über die chemische Affinität. *Journal für praktische Chemie*, **127**, 69 – 114.

Hammes, G.G. (2002) Multiple conformational changes in enzyme catalysis. *Biochemistry*, **41,** 8221 – 8228.

Hammond, P. M., Price, C. P. & Scawen, M. D. (1983) Purification and properties of aryl acylamidase from Pseudomonas fluorescens ATCC 39004. *European Journal of Biochemistry*, **132**, 651-655.

Henley, J.P. & Sadana, A. (1986) Deactivation Theory. *Biotechnology and Bioengineering*, **28**, 1277 – 1285.

Hollander, V. P. (1971) Acid Phosphatases, in *The Enzymes*, Vol. 4 (ed. Boyer, P. D.) 449-498 (Academic Press, New York)

Hsu, Y.P. & Kohlhaw, G.B. (1980) Leucine biosynthesis in *Saccharomyces cerevisiae*. Purification and characterization of beta-isopropylmalate dehydrogenase. *Journal of Biological Chemistry*, **255**, 7255-7260.

Hudson, R.C., Ruttersmith, L.D. & Daniel, R.M. (1993) Glutamate dehydrogenase from the extremely thermophilic archaebacterial isolate AN1. *Biochimica et Biophysica Acta*, **1202**, 244 – 250.

Hwang, C., Sinskey, A. J., & Lodish, H. F. (1992) Oxidized redox state of glutathione in the endoplasmic reticulum. *Science* **257**, 1496 – 1502.

Jaenicke, R. & Bohm, G.(1998) The stability of proteins in extreme environments. *Current Opinion in Structural Biology*, **8**, 738 – 748.

James, L.C. & Tawfik, D.S. (2003) Conformational diversity and protein evolution – a 60-year-old hypothesis revisited. *Trends in Biochemical Sciences*, **28**, 361 – 368.

Jansson, J.A. (1965) A Direct Spectrophotometric Assay for Pencillin Beta-Lactamase (Penicillinase). *Biochimica et Biophysica Acta*, **99**, 171 – 172.

Jiang, R.F. & Tsou, C.L. (1994) Inactivation precedes changes in allosteric properties and conformation of D-glyceraldehyde-3-phosphate dehydrogenase and fructose-1,6-bisphosphatase during denaturation by guanidinium chloride. *Biochemical Journal*, **303**, 241 – 245.

John, R.A. (1992) Photometric Assays, in *Enzyme Assays, a Practical Approach* (ed. Eisenthal, R. & Danson, M.J.) p59-92. Oxford University Press, Oxford, UK.

Kawaguchi, H., Inagaki, K., Kuwata, Y., Tanaka, H. & Tano, T. (1993) 3-Isopropylmalate dehydrogenase from chemolithoautotroph *Thiobacillus ferrooxidans*: DNA sequence, enzyme purification, and characterization. *Journal of Biochemistry*, **114**, 370-377.

Kawamura, Y., Nakanishi, K., Matsuno, R. & Kamikubo, T. (1981) Stability of immobilized α-chymotrypsin. *Biotechnology and Bioengineering*, **23**, 1219 – 1236.

Kistiakowsky, G.B. & Lumry, R. (1949) Anomalous Temperature Effects in the Hydrolysis of Urea by Urease. *Journal of the American Chemical Society*, **71**, 2006 – 2013.

Kittel, C. & Kroemer, H. (1980) In *Thermal Physics*, 2nd Edition, Freeman & Co, New York.

Knapp, S., Ladenstein, R. & Galinski, E.A. (1999) Extrinsic protein stabilization by the naturally occurring osmolytes beta-hydroxyectoine and betaine. *Extremophiles*, **3**, 191 – 198.

Ladbrooke, B.D. & Chapman, D. (1969) Thermal analysis of lipids, proteins and biological membranes. A review and summary of some recent studies. *Chemistry and Physical Lipids*, **3,** 304 – 356.

Laidler, K.J. & Bunting, P.S. (1973) In *The Chemical Kinetics of Enzyme Action*, 2nd Ed., pp426, Clarendon Press, Oxford, UK.

Lee, C.K., Peterson, M.E., Eisenthal, R., Danson, M.J., Cary, S.C. & Daniel, R.M. (2005) Growth temperature correlates with T_{eq}, a new intrinsic thermal property of enzymes. *In Progress.*

Lin, Y.Z., Liang, S.J., Zhou, J.M., Tsou, C.L., Wu, P.Q. & Zhou, Z.K. (1990) Comparison of inactivation and conformational changes of D-glyceraldehyde-3-phosphate dehydrogenase during thermal denaturation. *Biochimica et Biophysica Acta*, **1038**, 247 – 252.

Lonhienne, T., Gerday, C. & Feller, G. (2000) Psychrophilic enzymes: revisiting the thermodynamic parameters of activation may explain local flexibility. *Biochimica et Biophysica Acta,* **1543**, 1 – 10.

Lu, W & Fei, L. (2003) A logarithmic approximation to initial rates of enzyme reactions. *Analytical Biochemistry*, **316**, 58 – 65.

Matthews, B.W. (1993) Structural and genetic analysis of protein stability. *Annual Review of Biochemistry*, **62**, 139 – 160.

Medina, D.C., Hanna, E., MacRae, I.J., Fisher, A.J., & Segel, I.H. (2001) Temperature Effects on the Allosteric Transition of ATP Sulfurylase from *Penicillium chrysogenum*. *Archives of Biochemistry and Biophysics,* **393**(1), 51 – 60.

Millipore Corporation, Improving Protein and RNA Recovery with Microcon™ microconcentrators. *Fax Solutions Document 301*, Millipore Corporation, Bedford, Massachusetts, USA.

O'Callaghan, C. H., Morris, A., Kirby, S. M. & Shingler, A. H. (1972) Novel method for detection of beta-lactamases by using a chromogenic cephalosporin substrate. *Antimicrobial Agents and Chemotherapy*, **1**, 283 – 288.

Patnaik, P.R. (2002) Temperature optima of enzymes: sifting fact from fiction. *Enzyme and Microbial Technology*, **31**, 198 – 200.

Peterson, M.E. (2002) The Effect of Temperature on Enzyme Activity. MSc thesis, University of Waikato.

Peterson, M.E., Eisenthal, R., Danson, M.J. & Daniel, R.M. (2005) The determination of T_{eq}, the new and fundamental third thermal parameter of enzymes. *In Progress*.

Peterson, M.E., Eisenthal, R., Danson, M.J., Spence, A. & Daniel, R.M. (2004) A new, intrinsic, thermal parameter for enzymes reveals true temperature optima. *The Journal of Biological Chemistry*, **279**, 20717 – 20722.

Pfrogner, N. (1967) Adenosine Deaminase from Calf Spleen. II. Chemical and Enzymological Properties. *Archives of Biochemistry and Biophysics*, **119**, 141 – 146.

Porumb, H., Zargarian, L., Merad, H., Maroun, R., Mauffret, O., Troalen, F. & Fermandjian, S. (2004) Circular dichroism and fluorescence of a tyrosine side-chain residue monitors the concentration-dependent equilibrium between U-shaped and coiled-coil conformations of a peptide derived from the catalytic core of HIV-1 integrase. *Biochimica et Biophysica Acta*, **1699**, 77 – 86.

Powell, M.J.D. (1970) In *Numerical Methods for Nonlinear Algebraic Equations*, (ed. Robinowitz, P.) Chapter 7, Gordon & Breach Science Publishers, New York, New York, USA.

Raison, J.K. (1973) Temperature-induced phase changes in membrane lipids and their influence on metabolic regulation. *Symposia of the Society for Experimental Biology*, **27**, 485 – 512.

Renosto, F., Seubert, P.A., Knudson, P. & Segel, I.H. (1985) Adenosine 5'-phosphosulfate kinase from Penicillium chrysogenum. Determining ligand dissociation constants of binary and ternary complexes from the kinetics of enzyme inactivation. *Journal of Biological Chemistry*, **260**, 11903 – 11913.

Santoro, M.M., Liu, Y., Khan, S.M., Hou, L.X. & Bolen, D.W. (1992) Increased thermal stability of proteins in the presence of naturally occurring osmolytes. *Biochemistry*, **31**, 5278 – 5283.

Schellman JA. (2003) Protein stability in mixed solvents: a balance of contact interaction and excluded volume. *Biophysical Journal*, 85(1):108 – 125.

Scopes, R. K. (1994) in *Protein Purification: Principles and Practice*, 3rd Edition, (ed. Cantor, C. R.) 44 – 50 (Springer Verlag: San Diego).

Sekiguchi, T., Harada, Y., Shishido, K. & Nosoh, Y. (1984) Cloning of beta-isopropylmalate dehydrogenase gene from *Bacillus coagulans* in *Escherichia coli* and purification and properties of the enzyme. *Biochimica et Biophysica Acta*, **788**, 267-273.

Shoichet, B.K., Baase, W.A., Kuroki, R.& Matthews, B.W. (1995) A relationship between protein stability and protein function. *Proceedings of the National Academy of Sciences of the United States of America*, **92**, 452 – 456.

Sizer, I.W. (1943) Effects of temperature on enzyme kinetics. *Advances in Enzymology*, **3**, 35 – 62.

Sizer, I.W. (1944) Temperature activation and inactivation of the crystalline catalase-hydrogen peroxide system. *Journal of Biological Chemistry*, **154**, 461 – 473.

Stearn, A.E. (1949) Kinetics of biological reactions with special references to enzymatic processes. *Advances in Enzymology*, **9**, 25 – 74.

Stein, R.L. (2002) Enzymatic Hydrolysis of *p*-Nitroacetanilide: Mechanistic Studies of the Aryl Acylamidase from *Pseudomonas flourescens*. *Biochemisty,* **41**, 991 – 1000.

Stevens, L. (1992) in *Enzyme Assays, a Practical Approach* (ed. Eisenthal, R. & Danson, M.J.) p320. Oxford University Press, Oxford, UK.

Svensson, A-K.E., O'Neill, J.C. & Matthews, C.R. (2003) The coordination of the isomerization of a conserved non-prolyl cis peptide bond with the rate-limiting steps in the folding of dihydrofolate reductase. *Journal of Molecular Biology*, **326**, 569 – 583.

Thomas, T.M. & Scopes, R.K (1998) The effects of temperature on the kinetics and stability of mesophilic and thermophilic 3-phosphoglycerate kinases. *Biochemical Journal*, **330**, 1087 – 1095.

Tipton, K.F. (1992) Principles of enzymes assays and kinetic studies, in *Enzyme Assays, a Practical Approach* (ed. Eisenthal, R. & Danson, M.J.) p1-58. Oxford University Press, Oxford, UK.

Trépanier, S., Knox, J.R., Clairoux, N., Sanschagrin, F., Levesque, R.C. & Huletsky, A. (1999) Structure-Function Studies of Ser-289 in the Class C β-Lactamase from *Enterobacter cloacae* P99. *Antimicrobial Agents and Chemotherapy*, **43**, 543 – 548.

Tsou, C.L. *Biochim. Biophys. Acta* 1253, 151-162 (1995).

Volkin, D.B. & Klibanov, A.M. (1984) in *Protein function: A practical approach*, (ed. Creighton, T.E.) pp6 – 8, IRL Press, Oxford, England.

Waley, S. G. (1974) A spectrophotometric assay of β-lactamase action on penicillins. *Biochemical Journal*, **139,** 789 – 790.

Wallon, G., Yamamoto, K., Kirono, H., Yamagashi, A., Lovett, S.T., Petsko, G.A. & Oshima, T. (1997) Purification, catalytic properties and thermostability of 3-isopropylmalate dehydrogenase from *Escherichia coli*. *Biochimica et Biophysica Acta*, **1337**, 105-112.

Walsh, K.A.J., Daniel, R.M. & Morgan, H.W. (1983) A soluble NADH dehydrogenase (NADH: ferricyanide oxidoreductase) from *Thermus aquaticus* strain T351. *Biochemical Journal*, **209**, 427 – 433.

Wintrode, P.L., Zhang, D., Vaidehi, N., Arnold, F.H. & Goddard III, W.A. (2003) Protein dynamics in a family of laboratory evolved thermophilic enzymes. *Journal of Molecular Biology*, **327**, 745 – 757.

Wright, G. G. & Pauling, L. (1944) A note on the Serological Activity of Denatured Antibodies. *Science* **99**, 198 – 199.

Wright, G.G. & Schomaker, V. (1948) Studies on the Denaturation of Antibody III. Kinetic Aspects of the Inactivation of Diphtheria Antitoxin by Urea. *Journal of the American Chemical Society*, **70**, 356 – 364.

Wu, J., Patel, M.A., Sundaram, A.K. & Woodard, R.W. (2004) Functional and biochemical characterization of a recombinant Arabidopsis thaliana 3-deoxy-D-manno-octulosonic 8-phosphate synthase. *Biochemical Journal*, **381**,185 – 193.

Wynne, S.A., Nicholls, D.J., Scawen, M.D. & Sundaram, T.K. (1996) Tetrameric malate dehydrogenase from a thermophilic *Bacillus*: cloning, sequence and overexpresssion of the gene encoding the enzyme and isolation and characterization of the recombinant enzyme. *Biochemical Journal*, **317**, 235-245.

Yamada, T., Akutsu, N., Miyazaki, K., Kakinuma, K., Yoshida, M. & Oshima, T. (1990) Purification, catalytic properties, and thermal stability of threo-Ds-3-isopropylmalate dehydrogenase coded by leuB gene from an extreme thermophile, *Thermus thermophilus* strain HB8. *Journal of Biochemistry*, **108**, 449-456.

Yao, Q.Z., Tian, M. & Tsou, C.L. (1984) Comparison of the rates of inactivation and conformational changes of creatine kinase during urea denaturation. *Biochemistry*, **23**, 2740 – 2744.

Yoda, E., Anraku, Y., Kirino, H., Wakagi, T. & Oshima, T. (1995) Purification and characterization of 3-isopropylmalate dehydrogenase from a thermoacidophilic archaebacterium *Sulfolobus* sp. strain 7. *FEMS Microbiology Letters*, **131**, 243-247.

Zale, S.E. & Klibanov, A.M. (1986) Mechanisms of irreversible thermoinactivation of enzymes. *Biochemistry*, **25**, 5432 – 5444.

Zhang, Y.L., Zhou, J.M. & Tsou, C.L. (1993) Inactivation precedes conformation change during thermal denaturation of adenylate kinase. *Biochimica et Biophysica Acta*, **1164**, 61 – 67.

Zhou, H.M., Zhang, X.H., Yin, Y. & Tsou, C.L. (1993) Conformational changes at the active site of creatine kinase at low concentrations of guanidinium chloride. *Biochemical Journal*, **291**, 103 – 107.